INL/RPT-24-77205

Techno-Economic Analysis of Greenfield Geothermal Hybrid Power Plants using a Solar or Natural Gas Steam Topping Cycle

March 2024

Daniel Wendt and Ghanashyam Neupane
Idaho National Laboratory

Juliet G. Simpson, Joshua McTigue, and Guangdong Zhu
National Renewable Energy Laboratory

Idaho National Laboratory

INL is a U.S. Department of Energy National Laboratory
operated by Battelle Energy Alliance, LLC

INL/RPT-24-77205

Techno-Economic Analysis of Greenfield Geothermal Hybrid Power Plants using a Solar or Natural Gas Steam Topping Cycle

Daniel Wendt and Ghanashyam Neupane
Idaho National Laboratory
Juliet G. Simpson, Joshua McTigue, and Guangdong Zhu
National Renewable Energy Laboratory

March 2024

Idaho National Laboratory
Idaho Falls, Idaho 83415

http://www.inl.gov

Prepared for the
U.S. Department of Energy
Geothermal Technologies Office
Under DOE Idaho Operations Office
Contract DE-AC07-05ID14517

Page intentionally left blank

ABSTRACT

The relatively low generation costs associated with wind, solar photovoltaic (PV), and natural-gas power plants make it challenging for geothermal power plants to produce and sell the power that has the reliability and sustainability characteristics that are greatly needed in U.S. power markets. This is especially true for geothermal resources with low-to-medium temperatures, which results in relatively low-thermal efficiency and generation costs that are higher than those for wind, solar PV, and natural gas.

This analysis evaluates solar thermal- and natural-gas combustion waste heat recovery-based topping cycle hybridization of geothermal binary power plants. This approach provides several benefits that may allow geothermal power plants to generate power at more competitive costs. First, the addition of solar thermal energy or natural-gas combustion waste heat input to a geothermal power plant provides additional heat input that can be converted to electrical power. Second, the temperature level of the heat obtained from concentrating solar collectors or natural-gas combustion exhaust is higher than that of geothermal heat, which provides opportunities for improving the efficiency of the conversion of thermal energy to electrical power. Third, the ease with which solar thermal systems integrate with energy storage and the flexibility of natural gas means power generation can occur during peak demand periods.

The hybrid cycles are compared to equivalently sized, co-located, independent geothermal, concentrating solar, and/or natural-gas power plants. The hybrid cycle tends to produce slightly more power than the standalone plants combined. However, the hybrid plant Levelized Cost of Energy (LCOE) is slightly higher than the LCOE of the combined standalone power plants for each of the case study locations investigated.

Using the steam-topping cycle, organic Rankine cycle (ORC)-bottoming cycle hybrid plant design to combine a solar thermal resource and low-temperature geothermal resource (<120°C) leads to a hybrid plant with a lower LCOE than a standalone geothermal-only system. Thus, hybrid plants may enable the economic development of geothermal resources in locations with low geothermal resource temperatures. However, in areas with higher geothermal resource temperatures (>120°C), the geothermal-only plant has a lower LCOE than the hybrid cycle and thus could be developed without the need for solar heat addition.

A geothermal-natural-gas reciprocating engine hybrid plant was evaluated for an Elk Hills, California case study location. The Elk Hills case study analysis indicates that when the natural-gas engine operates for more than 12 hours per day the hybrid plant can produce power at an LCOE lower than a standalone geothermal plant, and comparable to that of the standalone natural-gas reciprocating engine, while also reducing the carbon intensity of the power generated relative to the standalone natural-gas engine. This may represent a scenario in which the hybrid plant provides an opportunity for the deployment of a low-temperature geothermal resource that otherwise may have an LCOE too high to develop and operate as a standalone resource, while also reducing the carbon intensity of natural-gas generation sources.

A "triple-hybrid" plant that combines natural gas, solar thermal, thermal energy storage, and geothermal was also investigated. A natural-gas combustion turbine (NGCT) is added to the geothermal-solar hybrid such that the hot exhaust gas from the gas turbine provides an alternative source of heat to the steam turbine of the hybrid cycle. Analysis results suggest that the triple-hybrid plant has a significantly higher energy generation and revenue than a standalone NGCT or the original geothermal-solar hybrid. The triple-hybrid design benefits most from using a smaller solar field so that the solar energy can be dispatched at the most valuable times available. The triple-hybrid plant also has a lower LCOE than the standalone NGCT. The triple-hybrid plant was evaluated making simple assumptions about the dispatch profile of the gas cycle, and more nuanced and realistic dispatching schedules should be analyzed in future work.

Page intentionally left blank

CONTENTS

ABSTRACT iii
ACRONYMS xii
1. Introduction 1
1.1 Project Objectives 2
1.2 Recap of Previous Projects 2
1.3 Literature Review 3
2. Case Study Locations 3
3. Cycle Configurations 6
3.1 Standalone Geothermal 7
3.1.1 Single-Pressure Level Subcritical ORC (Recuperated and Non-Recuperated) 7
3.1.2 Dual-Pressure Level Subcritical ORC 7
3.1.3 Supercritical ORC 9
3.2 Standalone CSP 10
3.3 Hybrid Geothermal-CSP 11
3.3.1 Description of Hybrid Plant Configuration 11
3.3.2 Hybrid Cycle Design Characteristics 13
3.3.3 Off-design Operation 14
3.4 Hybrid Geo-Gas Engine 15
3.5 Triple-Hybrid Geo-Gas-Solar 18
4. Modeling Methods 19
4.1 Plant-specific Modeling Considerations 20
4.1.1 Standalone Geothermal 20
4.1.2 Standalone CSP 20
4.1.3 Hybrid Geothermal-CSP 21
4.1.4 Hybrid Geo-Gas Reciprocating Engine 21
4.1.5 Triple-Hybrid Geo-Gas-Solar 21
4.2 Cost Assumptions 21
4.2.1 Solar Components 22
4.2.2 Geothermal Components 22
4.2.3 Natural-Gas Reciprocating Engine Components 22
4.2.4 Gas Turbine Costs 23
4.2.5 General Components 23
4.2.6 Combined Costs and Final Components 24
4.3 Metrics 24
4.4 Annual Simulations 26
5. Hybrid Geo-Solar Results 27

5.1 Design Point Results 27
5.2 Off-Design Results 27
5.3 Annual Results 29
5.3.1 "Baseload" Hybrid Plant 29
5.3.2 "Peaking" Hybrid Plant 34
6. Hybrid Geo-Gas Reciprocating Engine Results 38
6.1 Design Point Results 38
6.2 Off-Design Behavior 39
6.3 Annual Results 40
7. Hybrid Geo-Gas-Solar Results 45
7.1 Design Point Results 45
7.2 Off-Design Behavior 46
7.3 Annual Results 46
8. CONCLUSIONS 51
9. FUTURE WORK 53
10. REFERENCES 54
Appendix A Design Considerations and Set Points in IPSEpro and SAM 58
Appendix B Detailed Results Tables 62
Appendix C Additional Results for a "Peaking" Hybrid Plant 68

FIGURES

Figure 1. Geo-solar, geo-gas engine, and geo-gas turbine hybrid plant configurations. In this diagram heat flow is denoted with the letter Q and power is denoted with the letter W. 2
Figure 2. Selected study sites plotted on a geothermal resource map of the contiguous United States [24] 4
Figure 3. Selected study sites plotted on direct normal solar irradiance map of the contiguous United States [23]. 4
Figure 4. Standalone single-pressure level ORC. 7
Figure 5. Standalone dual-pressure level ORC. 8
Figure 6. Dual-pressure level isobutane ORC T-s diagram (left) and heating curve (right) 9
Figure 7. Standalone supercritical ORC. 9
Figure 8. Supercritical propane ORC T-s diagram (left) and heating curve (right). 10
Figure 9. Standalone steam Rankine cycle CSP plant. 10
Figure 10. Standalone steam Rankine cycle CSP plant T-s diagram. 11
Figure 11. Hybrid geo-solar configuration. 12

Figure 12. Hybrid geothermal-solar plant with steam-topping cycle and ORC-bottoming cycle operation with (left) and without (right) solar heat input. 12
Figure 13. Hybrid geothermal-solar plant steam Rankine topping cycle T-s diagram (left) and ORC-bottoming cycle T-s diagram (right). 13
Figure 14. Hybrid geothermal-solar plant steam-topping cycle heating curve (left) and ORC-bottoming cycle heating curve (right)..... 13
Figure 15. Standalone natural-gas reciprocating engine (top) and standalone natural-gas reciprocating engine with waste heat recovery (bottom). 16
Figure 16. Hybrid geothermal-gas reciprocating engine power plant..... 17
Figure 17. Standalone NGCT power plant (top) and standalone NGCC power plant (bottom) 18
Figure 18. Hybrid geo-gas plant with steam-topping cycle and ORC-bottoming cycle 19
Figure 19. Off-design performance for hybrid cycle in Elk Hills, California. 28
Figure 20. Example summer series performance of hybrid cycle in Elk Hills, California with a solar multiple of 3 and 12 hours of storage. 30
Figure 21. Monthly energy generation from standalone plants versus hybrid plants. 32
Figure 22. Tornado chart for cost sensitivities and impact on LCOE for Elk Hills, California design with SM = 3 and hours = 12. 33
Figure 23. Capital cost components compared between standalones and hybrid system for Elk Hills, California design with SM = 3 and hours = 12. 33
Figure 24. LCOE components for standalones versus hybrid cycle designs for each location. 34
Figure 25. Average daily power and electricity price profiles for 4 months in Elk Hills, California, 2021. 35
Figure 26. Heatmap showing electricity price and hybrid power plant energy output for each hour of the year in Elk Hills, California, 2021..... 36
Figure 27. Heatmaps showing hourly values of electricity price, ambient temperature, energy output from the bottoming cycle (normalized by the design value), and energy output from a standalone geothermal plant (normalized by the design value). Results are for Elk Hills, California, 2021. 37
Figure 28. Standalone gas engine, standalone geothermal, and hybrid geo-gas-cycle net power generation at Elk Hills, CA case study location during a sample one-week period with gas engine operated daily between the hours of 6:00 p.m. and 10:00 p.m. 40
Figure 29. Comparison of annual power generation for hybrid geo-gas versus sum of standalone geothermal and gas plants based on Elk Hills, California resource and ambient conditions..... 42
Figure 30. Additional generation of hybrid geo-gas plant relative to sum of standalone geothermal and gas plants based on Elk Hills, California resource and ambient conditions. 42
Figure 31. Comparison of CO_2 emissions for hybrid geo-gas plant versus sum of standalone geothermal plant and standalone gas engine based on Elk Hills, California resource and ambient conditions..... 43

Figure 32. LCOE comparison of hybrid geo-gas plant, standalone geothermal plant, and standalone gas engine with and without WHR as a function of hours per day of gas engine dispatch. 44

Figure 33. Comparison of LCOE for hybrid geo-gas plant versus sum of standalone geothermal plant and standalone gas engine based on Elk Hills, CA resource and ambient conditions..... 45

Figure 34. Scatter plot showing the electricity price and energy delivered by natural-gas power plants for each hour of the year in California 2023 [56]. 46

Figure 35. Average energy generated by natural-gas power plants for each month in California, 2023 [56]..... 47

Figure 36. Average daily energy profiles for several months for a triple-hybrid gas-geo-solar plant located in California, 2021. Solar multiple = 1.5 and TES duration = 12 hr..... 48

Figure 37. Breakdown of contributions to the LCOE for a standalone NGCT, a hybrid geothermal-solar system, and a triple-hybrid gas-geothermal-solar system. Solar multiple = 1.5 and thermal storage duration is 12 hr. California, 2021..... 50

Figure C-1. Heatmap showing electricity price and hybrid power plant energy output for each hour of the year in Elk Hills, California, 2021 70

Figure C-2. Heatmap showing electricity price and hybrid power plant energy output for each hour of the year in Fort Bliss, Texas, 2021..... 71

Figure C-3. Heatmap showing electricity price and hybrid power plant energy output for each hour of the year in Mississippi, 2021..... 71

Figure C-4. Heatmap showing electricity price and hybrid power plant energy output for each hour of the year in Idaho, 2021..... 72

Figure C-5. Heatmaps showing hourly values of electricity price, ambient temperature, energy output from the bottoming cycle (normalized by the design value), and energy output from a standalone geothermal plant (normalized by the design value). Results are for California, 2021 73

Figure C-6. Heatmaps showing hourly values of electricity price, ambient temperature, energy output from the bottoming cycle (normalized by the design value), and energy output from a standalone geothermal plant (normalized by the design value). Results are for Texas, 2021..... 74

Figure C-7. Heatmaps showing hourly values of electricity price, ambient temperature, energy output from the bottoming cycle (normalized by the design value), and energy output from a standalone geothermal plant (normalized by the design value). Results are for Mississippi, 2021 75

Figure C-8. Heatmaps showing hourly values of electricity price, ambient temperature, energy output from the bottoming cycle (normalized by the design value), and energy output from a standalone geothermal plant (normalized by the design value). Results are for Idaho, 2021 76

TABLES

Table 1. Geothermal and solar resource grades of the selected sites. 5
Table 2. Characteristics of selected case study site 6
Table 3. Natural-gas reciprocating engine generator set cost assumptions 23
Table 4. Cost assumptions for a topping gas turbine cycle. 23
Table 5. Design point power, efficiency, and parasitics at each location. 27
Table 6. Comparison of state-points and performance of the hybrid plant with and without solar heat addition. 29
Table 7. Annual simulation results for 2021 for four locations for hybrid geo-solar cycle. 31
Table 8. Annual simulation results for 2021 for four locations for hybrid geo-solar cycle. Each location uses a solar multiple of 1.5 and 8 hours of storage (except California, which uses 10 hours) 38
Table 9. Summary of standalone (SA) and hybrid power plant design point operation. 39
Table 10. Standalone (SA) reciprocating gas engine (without and with WHR), standalone geothermal plant, and hybrid geo-gas plant annual simulation results for Elk Hills, CA case study in which all plants operate in baseload mode (24/7 utilization of gas engine and geothermal resource) 41
Table 11. Comparison of LCOE and CO_2 emissions of hybrid plant relative to combined standalone (SA) geothermal and standalone gas plant for Elk Hills, California case study in which all plants operate in baseload mode (24/7 utilization of gas engine and geothermal resource). 41
Table 12. Comparison of power outputs from each cycle in gas-driven and solar-driven mods for a plant located in California. 45
Table 13. Techno-economic results for a triple-hybrid gas-geo-solar plant with different solar field sizes. 49
Table 14. Results comparing a standalone NGCT, with solar-geothermal hybrid, and triple gas-geothermal-solar hybrid for three solar field sizes, in California, 2021 50
Table A-1. Standalone and hybrid plant design parameters. 60
Table B-1. California annual simulation results for baseload operation. 65
Table B-2. Texas annual simulation results for baseload operation. 65
Table B-3. Mississippi annual simulation results for baseload operation. 66
Table B-4. Idaho annual simulation results for baseload operation. 67
Table C-1. California annual simulation results for peaking operation. 77
Table C-2. Texas annual simulation results for peaking operation. 77
Table C-3. Mississippi annual simulation results for peaking operation. 78
Table C-4. Idaho annual simulation results for peaking operation. 78

Page intentionally left blank

ACRONYMS

ACC	air-cooled condenser
AEP	annual energy production
APEA	Aspen Process Economic Analyzer
CAPEX	capital expenditure
CEPCI	Chemical Engineering Plant Cost Index
CHP	combined heat and power
CSP	concentrating solar power
DNI	direct normal insolation
DOE	Department of Energy
EDR	Exchanger Design & Rating
EIA	Energy Information Administration
GETEM	Geothermal Electricity Technology Evaluation Model
GW	gigawatt
HRSG	heat recovery steam generator
HTF	heat transfer fluid
IRR	internal rate of return
LCOE	levelized cost of electricity
LROE	levelized revenue of electricity
MITA	minimum internal temperature approach
MTD	mean temperature difference
MW	megawatt
NG	natural gas
NGCC	natural-gas combined cycle
NGCT	natural-gas combustion turbine
NPV	net present value
NREL	National Renewable Energy Laboratory
O&M	operations and maintenance
ORC	organic Rankine cycle
PPA	power purchase agreement
PV	photovoltaic
SA	standalone
SAM	System Advisor Model
SCC	Spencer Cotton Cannon

TES	thermal energy storage
USD	U.S. Dollar
VF	value factor
VRE	variable renewable energy
VSD	variable speed drive
WF	working fluid
WHR	waste heat recovery

Techno-Economic Analysis of Greenfield Geothermal Hybrid Power Plants using a Solar or Natural Gas Steam Topping Cycle

1. Introduction

Geothermal energy provides a reliable source of low-carbon power generation but has a higher LCOE at the point of delivery than variable renewable energy (VRE) sources such as wind and solar photovoltaics (PV). In the absence of grid-scale energy storage for VRE technologies, fossil fuel-based power plants are currently necessary to provide the generation capacity for energy markets with a large makeup of VRE sources. This arrangement is not amenable to achieving large scale carbon emission reduction goals including a carbon pollution-free power sector by 2035 and a net-zero emission economy by 2050 [1]. Development of geothermal power generation technologies that would enable more cost-effective deployment of geothermal resources is an approach that could help to provide firm backing for VRE technologies while maintaining a low carbon footprint.

Geothermal power plants face several challenges to competitively provide power to U.S. energy markets. Traditional PPAs do not compensate for flexible operation of geothermal plants, which tend to run as baseload systems, providing high capacity factors. These PPA structures limit the ability of the geothermal system to balance electricity supply and demand, such as by reducing generation when there is an oversupply of inflexible renewable power, such as solar energy during the day, or to ramp up production, providing energy reserves, or provide frequency regulation when other renewable generation decreases [4].

U.S. geothermal deployment has traditionally occurred in the Western United States where higher-temperature hydrothermal resources (e.g. 175–225°C) are most easily accessed. Low-to-medium temperature resources (e.g. 90–150°C) may be accessed over a larger proportion of the U.S. or at shallower well depths. This provides an opportunity to increase deployment of geothermal, but lower temperatures result in a lower thermal efficiency and increased generation costs.

This analysis evaluates solar thermal- and natural-gas combustion waste heat recovery-based topping cycle hybridization of geothermal binary power plants (Figure 1). This approach provides several benefits that may allow geothermal power plants to generate power at more competitive costs. First, the addition of solar thermal energy or natural-gas combustion waste heat input to a geothermal power plant provides additional heat input that can be converted to electrical power. Second, the temperature level of the heat obtained from concentrating solar collectors or natural-gas combustion exhaust is higher than that of geothermal heat, which provides opportunities for improving the efficiency of the conversion of thermal energy to electrical power. Third, the ease with which solar thermal systems integrate with thermal energy storage and the flexibility of natural gas means power generation can occur during peak demand periods.

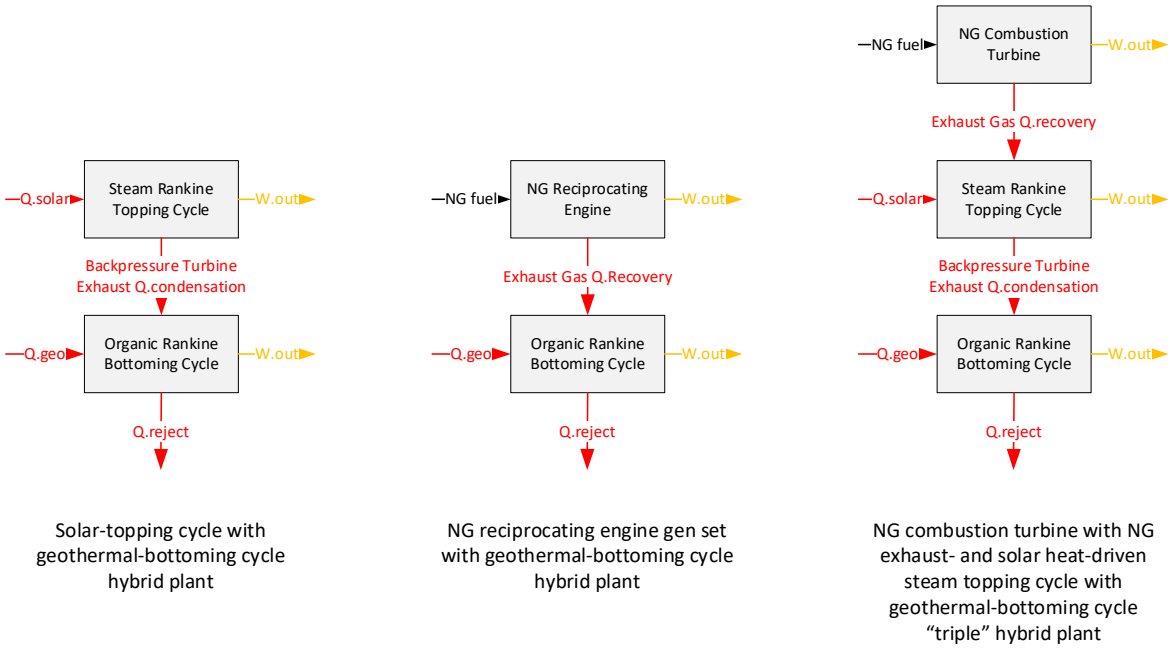

Figure 1. Geo-solar, geo-gas engine, and geo-gas turbine hybrid plant configurations. In this diagram heat flow is denoted with the letter Q and power is denoted with the letter W.

1.1 Project Objectives

The objective of this analysis is to determine the geothermal and solar resource conditions and the associated plant configurations and operating strategies for which a steam-topping cycle hybrid binary geothermal power plant would be able to profitably sell power to a representative electricity market. The analysis uses a case study approach to provide insight as to the resource types and plant configurations that will enable increased deployment of geothermal power plants, which will in turn increase the United States installed base load generation capacity of clean renewable geothermal power, reducing the need for generation backing from fossil-based power plants. While multiple cycle designs will be evaluated, the focus of this report is geothermal-solar hybrid power cycles.

1.2 Recap of Previous Projects

Idaho National Laboratory and the National Renewable Energy Laboratory have collaborated on several analyses of hybrid geothermal-solar power generation, including:

1. An analysis and validation of data from the Stillwater power plant that hybridized a medium enthalpy geothermal resource with solar photovoltaics and parabolic trough solar thermal collectors [5].
2. An investigation into the optimal addition of solar thermal to a double-flash geothermal plant based on the Coso geothermal field to exploit excess capacity in the steam turbine that arose due to geothermal resource decline [6].
3. The development of a solar-driven topping cycle using a back-pressure steam turbine to add heat to a bottoming geothermal binary cycle based on the Raft River power plant [7].
4. The use of solar thermal energy to heat the subsurface and create a geological thermal energy storage system [8], [9], [10].

The current study concentrates on the development of a new-build geothermal-solar or geothermal-gas hybrid plant [11], as opposed to the previous projects which largely considered retrofitting an existing geothermal plant with solar thermal.

1.3 Literature Review

Geothermal organic Rankine cycles (ORCs) that rely on air-cooled condensers (ACCs) are negatively affected by high-ambient temperatures. An increase in ambient temperature by just 10°C was found to result in about a 20% reduction in power output by Manente et al.'s 2013 article and Keshvarparast et al.'s 2020 article [12] and [13]. One option for improving geothermal power production during high-ambient temperature times (and over time as geothermal resource declines) is to gather additional supplemental heat from solar thermal.

Some hybrid cycle designs use solar thermal to heat the geothermal brine without a topping cycle. In Hu et al. [14] and Ghasemi et al. [15], solar is used to heat the geothermal brine without a topping cycle, and in Lentz and Almanza [16], solar thermal is used to assist an underperforming geothermal plant. Adding supplemental heat to the geothermal brine was also considered by Hu et al., Tranamil-Maripe et al. and Bassetti et al.'s articles [14], [17], [18].

Previous work by this group, including McTigue et al.'s 2020 article [7], considered starting from a known geothermal plant and adding solar in the form of a steam Rankine topping cycle which feeds additional heat into an ORC-bottoming cycle. McTigue et al. [19] studied the different possible options for moving heat from the solar thermal system to the geothermal cycle and found that using a topping cycle to add heat to the bottoming cycle working fluid provided the best compromise between efficiency and complexity. Variations on that design are common, including those found in McTigue et al., Bonyadi et al., Boukelia et al., and Song et al.'s articles [7], [20], [21], [22].

Starting from a greenfield site where there is not already an existing/planned solar or geothermal power cycle is less common. The only identified greenfield hybrid design, detailed in Hu et al.'s article, considered using solar to add heat to the geothermal brine without the use of a topping cycle [14]. Thus, investigating a greenfield hybrid system with a solar topping cycle and a geothermal bottoming cycle remains a novel area of research.

When comparing systems, common metrics used include LCOE used by McTigue et al., Tranamil-Maripe et al., and Bonyadi et al. [7], [17], [20], and annual energy production (AEP), McTigue et al., Tranamil-Maripe et al., and Song et al. [7], [17], [22].

Despite a well-established history in the literature, opportunities for novelty in this field still exist in the form of greenfield design and dispatch/design focused on value of the system.

2. Case Study Locations

In the United States, most of the identified geothermal resources are in the western part of the country. For this study, we also evaluated geothermal resources in the southeastern part of the country for their economic viability when hybridized with solar thermal resources. A review of hybrid systems literature found a range of temperatures considered from 90°C to 265°C for the geothermal brine, but the majority were around 150°C. Four low-to-medium temperature geothermal resources with a known temperature range of 90 to 135°C are selected for this study to evaluate the potential for hybridization of the geothermal heat with a secondary heat source to improve the viability of using low-to-medium temperature geothermal resources.

The selected sites are in Idaho, California, New Mexico/Texas, and Mississippi. (Note that the Fort Bliss site crosses between Texas and New Mexico and uses Texas energy market data for this report). The main criteria to select these sites for this study are (1) diversity in geographic areas, (2) geothermal resource grades, and (3) solar resource grade.

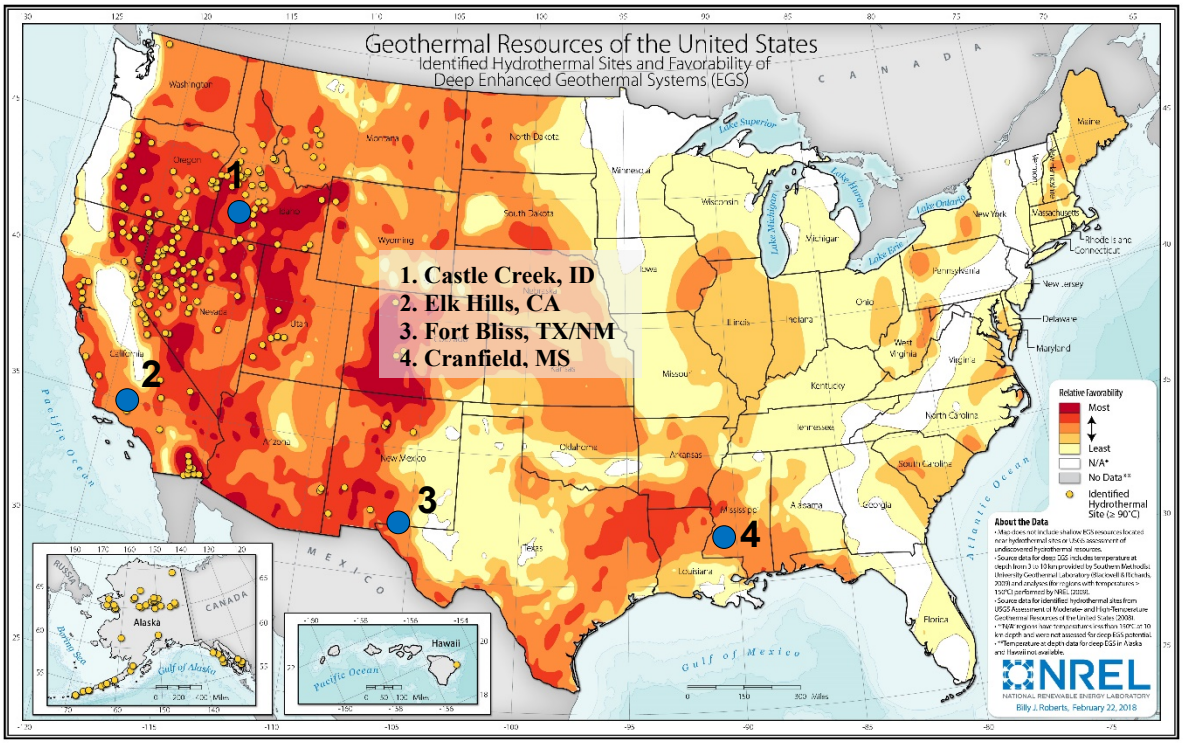

Figure 2. Selected study sites plotted on a geothermal resource map of the contiguous United States [24]

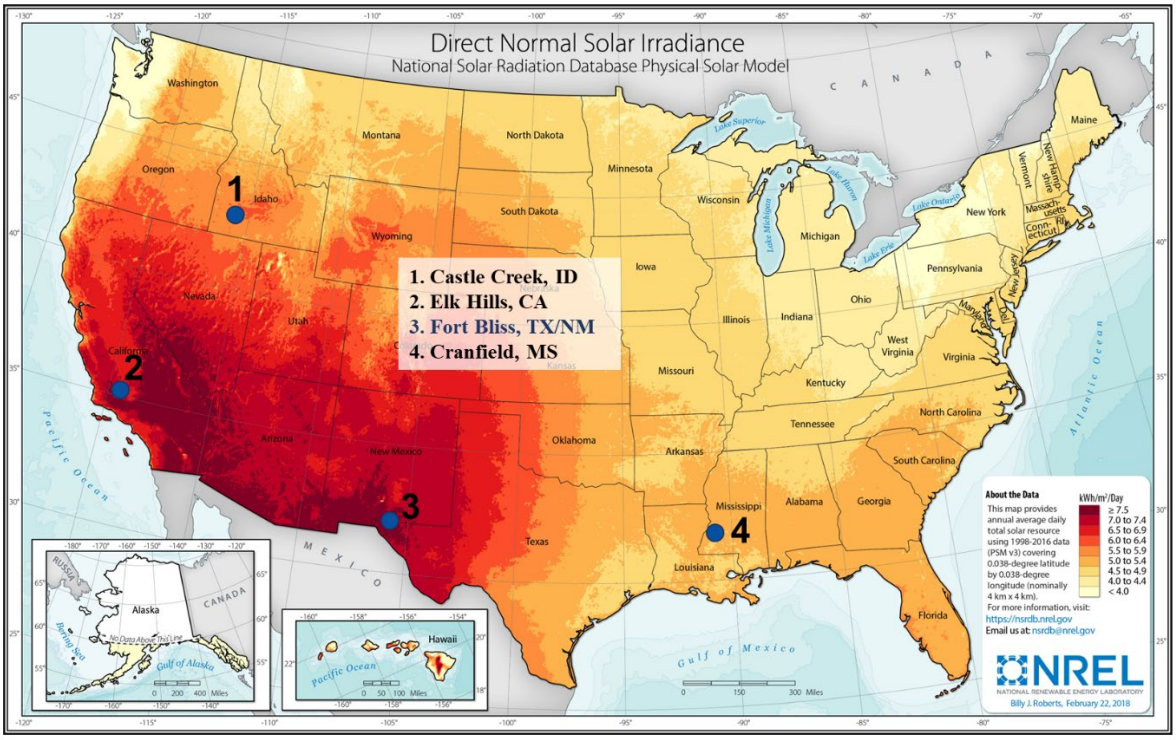

Figure 3. Selected study sites plotted on direct normal solar irradiance map of the contiguous United States [23].

These resources are subdivided into low-temperature (90 to 120°C) and high-temperature (120 to 150°C). Note that higher-temperature hydrothermal resources (>200°C) have been developed for geothermal in the U.S., and higher temperatures are achievable with Enhanced Geothermal Systems (Figure 2), so the 120-150°C is only high-temperature in the context of this study. The selected sites also represent diverse solar resource grades (Figure 3), which we categorize as having low-irradiance (<6.4 $kWh_{th}/m^2/day$) or high-irradiance (>6.5 $kWh_{th}/m^2/day$) in terms of concentrating solar thermal potential. The qualitative categories of the geothermal and solar grades for the selected sites are given in Table 1. Two reservoir systems representing low- and high-geothermal grades could be considered for the Elk Hills site. Salient characteristics of all selected sites are given in Table 2. The higher-temperature Elk Hills geothermal resource was considered in this study; the lower temperature resource that was not evaluated is denoted using gray font in Table 2.

Table 1. Geothermal and solar resource grades of the selected sites.

		Solar	
		Low	High
Geothermal	Low	Grand View, ID	Fort Bliss, TX
	High	Cranfield, MS	Elk Hills, CA

Table 2. Characteristics of selected case study site.

Sites		Grand View	Elk Hills	Fort Bliss / McGregor Range	Cranfield site
State		Idaho	California	Texas / New Mexico	Mississippi
Latitude		42.96333	35.280115	32.068639	31.563533
Longitude		-116.076655	-119.469009	-106.155008	-91.141487
Geothermal	Measured temp (°C)	108	89.5 @ 2250 m* 135 @ 2800 m	96	127
	Injection temp (°C)	51	52	51	51
	Province/Basin	Snake River Plain	San Juaquin	Tularosa Basin	Gulf Coast
	Resource depth (m)	2672	2225 2800	1500	3100
	Reservoir pressure, psi	213	3200 3645	1918	4641
	Pumping power (kW_e/MW_e)	181	125	284	98
	Resource grade	Low	Low to High	Low	High
	Geology	Sedimentary, volcanics	Sedimentary	Sedimentary, intrusive	Sedimentary
	Reservoir rock	Rhyolite	Sandstones	Carbonates	Sandstones
	Drilling difficulty	Low-Medium	Low-Medium	Low	Low
	Brine chemistry	<1000 mg/L TDS	<50k mg/L TDS; low sulfate	~10k mg/L TDS; sulfate rich	150K mg/L TDS; low sulfate
	Qualitative permeability	High	Low-Medium	Commercial	Medium
	Flow rate/well or hot springs (gpm)	1000	2000 1300	1000	2000
	# Prod well for 10 MW_e	8	4	12	2
Solar	Resource grade	Low	High	High	Low
	Direct Normal Irradiance ($kWh_{th}/m^2/day$)	5.7	6.6	7.1	5
Other energy source		Wind	Natural gas		Natural gas
Drilling cost estimates per well (in million 2020 USD)		6.8	5.5/7	4.9	7.3

*The gray font data for the Elk Hills area are for a shallower secondary reservoir.

Further details of the selected case study locations including discussion of brine chemistry and scaling potential as well as estimated well drilling costs and production and injection pumping power requirements is provided in Neupane et al.'s 2024 document [25].

3. Cycle Configurations

The focus of this report is geothermal-solar hybrid power cycles. These are compared to standalone geothermal cycles and solar thermal cycles. In addition, hybridization of natural-gas power cycles with geothermal and geothermal-solar are considered. Cycle concepts and models are developed for each of these configurations.

3.1 Standalone Geothermal

Several standalone geothermal cycle configurations were evaluated to provide a baseline for comparison of hybrid plant performance. The configurations evaluated include basic (single-pressure level) ORC (recuperated and non-recuperated configurations), dual-pressure level ORC, and supercritical ORC. Each standalone geothermal cycle configuration was evaluated using both isobutane and propane working fluid.

3.1.1 Single-Pressure Level Subcritical ORC (Recuperated and Non-Recuperated)

A basic single-pressure level ORC configuration includes a feed pump, preheater, vaporizer, expander, and condenser as shown in Figure 4. The basic single-pressure level configuration causes the ORC working fluid vaporization process to have a single pinch point that results in relatively high mean temperature difference (MTD), which limits the brine return temperature (and the quantity of heat that can be extracted from the brine) and results in thermodynamic inefficiencies (high exergy losses in the working fluid vaporization process).

Recuperation can be used to remove superheat from the turbine exhaust (this is primarily applicable for ORCs with working fluids having a temperature-entropy (T-S) diagram with a retrograde or "dry" condensation curve, as is the case for isobutane) with the heat recovered from the turbine exhaust used to increase the temperature of the condensed liquid prior to heat exchange with the geothermal brine. Recuperation can reduce the quantity of heat that must be rejected in the condenser, which can reduce the condenser capital costs. Recuperation can also be used to maintain a brine return temperature above the point at which minerals may begin to precipitate in the hot side of the preheater. However, based on our case study site analysis none of the case study locations require a brine outlet temperature constraint to prevent mineral precipitation so the inclusion or exclusion of a recuperator in the standalone geothermal plant was based entirely on which configuration resulted in the highest design point power generation. In the case studies considered, the single-pressure level subcritical ORC performed better without use of a recuperator.

The single-pressure level subcritical ORC was determined to provide a lower level of net power generation than the dual-pressure level and supercritical ORC configurations (described below) for all the case study locations evaluated. Therefore, the single-pressure level subcritical ORC was not selected as the baseline standalone geothermal plant configuration in the comparison of hybrid versus standalone plant performance and economics.

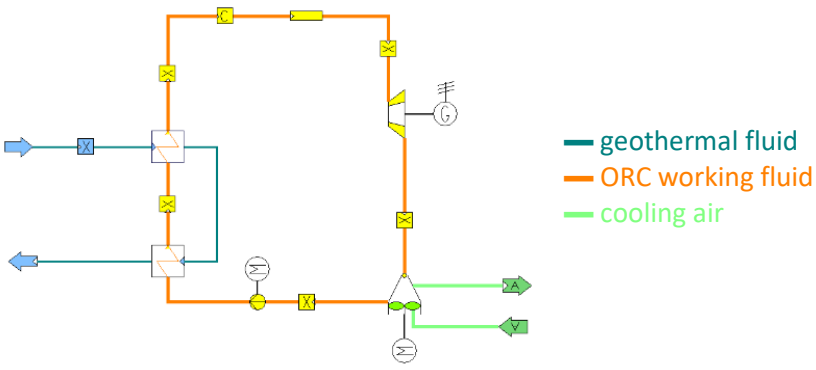

Figure 4. Standalone single-pressure level ORC.

3.1.2 Dual-Pressure Level Subcritical ORC

The dual-pressure level subcritical ORC includes low- and high-pressure cycles as shown in Figure 5. This configuration requires a high-pressure pump, high-pressure vaporizer, and high-pressure turbine in

addition to the low-pressure pump, low-pressure preheater and vaporizer, and low-pressure turbine. The condensate exiting the condenser is pressurized in the low-pressure pump and then heated to the low-pressure bubble point in the preheater. At this point the flow is split between the low- and high-pressure branches of the cycle. The low-pressure fraction is vaporized and expanded via the low-pressure turbine. The high-pressure fraction is further pressurized in the high-pressure pump and then sent to the high-pressure vaporizer, where the fluid is further heated to the high-pressure bubble point and then vaporized and expanded via the high-pressure turbine. The high-pressure turbine exhaust pressure is set equal to the low-pressure turbine inlet pressure so that the working fluid from both the high- and low-pressure branches of the cycle can be expanded in the low-pressure turbine. A T-s diagram of the dual-pressure level ORC is shown in Figure 6 (left).

The dual-pressure level configuration allows the ORC working fluid heating curve to have two preheating and two vaporization segments, which results in a "stepped" heating curve that allows the heat exchangers to operate with low MTD for increased cycle efficiency and allows the cycle to extract more heat from the brine than would typically be possible with a single-pressure level ORC. The dual-pressure level ORC heating curve is shown in Figure 6 (right).

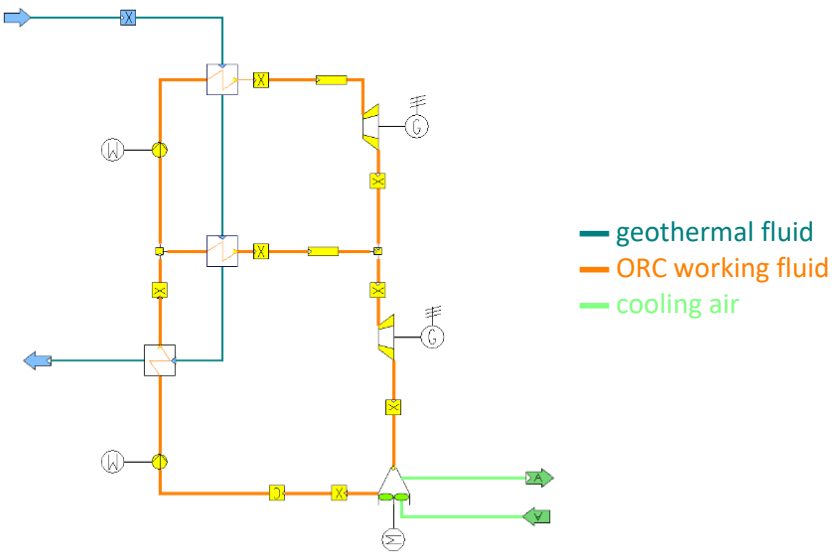

Figure 5. Standalone dual-pressure level ORC.

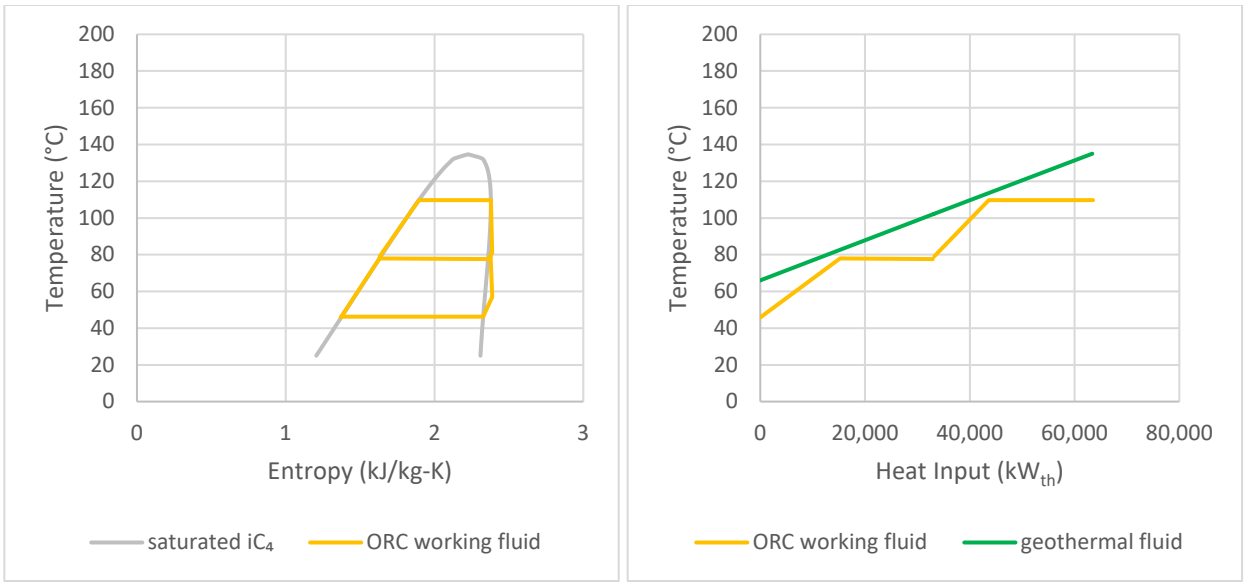

Figure 6. Dual-pressure level isobutane ORC T-s diagram (left) and heating curve (right).

3.1.3 Supercritical ORC

The supercritical ORC has a configuration similar to the basic single-pressure level ORC (Figure 7) but uses a working fluid selection and operating conditions that enable the working fluid to be kept at temperature and pressure combinations outside the two-phase region during heat addition. When the working fluid is maintained above the critical pressure, the vaporization curve never passes through the two-phase region of the T-s diagram, which eliminates the pinch point associated with subcritical fluid vaporization and allows an approximately parallel temperature profile in the geothermal fluid and working fluid heating curve to minimize exergy losses and maximize heat extraction from the geothermal brine. The supercritical ORC T-s diagram is shown in Figure 8 (left), while the supercritical ORC heating curve is shown in Figure 8 (right).

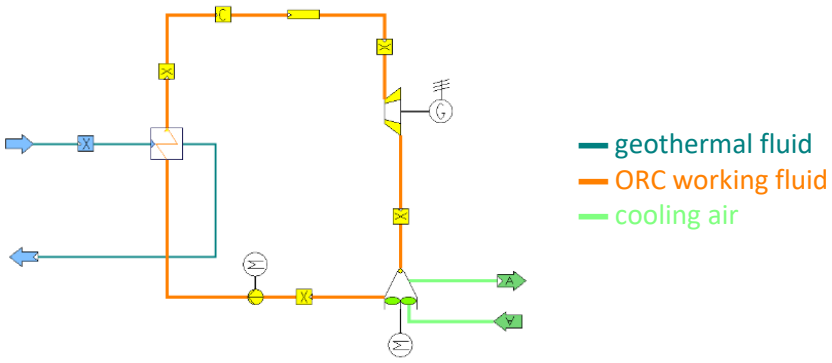

Figure 7. Standalone supercritical ORC.

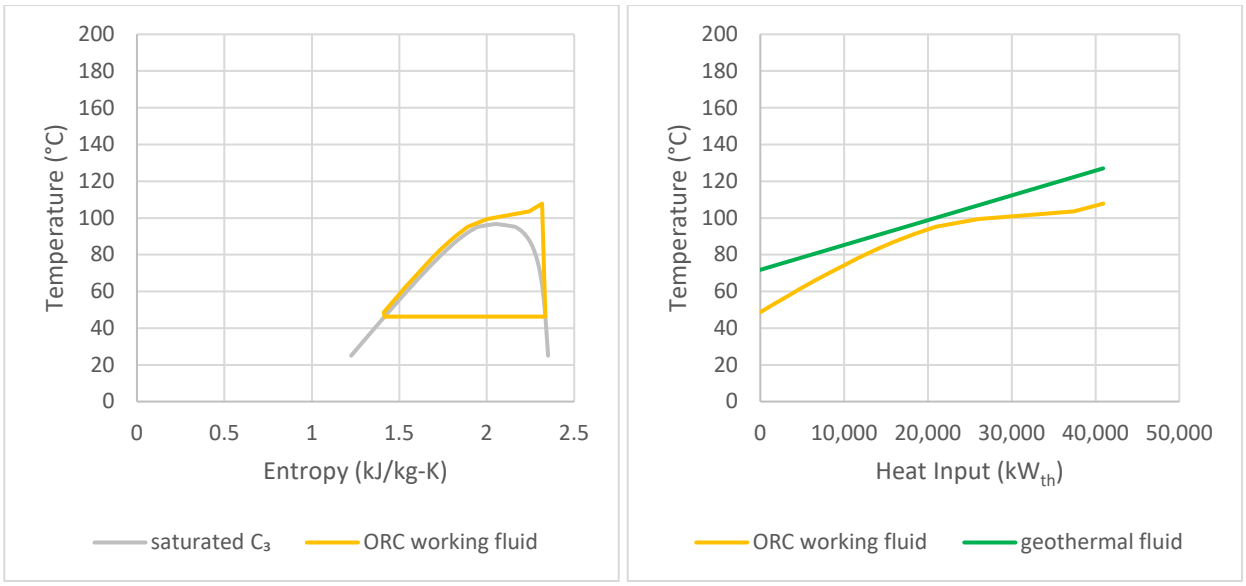

Figure 8. Supercritical propane ORC T-s diagram (left) and heating curve (right).

3.2 Standalone CSP

The steam Rankine cycle was selected as the baseline power cycle for the standalone concentrating solar power (CSP) power plant. The standalone CSP power plant was evaluated to provide a baseline for comparison of standalone versus hybrid plant performance. The steam Rankine cycle is a mature and robust commercial technology that has been used in fossil, biomass, nuclear, and renewable power generation applications. The steam Rankine cycle has been deployed in most, if not all, currently operational utility-scale commercial CSP power plants [26], [27], [28], [29].

The standalone CSP plant considered in this analysis uses a subcritical steam Rankine cycle that includes a feedwater pump, steam generator, condensing steam turbine, and an air-cooled condenser (Figure 9). The cycle is specified to use high-temperature CSP collectors and a molten salt heat transfer fluid with a supply temperature sufficient to provide a level of superheating that does not require the use of a reheater (to avoid excessive condensation in the final stages of the expansion process). The turbine inlet pressure is specified as 90 bar [30] with an exhaust pressure of approximately 0.1 bar. An air-cooled condenser is used to reject heat to ambient; this cooling technology has been deployed in multiple commercial CSP power plants [29], [31]. The T-s diagram for the CSP steam Rankine cycle is shown in Figure 10.

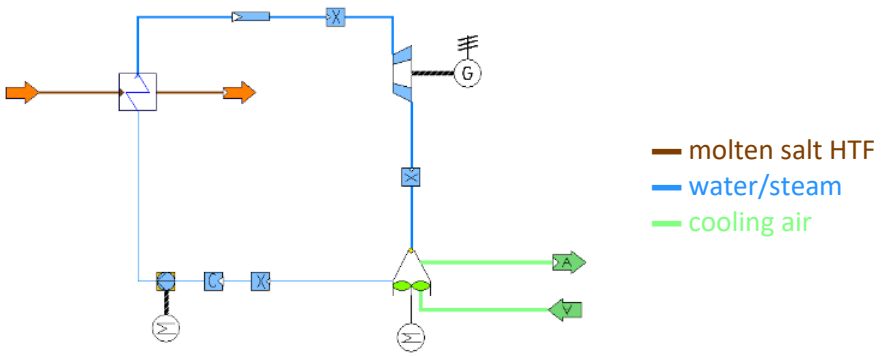

Figure 9. Standalone steam Rankine cycle CSP plant.

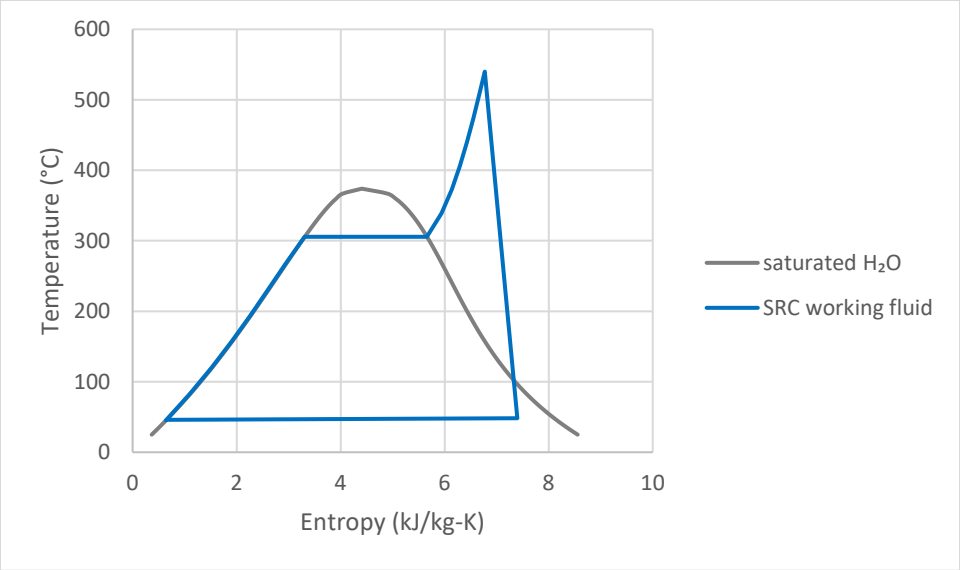

Figure 10. Standalone steam Rankine cycle CSP plant T-s diagram.

3.3 Hybrid Geothermal-CSP

3.3.1 Description of Hybrid Plant Configuration

A hybrid geothermal-solar power plant configuration with a steam Rankine topping cycle and an organic Rankine bottoming cycle was investigated. The cycle configuration is illustrated in Figure 11 and the IPSEpro cycle representation is shown in Figure 12 (left). T-s diagrams of the steam Rankine topping cycle and organic Rankine bottoming cycle are shown in Figure 13. High-temperature solar heat is input to the steam-topping cycle, which generates electrical power using a back-pressure turbine. Low-temperature geothermal heat is input to the ORC-bottoming cycle to preheat the working fluid. The steam-topping cycle back-pressure turbine exhaust pressure is specified such that the heat rejection associated with the steam condensation can provide heat input to the bottoming ORC cycle at a temperature that is complementary to the geothermal heat source.

Hybrid plant configurations were investigated in which both the geothermal heat and the solar heat rejected from the topping cycle were used to vaporize the ORC working fluid. However, evaluation of the fraction of geothermal heat to be used for ORC working fluid vaporization identified that the hybrid plant performance was maximized (relative to the combined performance of a standalone geothermal plant and standalone solar plant operating off of the same geothermal and solar thermal resources, respectively) when all geothermal heat was used for preheating the ORC working fluid and all solar heat rejected from the topping cycle was used for vaporizing the ORC working fluid (the optimal design point configuration does not use any geothermal heat for vaporizing the ORC working fluid).

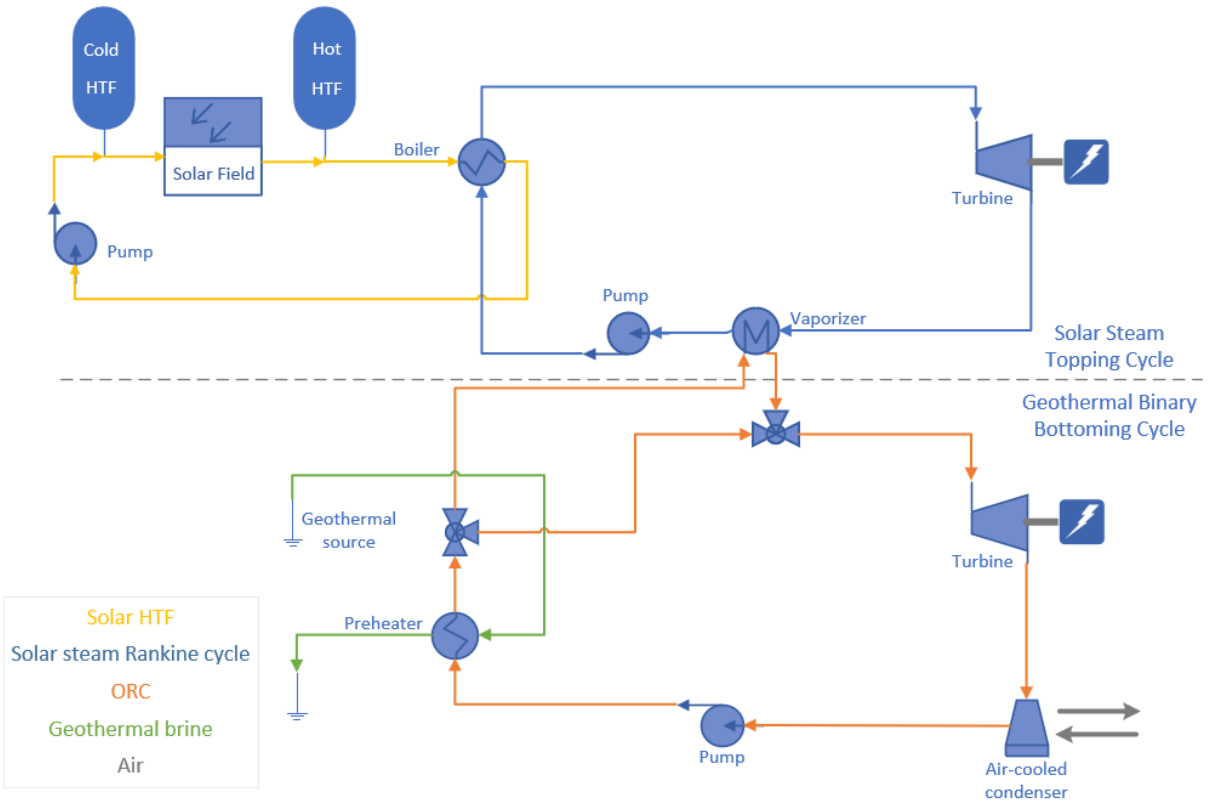

Figure 11. Hybrid geo-solar configuration.

The hybrid plant rejects heat to ambient by way of an ACC. Since the heat rejected from the topping cycle is input to the bottoming cycle, the bottoming cycle is responsible for all heat rejection to ambient. Use of an ACC eliminates the need for cooling water. However, the off-design operation of the air-cooled cycle is more sensitive to changes in the ambient temperature than if the cycle were based on a water-cooled configuration.

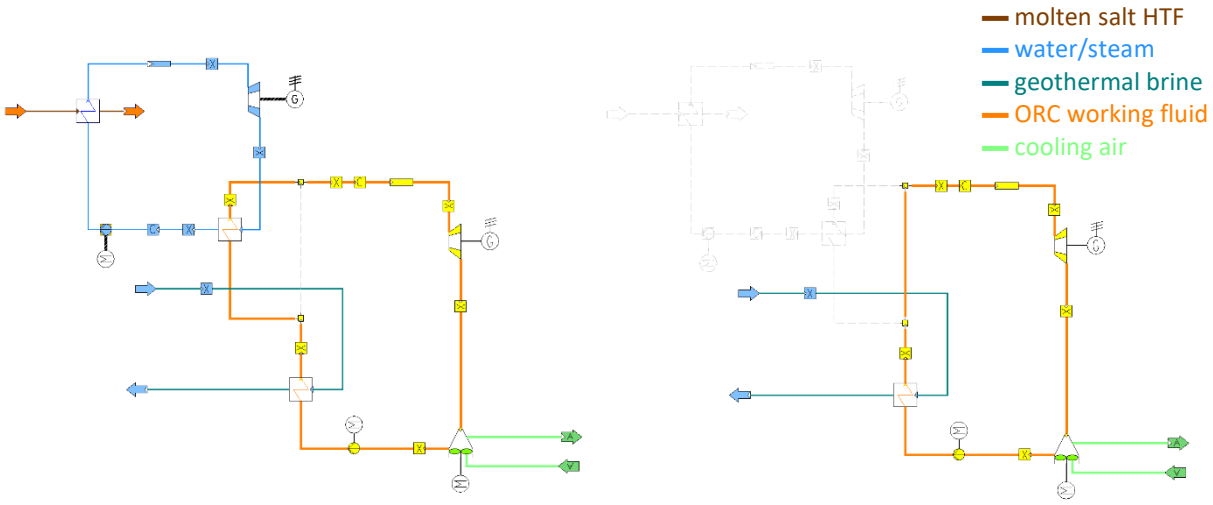

Figure 12. Hybrid geothermal-solar plant with steam-topping cycle and ORC-bottoming cycle operation with (left) and without (right) solar heat input.

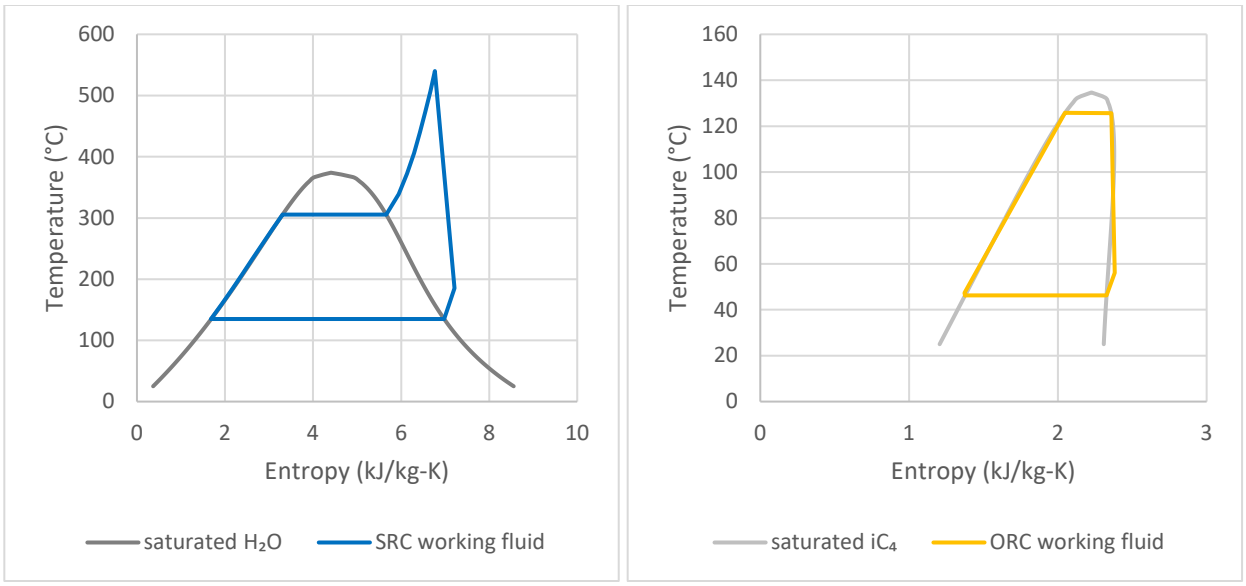

Figure 13. Hybrid geothermal-solar plant steam Rankine topping cycle T-s diagram (left) and ORC-bottoming cycle T-s diagram (right).

3.3.2 Hybrid Cycle Design Characteristics

The hybrid cycle configuration is selected to make efficient use of the high-temperature, high-exergy solar thermal heat source through use of a steam Rankine cycle. Use of a back-pressure steam turbine eliminates the need for rejection of the steam Rankine cycle to ambient as the configuration allows the heat rejected from the steam Rankine cycle to be input to the ORC-bottoming cycle. Use of a back-pressure steam turbine also reduces the amount of feedwater heating needed to achieve the correct boiler inlet temperature. The heating curve for the steam Rankine topping cycle is shown in Figure 14 (left).

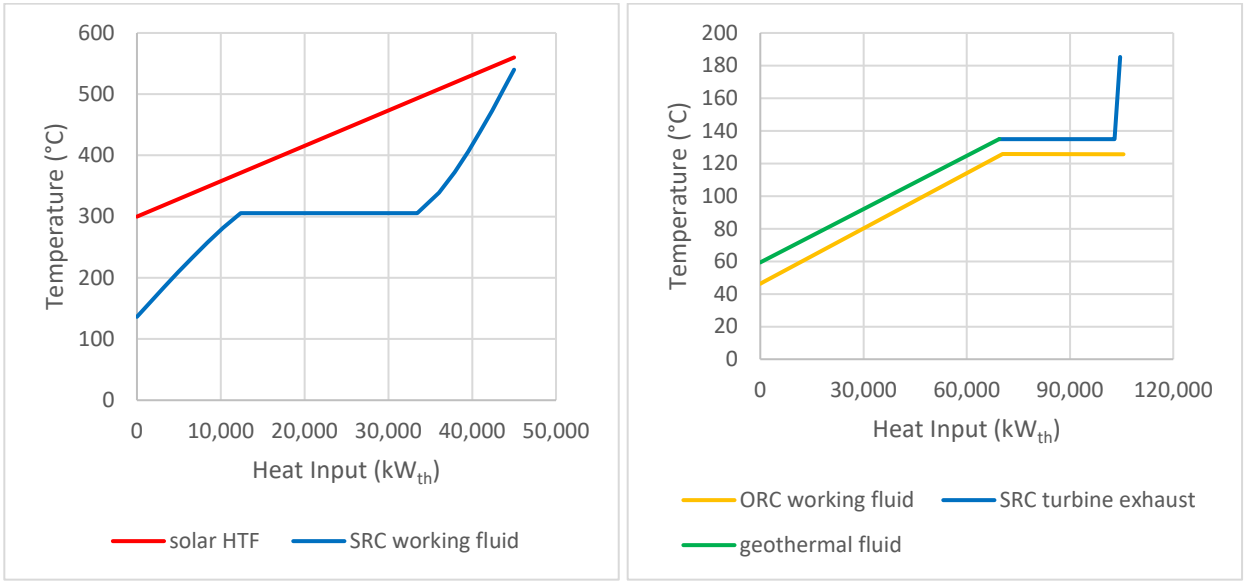

Figure 14. Hybrid geothermal-solar plant steam-topping cycle heating curve (left) and ORC-bottoming cycle heating curve (right).

While a small portion of the heat rejection from the steam-topping cycle is in the form of de-superheating the turbine exhaust, most of the heat rejected from the steam Rankine topping cycle is

associated with the condensation of the steam exiting the back-pressure turbine. The steam condensation provides an isothermal heat flow that is utilized in the bottoming cycle for the purpose of vaporizing the ORC working fluid (also an isothermal process). The bottoming cycle working fluid design point flow rate is set to the value that matches the heat duty of the steam condensation and ORC working fluid vaporization processes to achieve a heat exchanger heating curve with a nearly constant ΔT between the hot and cold fluids. This design strategy enables heat transfer from the topping cycle to the bottoming cycle with minimal exergy loss due to the well-matched temperature profile of the steam condensation and the ORC working fluid vaporization.

As the heat rejected from the topping cycle provides the heat duty required to vaporize the ORC working fluid, the heat extracted from the geothermal resource can be used entirely for preheating the ORC working fluid. This arrangement eliminates the pinch point that standalone subcritical ORCs encounter when the geothermal brine is used to both preheat and vaporize the ORC working fluid. Additionally, the hybrid plant's use of the geothermal brine entirely for preheating the ORC working fluid allows the preheater to have a heating profile with near constant temperature differential between the brine and ORC working fluid, which minimizes the thermodynamic losses (minimizes exergy losses) while also allowing the hybrid plant to extract the maximum possible heat from the brine by minimizing the brine return temperature. The heating curve for the organic Rankine bottoming cycle is shown in Figure 14 (right).

An air-cooled condenser is used to reject heat from the bottoming cycle (which includes heat from both the solar and geothermal resources) to ambient without the requirement for a cooling water source.

3.3.3 Off-design Operation

Despite the use of solar thermal energy storage, the hybrid plant solar heat input is likely to vary on hourly, daily, and seasonal time scales. The hybrid plant design point is based on the maximal use of the solar resource. When the heat input from the solar resource decreases due to the diurnal cycle, weather patterns, or seasonal effects the hybrid plant off-design operating point will change. The hybrid plant will respond to decreases in the solar resource heat input by decreasing the topping cycle steam production rate, which will both decrease the steam flow rate and decrease the heat flow from the topping cycle to the bottoming cycle. The geothermal flow rate is not subject to the same level of perturbations as the solar resource, and it is assumed to remain constant in the simulations performed for this analysis. Therefore, a reduction in the heat flow from the topping cycle to the bottoming cycle will require that the geothermal heat be used to provide a portion of the heat used to vaporize the ORC working fluid. Use of the geothermal heat for vaporizing the ORC working fluid in addition to preheating the ORC working fluid will necessitate a decrease in the ORC working flow rate and a corresponding decrease in the ORC-bottoming cycle gross power generation.

Changes in the ambient temperature also cause the hybrid plant to operate at off-design conditions in which the geothermal heat exchanger is not used solely for preheating and/or the topping cycle heat rejection exchanger is not used solely for vaporization (e.g., when the ambient temperature increases above the design condition, the ORC-bottoming cycle condensing pressure and turbine inlet pressure increase, which prevents the geothermal heat exchanger from preheating the ORC working fluid all the way to its saturation point).

The hybrid plant bottoming cycle includes a vaporizer bypass line that can be used to send vapor exiting the geothermal heat exchanger directly to the ORC turbine. When there is no heat input from the solar resource, the geothermal heat exchanger provides all the heat duty required to preheat and vaporize the ORC working fluid and the bypass is used to route all flow around the topping cycle heat rejection exchanger and directly to the ORC turbine. This operating mode is shown in Figure 12 (right).

The hybrid plant requires a geothermal heat exchanger that can operate as a pure preheater when the plant is operating at the design condition, but that can also operate as a preheater/vaporizer when

decreased solar resource availability causes the plant to operate at off-design conditions. Therefore, this heat exchanger would operate under conditions that would result in a liquid phase outlet fluid, two-phase mixture outlet fluid, or a vapor phase outlet fluid and would require an equipment configuration that would support these various operational strategies, such as inclusion of a vapor-liquid disengaging space and outlet pipe sizing that could accommodate either liquid, two-phase, or vapor phase flow. This study did not perform a detailed investigation of the specific geothermal heat exchanger design that would be necessary to accommodate these varying operating modes, and future studies of the steam-topping cycle hybrid plant configuration should consider the costs and operational implications of such a heat exchanger design.

3.4 Hybrid Geo-Gas Engine

Application of the design strategies described above for the hybrid geo-solar plant were also applied to a hybrid geo-gas plant configuration using a natural-gas reciprocating engine generator set. A basic natural-gas reciprocating engine generator set configuration is shown in Figure 15 (left). Natural-gas reciprocating engines used for power generation applications have the following characteristics [32]:

- Are available in sizes ranging from 10 kW_e to over 18 MW_e
- Have a fast startup time that makes them well suited for peaking and/or emergency power applications
- Can maintain their operating efficiency during partial load operation, which is important in electrical load following applications.

Reciprocating engines produce waste heat in the form of the heat rejected by the engine coolant as well as the heat in the engine exhaust. Engines with high-pressure or ebullient cooling systems can operate with water jacket temperatures up to 130°C. Engine exhaust heat may be available at temperatures in excess of 500°C, but to prevent corrosion from condensation of exhaust gases, this stream should not be cooled below about 120°C [32].

The waste heat from a reciprocating engine can be used to drive an ORC-bottoming cycle, as shown in Figure 15 (right). This analysis considers use of both the reciprocating engine cooling jacket heat along with heat recovered from the exhaust gas stream via a waste heat recovery (WHR) system to provide the heat input for the ORC-bottoming cycle. The engine coolant is used as the heat transfer fluid for delivering the waste heat from the engine jacket and exhaust gas WHR system to the ORC working fluid vaporizer. Use of an ebullient cooling system is specified such that steam can be used to deliver the waste heat from the reciprocating engine to the ORC-bottoming cycle working fluid.

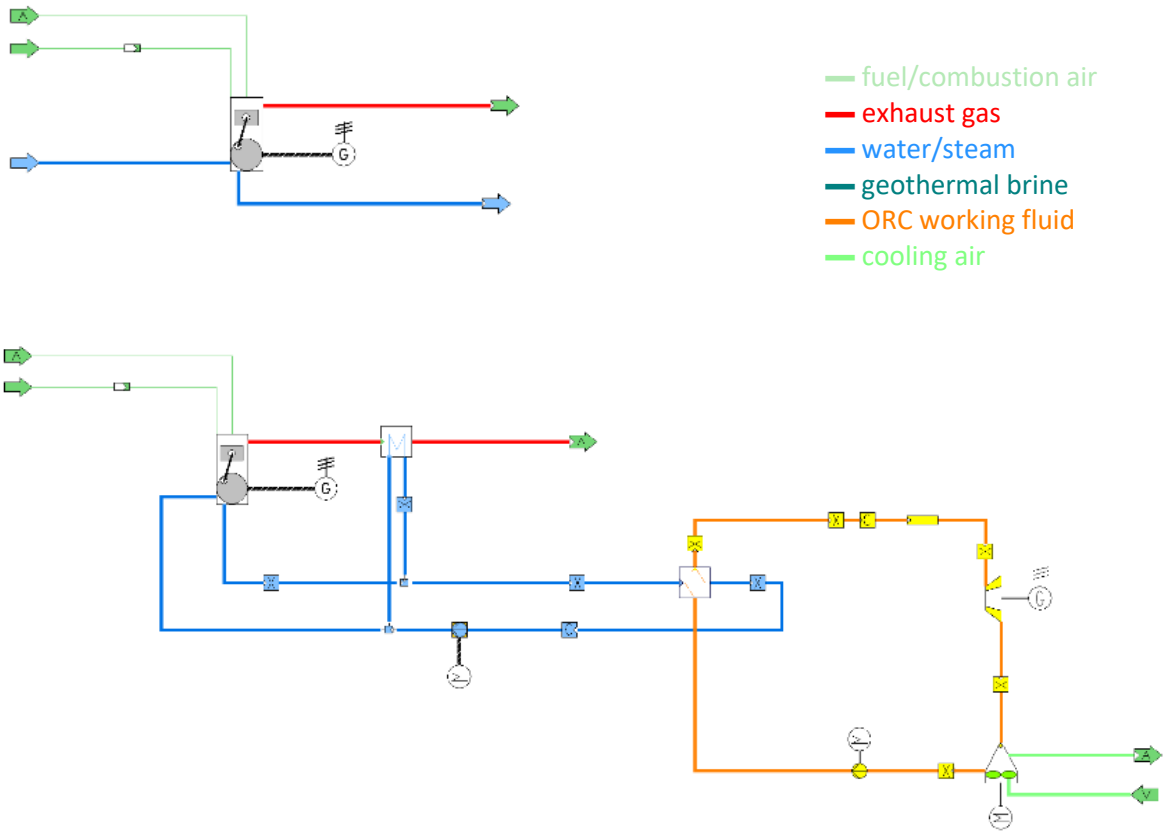

Figure 15. Standalone natural-gas reciprocating engine (top) and standalone natural-gas reciprocating engine with waste heat recovery (bottom).

The hybrid geothermal-gas reciprocating engine power plant uses similar concepts to those employed in the geo-solar hybrid plant design. The geothermal heat is used to preheat the ORC working fluid and the waste heat from the reciprocating engine is used to vaporize the ORC working fluid. This allows the ORC heat exchangers to have small MTD values while extracting the maximum quantity of heat from the geothermal fluid. The hybrid geothermal-gas reciprocating engine power plant configuration is shown in Figure 16.

As with the hybrid geo-solar plant, the ORC-bottoming cycle can continue to operate when the heat from the gas engine is unavailable. This requires the geothermal fluid to supply the heat for both preheating and vaporizing the ORC working fluid. Since the geothermal fluid flow rate is assumed to remain constant, the ORC working fluid flow rate and corresponding ORC net power generation will be reduced when only the geothermal heat source is available.

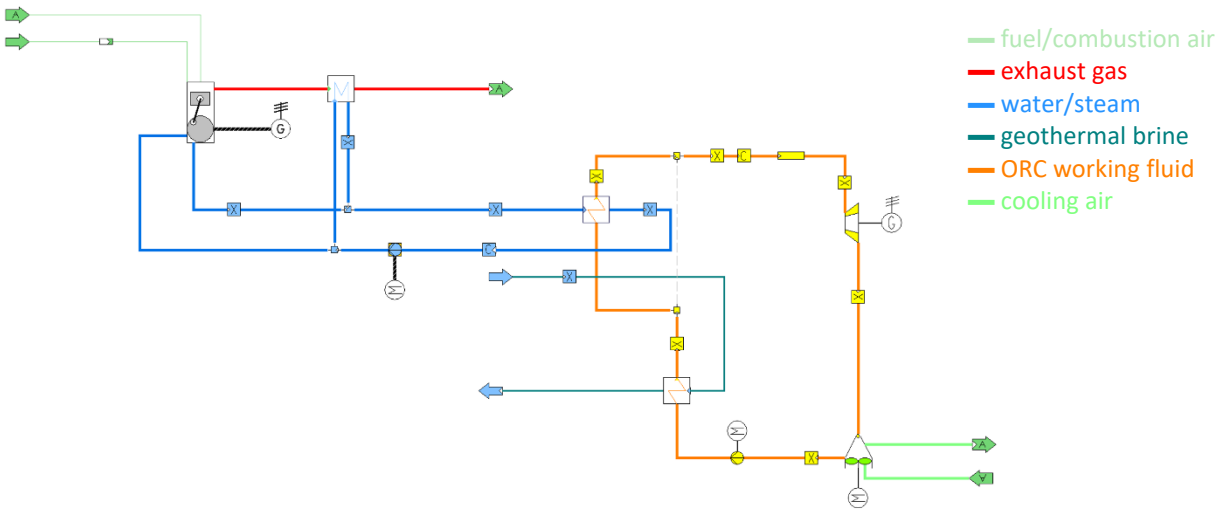

Figure 16. Hybrid geothermal-gas reciprocating engine power plant.

3.5 Triple-Hybrid Geo-Gas-Solar

Conventional natural-gas power generation cycles include natural-gas combustion turbine (NGCT) power plants and natural-gas combined cycle (NGCC) power plants. Illustrations of the NGCT and NGCC plant configurations are shown in Figure 17. NGCTs are commonly used for providing a reliable source of dispatchable power. In practice, NGCTs are typically operated during times of peak electrical power demand, especially when VRE generation sources are unavailable. NGCTs can ramp from cold shut down to full load in time periods ranging from less than 10 minutes to less than 1 hour [33]. However, NGCT operation results in CO_2 emissions on the scale of 560 kg/MWh [34]. NGCCs include equipment to recover waste heat from the gas turbine exhaust gas. The exhaust gas heat is used to vaporize steam for driving turbines in a steam Rankine bottoming cycle. NGCCs provide a more efficient method of power generation compared to NGCTs. NGCCs can be used as baseload power generators and used to complement VRE sources. NGCC operation CO_2 emissions are reported to be about 339 kg/MWh [34].

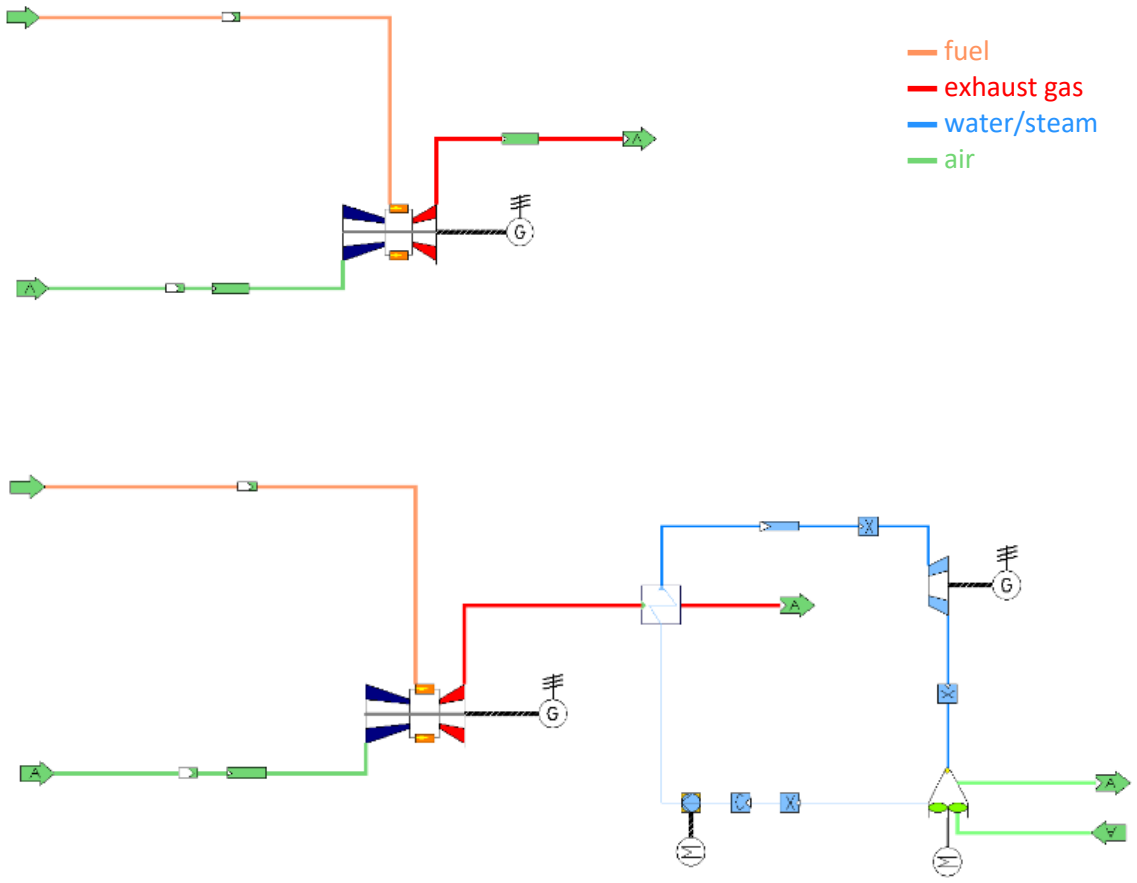

Figure 17. Standalone NGCT power plant (top) and standalone NGCC power plant (bottom)

A hybrid geothermal-gas cycle was considered to evaluate potential performance and CO_2 emissions reduction benefits. The hybrid geo-gas cycle configuration considered in this analysis is shown in Figure 18. The hybrid geothermal-gas cycle recovers heat from the gas turbine exhaust stream in a manner similar to the conventional NGCC cycle. However, in contrast with the conventional NGCC cycle, the hybrid geo-gas cycle uses a back-pressure steam turbine such that the heat rejected from the steam Rankine cycle can be transferred to an ORC-bottoming cycle. Similar to the hybrid geo-solar plant,

the ORC-bottoming cycle has a design point configuration in which the geothermal resource provides the heat to preheat the ORC working fluid while the heat rejected from the steam Rankine cycle is used to vaporize the ORC working fluid.

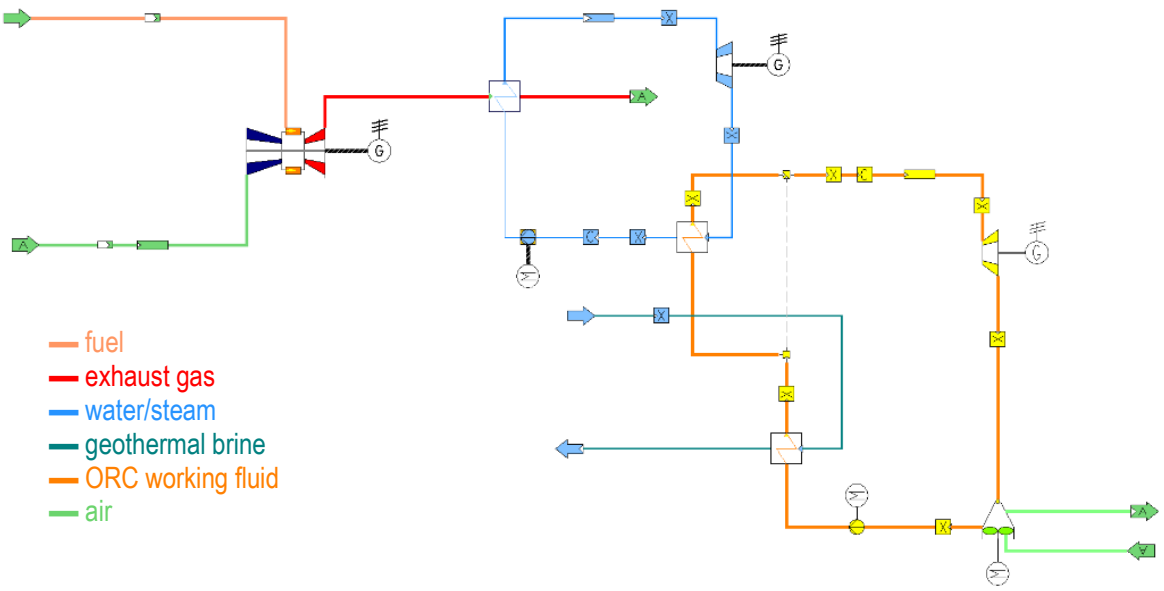

Figure 18. Hybrid geo-gas plant with steam-topping cycle and ORC-bottoming cycle

Since the hybrid geothermal-gas cycle utilizes the same steam Rankine cycle and organic Rankine cycle (ORC) configurations as the hybrid geothermal-solar cycle, a triple-hybrid plant could use heat from both solar and gas sources to augment the geothermal heat. This triple-hybrid plant configuration may be able to reduce or eliminate the amount of solar thermal energy storage required by operating the gas turbine during times when no solar resource is available, but the power demand is high.

4. Modeling Methods

Standalone and hybrid plant design and off-design models were simulated using IPSEpro V8 process modeling software [35]. Standalone (geothermal, CSP, natural-gas reciprocating engine, and natural-gas combustion turbine) and hybrid (geo-solar, geo-gas engine, and geo-gas turbine) power plants designs were established for each of the case study locations using the geothermal resource conditions specified in Section 2. Solar resource and ambient conditions were obtained using typical meteorological year data from the National Renewable Energy Laboratory (NREL) System Advisor Model (SAM). All cycle configurations use ACCs for heat rejection. The ambient design temperature was specified as 25°C for the CA, MS, and TX case study locations and 20°C for the ID case study location; these temperature specifications are higher than the median temperature at each of these locations to obtain a condenser design that will minimize power plant performance degradation during times with elevated ambient temperature. Design parameters and off-design relations are listed in Appendix A. Power plant-specific design considerations for each of the standalone and hybrid plant configurations are discussed in subsequent sections.

Off-design plant operation was simulated using IPSEpro partial load heat exchanger, turbine, condenser, etc. equipment component models to evaluate the impact of changes in the thermal resource (variation in the solar heat input and operational status of the natural-gas engine generator set were considered; the geothermal resource was assumed to be always available) and ambient temperature on plant performance.

The standalone and hybrid plant off-design net power generation data was used to create off-design performance "maps" that are interpolated to estimate plant performance as functions of resource and ambient temperature. The off-design performance maps allow the net power generation of the standalone and hybrid plants to be estimated for different combinations of resource heat input and ambient temperature without having to re-run the IPSEpro off-design simulations. This approach expedites the process of simulating hourly plant performance over extended time periods (e.g., annual simulation of power plant operation using an hourly time interval to evaluate hourly, daily, and seasonal variations in plant performance resulting from variation in the resource and ambient conditions).

Annual performance for the standalone and hybrid plants was estimated using the off-design model performance predictions (i.e., the performance map developed from the collection of off-design simulations) with the specified solar resource availability or natural-gas dispatch strategy along with historical ambient temperature data at each of the case study locations to evaluate the plant output on an hourly basis. The standalone and hybrid plant annual generation was then computed by summing the generation from each hour of the year simulated.

4.1 Plant-specific Modeling Considerations

4.1.1 Standalone Geothermal

Multiple standalone geothermal cycles were evaluated to identify the configuration with the maximal design point power generation at each of the case study locations. Configurations evaluated included single-pressure level basic (non-recuperated), single-pressure level recuperated, dual-pressure level, and supercritical ORCs. Several ORC working fluids were considered, but for the geothermal resource conditions considered in this study propane and isobutane were determined to provide near optimal performance while also having acceptable costs and low global warming potential [36]. The design point net power generation of each standalone geothermal cycle was maximized by optimizing the turbine inlet pressure. The standalone geothermal cycle configuration and working fluid selection with the greatest design point net power generation at each case study location was then selected as the baseline. The optimal standalone geothermal cycles for each case study location were determined to be the dual-pressure level isobutane configuration for the CA, ID, and TX case study locations and the supercritical propane configuration for the MS case study location.

4.1.2 Standalone CSP

The standalone CSP plant was simulated as a simplified power cycle configuration using a single heat exchanger to represent the steam generator and a single expander to represent all steam turbine stages. These simplifications were also used in the hybrid plant steam-topping cycle to provide a consistent basis for the evaluation of steam cycle performance. The CSP plant design includes use of molten salt heat transfer fluid with the heat transfer fluid (HTF) supply temperature specification of 560°C and return temperature of 300°C. The steam generator heat input is specified as 45 MW_{th} with steam turbine inlet conditions of 90 bar and 540°C. Steam has a two-phase region in which the saturated vapor entropy increases as the temperature decreases (i.e., a "wet" power cycle working fluid), such that the steam must be superheated to avoid excessive condensation within the turbine during the expansion process (see Figure 10).

The parabolic trough collectors are modeled using the SAM, which calculates the optical efficiency for each hour of the year for a given location. This is used to calculate the thermal energy generated at each hour given the solar field size, which is specified by the "solar multiple." A solar field area that corresponds to a solar multiple of one generates enough heat at nominal conditions (irradiance of 1000 W/m² and normal incidence angle) to provide the design heat to the thermal power cycle. A larger solar multiple generates too much heat at these conditions to be used by the power cycle and the excess is stored. However, solar multiples greater than one enable the system to provide the design power when the irradiance is less than the design irradiance and thus deliver rated power for a larger portion of the year.

4.1.3 Hybrid Geothermal-CSP

The hybrid geo-solar plant uses the same geothermal resource (brine temperature and flow rate) and solar resource (design point heat input) as the respective standalone plants. The hybrid plant configuration includes a steam-topping cycle configuration similar to that of the standalone CSP plant (with the hybrid plant using a back-pressure steam turbine in place of the condensing steam turbine in the standalone CSP plant) and a single-pressure level, non-recuperated ORC-bottoming cycle.

A lower bottoming cycle turbine inlet pressure specification results in more of the solar heat being converted to power via the topping cycle, while a higher bottoming cycle turbine inlet pressure specification results in more of the solar heat being used along with the geothermal heat to produce power via the ORC-bottoming cycle. The hybrid geo-solar cycle performance is optimized by selecting the ORC turbine inlet pressure that maximizes the hybrid plant net power generation. The hybrid plant can then be compared to the combined output of the standalone geothermal plant and standalone solar plant at the same location to assess the benefits of plant integration. The IPSEpro solver then calculates the topping cycle back-pressure turbine exhaust pressure as the value that satisfies the steam-to-ORC working fluid heat exchanger design specifications.

4.1.4 Hybrid Geo-Gas Reciprocating Engine

The hybrid geo-gas reciprocating engine cycle configuration involves use of waste heat recovered from the gas engine to provide the heat input to vaporize the ORC working fluid. Similar to the geo-solar hybrid plant configuration, the geothermal resource is used in the geo-gas hybrid for preheating the ORC working fluid to its bubble point. Therefore, the hybrid plant reciprocating engine and geothermal resource must be sized such that the heat available from the geothermal resource for ORC working fluid preheating is aligned with the waste heat available from the natural-gas reciprocating engine for ORC working fluid vaporization (at the specified turbine inlet pressure of the ORC-bottoming cycle). The hybrid plant natural-gas engine capacity was specified at the value that resulted in a geothermal resource flow rate equal to that for the geo-solar hybrid plant such that the geothermal resource flow rate, parasitic load, costs, etc., would be consistent for both the geo-solar and geo-gas hybrid plant analyses.

The reciprocating engine in the IPSEpro gas reciprocating engine models was based on specifications corresponding to a Jenbacher Type 6 unit [37], [38]. This unit has been deployed in both standalone installations as well as installations that utilize WHR for combined heat and power (CHP) applications [39]. In this analysis, the gas engine was only operated at 100% load or 0% load so off-design performance maps were required only for variation of the standalone gas engine w/WHR and hybrid geo-gas engine performance with respect to the ambient temperature and its effect on the heat rejection from the ORC-bottoming cycles.

4.1.5 Triple-Hybrid Geo-Gas-Solar

This system involves the addition of a topping gas turbine to the hybrid geothermal-solar hybrid plant. Therefore, the back-pressure steam turbine, ORC, and assumptions about the geothermal and solar resource are the same as previously discussed. The gas turbine is modeled in IPSEpro, as is a gas-to-steam heat exchanger (effectively a simplified Heat Recovery Steam Generator [HRSG]). The HRSG is sized so that it delivers the same thermal power to the back-pressure steam turbine as the molten-salt-to-steam heat exchanger (45 MW_{th}). Specifying the waste heat available in the gas turbine exhaust effectively fixes the power output and fuel consumption of the gas engine. In this analysis, the gas turbine was only operated at 100% load or 0% load so off-design performance maps were not required.

4.2 Cost Assumptions

Note that all costing was converted to installed costs in 2022 USD for final analysis but may be reported in its given year's USD equivalent based on the source.

4.2.1 Solar Components

The parabolic trough solar field (including collectors, heat transfer fluid system, land, and installation) is estimated as \$200/m² based on [7] in 2020 USD. For comparison, [40] CSP report estimated total cost to be \$235/m². Note, that state-of-the-art parabolic troughs use thermal oil as the heat transfer fluid, which are limited to maximum temperatures of 300–400°C. This study envisions the use of molten salts in the parabolic troughs that facilitates higher maximum temperatures (e.g. 565°C for nitrate molten salt mixtures); therefore, higher efficiencies and lower thermal storage costs. The thermal storage is estimated as \$20/kWh$_{th}$ in 2015 USD based on CSP Gen3 roadmap [41] using real installed cost numbers for a thermal system with comparable temperatures and sizing. For the solar system and topping cycle, the operation and maintenance (O&M) costs are estimated as \$66/kW$_e$-yr fixed and \$4/MWh$_e$ variable in 2018 USD based on the CSP report [40].

4.2.2 Geothermal Components

Costs for the geothermal brine extraction are based on the Geothermal Electricity Technology Evaluation Model (GETEM) [42] and are in 2010 USD. The subsurface costing includes drilling costs, equipment (including pumps and piping) to transport brine to the power cycle, and O&M costs including make up water. State taxes were not included because many states exempt renewable energy from state taxes. Inputs to this costing model include:

- Brine temperature
- Reinjection temperature
- Resource depth
- Reservoir thickness
- Flow rate per well
- Wellhead pressure
- Productivity and injectivity.

Input data for the subsurface model came from site data and design results. For productivity and injectivity, the "moderate" values from the Annual Technology Baseline were used [43]. In addition to cost, other outputs used in the analysis include the parasitic pumping power and number of wells needed.

4.2.3 Natural-Gas Reciprocating Engine Components

Natural-gas reciprocating engine gen set costs were estimated based on values reported in the U.S. EPA CHP analysis [32]. The hybrid plant analysis used the normalized capital cost reported for a large scale (~10 MW$_e$) natural-gas reciprocating engine generator in a grid interconnected CHP application since this configuration is most representative of the configuration considered in the hybrid plant analysis. The capital cost reported in the U.S. EPA CHP analysis were adjusted to 2022 USD using the Chemical Engineering Plant Cost Index (CEPCI) Annual Index [44] as basis for hybrid and standalone plant analyses.

Fixed and Variable O&M costs for the natural-gas reciprocating engine were estimated based on values reported in the U.S. Energy Information Administration (EIA) Annual Energy Outlook [45]. Hybrid plant O&M costs were assumed as the weighted average of the standalone natural-gas reciprocating engine and standalone geothermal plant O&M costs, with natural gas and geothermal thermal energy input, respectively, used as the weighting factors. The natural-gas fuel price was assumed to be \$5.5/MMBtu based on Lazard LCOE Version 11 [46]. A summary of the cost assumptions used in the natural-gas reciprocating engine gen set analysis is included in Table 3.

Table 3. Natural-gas reciprocating engine generator set cost assumptions.

Parameter	Value	Reference
Gen Set Package (2022$/kW$_e$)	827	U.S. EPA [32]
Waste Heat Recovery (2022$/kW$_e$)	252	U.S. EPA [32]
Interconnect/Electrical (2022$/kW$_e$)	36	U.S. EPA [32]
Exhaust Gas Treatment (2022$/kW$_e$)	216	U.S. EPA [32]
Labor/Materials (2022$/kW$_e$; 25% of equipment costs)	1,331	U.S. EPA [32]
Fixed O&M (2021$/kW$_e$-yr)	36.81	U.S. EIA [45]
Variable O&M (2021$/MWh$_e$)	5.96	U.S. EIA [45]
Natural-Gas Fuel Price ($/MMBtu)	5.5	Lazard [46]

4.2.4 Gas Turbine Costs

The gas turbine capital cost is estimated using data from [47] and provided in Table 4. HRSG costs are also available in that reference for HRSGs that are considerably larger than the one required in this application. Therefore, the HRSG cost is scaled using a power law with an exponent of 0.6. O&M costs are assumed to be the same as in the gas-geothermal hybrid analysis in Section 4.2.3. Natural-gas costs are obtained from the U.S. EIA [48] and are the average value paid by electric power utilities in California 2023.

Table 4. Cost assumptions for a topping gas turbine cycle.

Gas Turbine Cost Parameters		Value
Gas turbine cost	$/kW$_e$	1282
HRSG	$/kW$_{th}$	544
Fixed O&M	$/kW$_e$	36.8
Variable O&M	$/MWh$_e$	5.96
Natural gas	$/kWh$_{th}$	0.027

4.2.5 General Components

Additional components installed cost estimates include:

- Back-pressure steam turbine (with generator): $674/kW$_e$. The back-pressure steam turbine with generator cost was used for both the topping cycle and the solar standalone cycle turbine. Note, this likely underestimates the standalone solar turbine cost because it would be a condensing turbine. The installed cost for the back-pressure turbine is based on the 2016 Department of Energy (DOE) "Combined Heat and Power Fact Sheet Series" [49] and is comparable to costs in the U.S. EPA's "Catalog of CHP Technologies" [50].
- ORC turbine (with generator): $750/kW$_e$. The ORC turbine and generator cost were used for the bottoming cycle and geothermal standalone cycle. This cost is for geothermal power cycles from Black and Veatch's 2012 cost report for NREL [51].
- AspenTech, Inc. cost estimation software was used for estimating installed costs of pumps, heat exchangers, and ACCs for all cycles:
  - Pump specifications were obtained from IPSEpro simulations for each case study location evaluated. Pump costs were estimated using Aspen Process Economic Analyzer (APEA) V11 for a centrifugal pump with carbon steel casing and electric motor driver configuration [52].

- Steam Rankine cycle molten salt HTF to steam heat exchanger heat transfer areas were estimated based on an iterative script for heat transfer in/around tubes. The corresponding heat exchanger costs were estimated using APEA for a BEM Shell & Tube exchanger configuration with Hastelloy C tubes (hot side) and SS 304 shells (cold side).
- The topping cycle steam-to-ORC working fluid heat exchanger heat transfer areas were estimated based on an iterative script for heat transfer in/around tubes. The corresponding heat exchanger costs were estimated using APEA for a BEM Shell & Tube exchanger configuration with carbon steel shell and tube construction.
- Heat exchanger areas of the geothermal heat driven ORC preheater and vaporizer (standalone case studies) were calculated using AspenTech Exchanger Design and Rating (EDR) V11 software [53] for each case study location. The corresponding heat exchanger costs were estimated using APEA for a BEM Shell & Tube exchanger configuration with carbon steel shell and tube construction.
- Air-cooled condenser specifications were calculated using AspenTech EDR software for each case study location. The corresponding costs were estimated using APEA for an induced flow, finned tube multi-bay configuration with carbon steel tubes and aluminum fins.
- Capital costs estimated using APEA were adjusted to 2022 USD using the CEPCI Annual Index.

Additionally, the ORC cycle is allowed to be overrated by a maximum of 20% above its rated generator power. This is necessary because the system was designed for relatively high ambient temperature, which resulted in a large condenser and power generation significantly above the design point at low temperatures. The cost for oversizing the generator relative to the turbine is calculated using the following cost relation from Benato and Stoppato's 2019 article [54]

$$C = 40 * P^{0.67} \quad (4\text{-}1)$$

where P is the rated power in W. Additional generator cost is calculated as the cost for ORC-rated power plus 20% extra minus the cost calculated for ORC-rated power.
For the non-solar cycle and subsurface components, O&M is estimated as 2% of the capital cost, applied annually [55].

4.2.6 Combined Costs and Final Components

All the installed costs are converted to 2022 USD using the CEPCI Index. An additional 11% EPC and 7% contingency are applied [40]. Finally, the IRA investment tax credit is applied, reducing the total capital cost by 30%. Note, this has many assumptions including that the owners/financers of the project can make use of a 30% tax credit and that it is applied at the same time as the costs are incurred at the beginning of the project. All cost results presented, including LCOE, are using the 30% investment tax credit.

Thus, the final capital cost is calculated as:

$$Capital\ Cost = \Sigma(\text{installed costs in 2022 USD}) * (1 + EPC + contingency) * (1 - ITC) \quad (4\text{-}2)$$

4.3 Metrics

The capital costs and O&M costs can be annualized based on additional financial metrics. A fixed charge rate (FCR) of 6.62% was calculated based on the following assumptions (before tax incentives are applied):

- 30-year lifetime
- 2.5% inflation
- 10% IRR

- 60% debt fraction
- 8% debt interest rate
- 40% tax rate
- Depreciation table.

Thus, LCOE ($/MWh$_e$) is calculated as:

$$LCOE = \frac{CC * FCR + OM_{annual}}{AEP} \tag{4-3}$$

CC is the capital cost, O&M is the annual operating and maintenance cost, and AEP is annual energy generation.

The AEP is the sum of net energy generated over 1 year.

$$AEP = \int \left(P_{topping} + P_{bottoming} - P_{parasitics}\right) \tag{4-4}$$

The capacity factor is the ratio of the AEP to the potential AEP if rated power were produced continuously all year long.

$$CF = \frac{AEP}{\left(P_{topping,rated} + P_{bottoming,rated} - P_{parasitics,rated}\right) * 8760} \tag{4-5}$$

The revenue herein only considers revenue from selling electricity on the spot market. Note that this is not reflective of the more common nature of geothermal plants to sell to PPAs, but it does help capture the potential benefits of variable plant output. Additionally, depending on the location and market, capacity payments could be a significant portion of the revenue. Revenue is calculated herein as:

$$\text{revenue} = \int P_{net} * p \tag{4-6}$$

where P_{net} is the hourly net power produced and p is the hourly spot market price of electricity. The levelized revenue of energy (or weighted average price of energy) is then calculated as follows.

$$LROE = \frac{\int P_{net} * p}{AEP} \tag{4-7}$$

The value factor (VF) is calculated as the ratio of the weighted average price of energy to the straight average price of energy ($\bar{p}$), thus it reflects how much energy revenue a plant makes in comparison to one with continuous output. A VF above one means the plant is producing more energy at times when the price is above average, while a VF below one means the plant is producing energy at times when the electricity price is below average.

$$VF = \frac{\int P_{net} * p}{\int p} = \frac{LROE}{\bar{p}} \tag{4-8}$$

The net present value (NPV) is calculated as:

$$NPV = profit_{PV} - cost_{PV} \tag{4-9}$$

where the present value of profit is calculated as the present value of an annuity of the expected annual revenue less the expected annual O&M costs, discounted to present value via the weighted average cost of capital. The present value of cost is the expected total plant capital cost.

The benefit to cost ratio is calculated as the ratio of the present value of the annual profits over the plant lifetime to the present value of the capital cost investment.

$$BC = \frac{profit_{PV}}{cost_{PV}} \tag{4-10}$$

4.4 Annual Simulations

The annual simulations and techno-economic analysis were performed in MATLAB. A central code pulled together the following data sets for analysis:

- Local weather files for each location including direct normal insolation (DNI) and ambient air temperatures
- Local spot market electrical prices for each location
- Power cycle off-design performance map from IPSEpro simulations
- Cost and financial model inputs and assumptions.

The modeling process includes the following steps:

- Specify initial inputs
- Import datasets
- Run SAM; output the size of the solar field and thermal output hourly over a year
- Run dispatch model, hourly over a year
- Cost model and financial calculations
- Dispatch standalone cycles and compare
- Post-process.

The SAM software is used to model the parabolic trough thermal energy production and parasitic freeze protection and pumping loads for a given location's solar DNI.

The IPSEpro off-design performance map was linearly interpolated at each hour to find net power generation based on weather and chosen storage dispatch. As a comparison, a standalone solar and standalone geothermal plant with the same resources available were evaluated using the same methodology including IPSEpro cycle modeling, SAM simulation, annual dispatch, and economic analysis.

Two dispatch controllers were developed to achieve different objectives and are referred to as the "constant solar" controller and the "price-based" controller.

The "constant solar" controller is used as the baseline dispatch scheme. The objective of this controller is to continuously supply the design solar thermal energy to the hybrid plant. Thus, any excess solar thermal energy is stored in the thermal energy storage. Once the thermal energy storage is full, excess solar thermal is curtailed. Whenever solar field production drops below the design value, the thermal energy storage is discharged to provide the correct thermal input to the power cycle. This controller does not consider the timing of production of the value of electricity at the time of production.

The "price-based" controller considers the electricity prices as well as solar resource with the objective of dispatching electricity at the most valuable times to maximize the revenue. Electricity price data for each hour of the year was obtained for 2 years at each case study location from the relevant Independent System Operator. The controller uses "goals" to determine when electricity should be delivered, rather than using a sophisticated optimization scheme that would maximize revenue by

considering time-series interactions between solar, thermal storage, and electricity prices. The controller "looks" 24 hours ahead at electricity prices and solar irradiance data. The solar data is used to calculate the total solar energy that is available and the number of hours that the rated power can be delivered, $N_{available}$. Each hour is ranked by the electricity price, and the $N_{available}$ most valuable hours are given a target power output (the rated power output). The full year is then simulated, with the model dispatching the target thermal power in each hour and storing solar energy in hours where there is no target power output. If storage is full, then power is dispatched regardless of the electricity price. Therefore, this simple dispatch strategy does not consider the order that valuable hours occur in, so it is possible that energy will not have been stored in time for valuable hours. Therefore, improvements can be made to this model, but it was found to operate reasonably well.

5. Hybrid Geo-Solar Results

5.1 Design Point Results

As discussed above, the cycles were designed in IPSEpro and modified for optimal performance in each location. The solar cycle design was kept constant for each location and the geothermal flow rate and bottoming cycle size was allowed to vary to find the best combination. Additionally, the parasitic loads are different for each location. The parasitic loads on each system are very location specific. For example, the design in Idaho has the lowest parasitic loads because it has the lowest ambient air temperature and a nearly artesian geothermal well source.

Thus, the rated net power varies by location, as seen in Table 5. The design point thermal efficiencies are calculated as the ratio of net power (P) in MW_e to thermal input (Q) in MW_{th}:

$$\eta = \frac{P_{top} + P_{bottom} - P_{parasitic}}{Q_{solar} + Q_{geo}} \tag{5-1}$$

The parasitic loads as a percent of gross power production are calculated as:

$$\frac{P_{parasitic}}{P_{top} + P_{bottom}} \tag{5-2}$$

Design point parasitic loads include geothermal production and injection pumps, topping and bottoming cycle pumps, and air-cooled condenser.

Table 5. Design point power, efficiency, and parasitics at each location.

	CA	MS	ID	TX
Rated net power (MW_e)	19.1	17.4	16.1	14.2
Thermal efficiency (%)	16.7%	18.2%	21.9%	22.5%
Parasitics (%)	18.5%	15.8%	9.9%	10.5%

5.2 Off-Design Results

The off-design performance map from IPSEpro for the Elk Hills, CA hybrid geothermal-solar cycle design is shown in Figure 19. The topping cycle does not vary noticeably with ambient air temperature, thus it is only plotted with open squares based on the solar thermal input. The bottoming cycle gross power generation varies both with solar thermal input into the topping cycle (and thus heat input into the bottoming cycle) and with ambient air temperature. The most power is produced from the bottoming

cycle at times of high solar thermal input and low ambient temperature. Because this swing in potential power generation is great, the bottoming cycle generator is oversized by 20%, but then power generation is capped and not allowed to exceed that point. When there is no solar thermal input, the bottoming cycle is still able to produce some power regardless of ambient air temperature. The air-cooled condenser power setting was reduced for low temperature cases, but additional potential improvements to the condenser operation are discussed in the future work section.

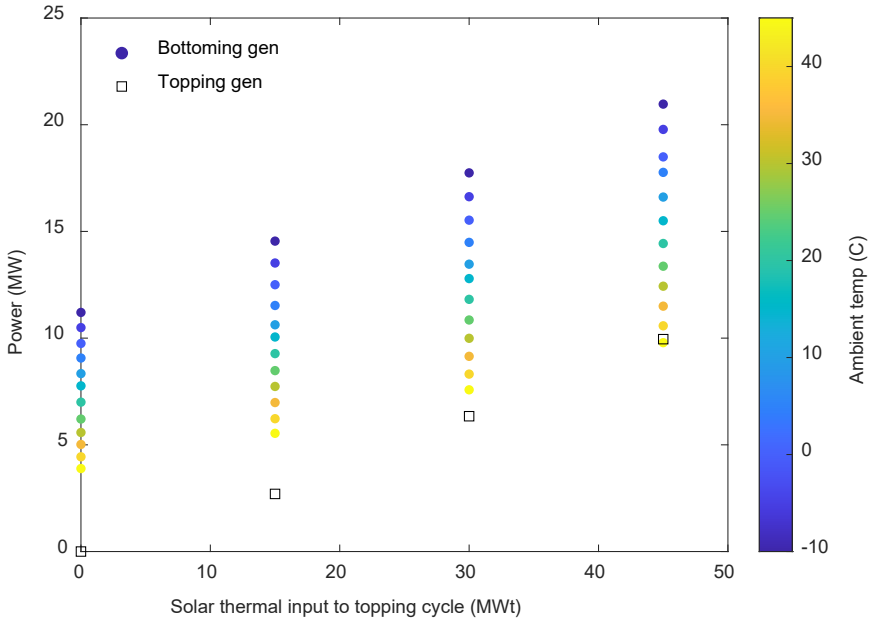

Figure 19. Off-design performance for hybrid cycle in Elk Hills, California.

The hybrid plant can be considered to have two major operating points: (1) design solar thermal energy is available and (2) no solar energy is available. When the design solar energy is available, the components operate at their design conditions (if the ambient temperature is also at the design value). When no solar energy is available, the geothermal resource must provide all the energy to preheat and vaporize the ORC working fluid. Table 6 presents the temperatures and pressures around the ORC when solar heat is and is not available, as well as energy flow information. When no solar heat is available, the geothermal fluid provides all the heat input, and due to pinch points in the vaporizer, the turbine inlet temperature reduces. As a result, the turbine inlet pressure and working fluid mass flow rate also reduce to maintain near constant volumetric flow through the turbine. Therefore, this reduces the power output of the ORC and since the cycle is operating at off-design conditions it is less efficient than a dedicated geothermal power cycle. Another significant result is that less heat is extracted from the geothermal fluid when no solar heat is available; although the geothermal mass flow rate is kept constant, the reinjection temperature increases. This feature can be exploited to enable the geothermal system to provide a level of flexibility (i.e., the geothermal energy extracted [and power generation] can be varied by the plant operator depending on the requirements of the grid). When there is a surplus of renewable energy on the grid (e.g., during daylight hours in California), geothermal power production can be reduced by not adding solar thermal energy to the geothermal cycle. When renewable generation reduces, thermal energy can be added to the ORC cycle (via the thermal energy storage), and the geothermal electricity generation can increase to meet demand.

Table 6. Comparison of state-points and performance of the hybrid plant with and without solar heat addition.

		No solar heat		Design solar heat	
		T, °C	P, bar	T, °C	P, bar
Pump inlet		36.3	4.9	45.3	6.2
Preheater inlet		37.3	18.6	47.3	31.4
Vaporizer inlet[a]		–	–	125.8	31.3
Turbine inlet		85.9	15.0	125.2	31.0
ACC		4.9	50.4	56.0	6.4
Solar heat	MW_{th}	0.0		45.0	
Working fluid mass flow	kg/s	139.8		283.7	
Geothermal heat	MW_{th}	27.7		69.5	
Production temperature	°C	135.0		135.0	
Injection temperature	°C	67.5		59.4	
Gross Electricity generation	MW_e	4.7		13.5	

[a] When no solar heat is available, the vaporizer is bypassed, and the preheater provides all the preheating and vaporization

5.3 Annual Results

5.3.1 "Baseload" Hybrid Plant

The hybrid geothermal-solar system could be designed for multiple purposes. One would be a more "baseload" operation where the solar thermal plant is large and has a long duration of storage available to provide nearly constant power output when there is ample solar resource available. An example time-series output from this type of operation is shown in Figure 20 for the Elk Hills, California design with a solar multiple of three, 12 hours of storage, and the "constant solar" dispatch operation. The solar multiple is defined in Section 4.1.2 and indicates how much larger the solar field is than a solar field that can produce the design power at nominal conditions. The solar cycle output is kept fairly constant, with dips occurring only when the topping cycle storage runs out. The bottoming cycle shows sharp dips when the topping cycle reduces power output (though it still never drops to zero output) and shows variation in power output with ambient temperature. A different controller could be used for the solar thermal storage to avoid sharp drops in power output if wanted.

For this baseload operation, all locations were given a solar multiple of three and the storage was varied to find the storage duration that minimized the LCOE. Adding some storage reduces curtailment of solar energy and increases the annual energy output, thereby reducing the LCOE. As storage continues to be added, capacity is used less frequently and may not be used at all, which increases the capital cost but not the energy output, thus increasing the LCOE. For Idaho, California, and Texas it was 12 hours, and for Mississippi it was 10 hours.

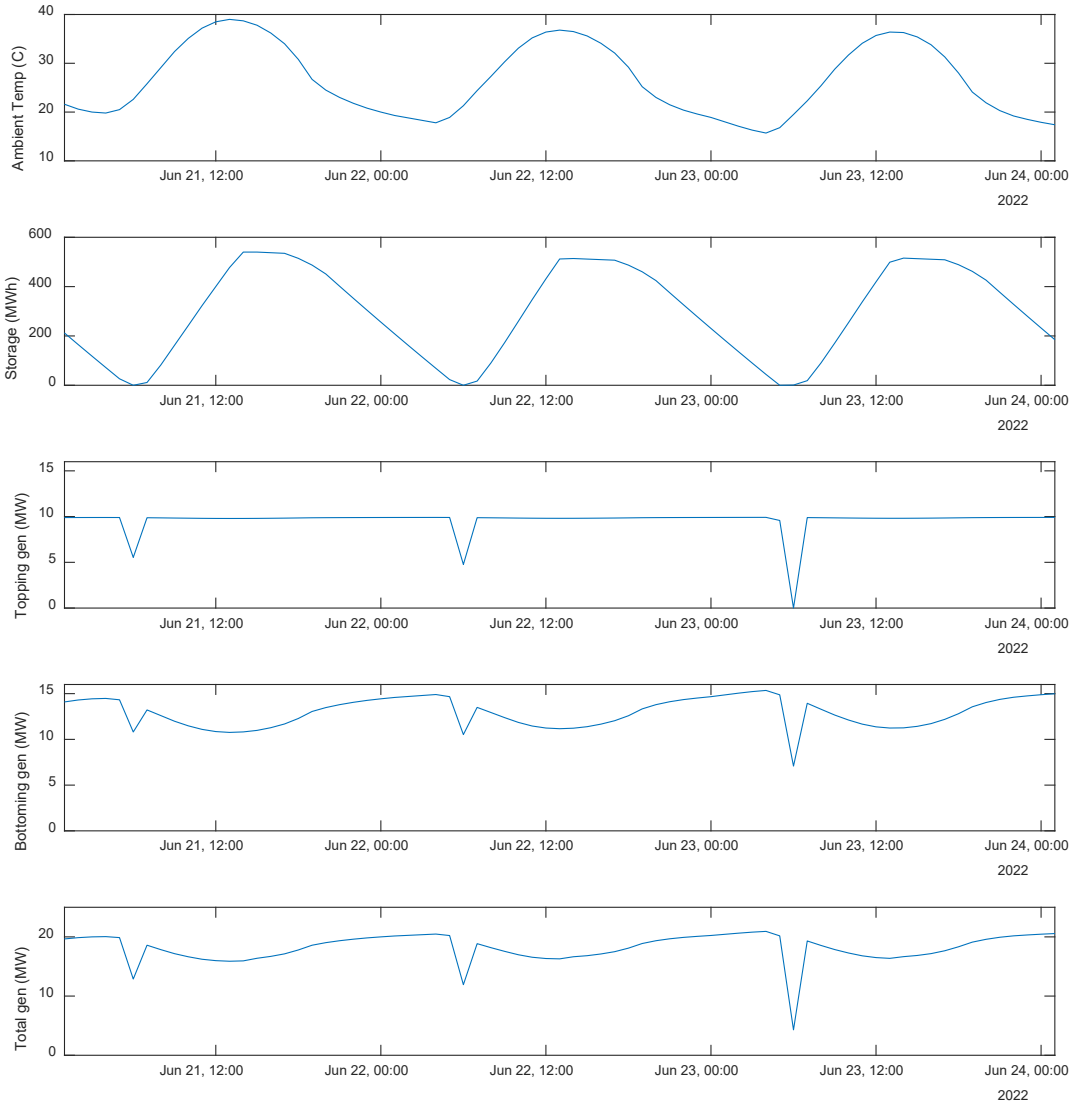

Figure 20. Example summer series performance of hybrid cycle in Elk Hills, California with a solar multiple of 3 and 12 hours of storage.

The annual results for the four locations are shown in Table 7 for 2021. Additional results and a detailed comparison to the standalone cycles can be found in Appendix B.

Table 7. Annual simulation results for 2021 for four locations for hybrid geo-solar cycle.

	CA	TX	MS	ID
Solar multiple	3	3	3	3
Storage discharge duration (h)	12	12	10	12
Geothermal brine temperature (°C)	135	96	127	108
Annual energy production (MWh_e)	115,516	75,227	74,514	69,051
Capacity factor	0.70	0.61	0.49	0.49
Capital Cost ($MM)	$138.81	$109.43	$118.38	$121.39
O&M Cost ($MM/yr)	$2.50	$2.23	$2.06	$2.23
Revenue ($MM/yr)	$5.67	$5.42	$2.63	$2.83
LCOE ($/$MWh_e$)	$98.22	$125.88	$132.84	$148.60
LROE ($/$MWh_e$)	$47.61	$71.99	$35.29	$41.04
VF	0.97	0.51	1.07	1.02
NPV ($MM)	-$85.91	-$56.06	-$108.89	-$111.22
Benefit / cost ratio	0.38	0.49	0.08	0.08

A standalone geothermal and standalone CSP plant were used for comparison against the hybrid plant. Detailed breakdowns for the standalones and the standalones combined can be found in Appendix B. The monthly energy production from each plant is compared in Figure 21 for the four locations. Many different trends from the different cycles are shown. The locations with low geothermal resource temperature show very little energy each month from the geothermal-only plant, while the locations with low solar resource show reduced energy from the solar-only plant. The reduction in energy from the solar-only plant in the winter is noticeable in all locations, but it is particularly clear in the low solar locations. Additionally, all locations show a reduction in geothermal-only power production in the summer due to increased ambient temperatures. The hybrid plant tends to have a higher AEP than the combined output of two hybrid plants, being 2.9%, 4.2%, and 4.1% greater in California, Mississippi, and Idaho, respectively. However, in Texas, the hybrid AEP was 4.2% lower than the two standalone plants.

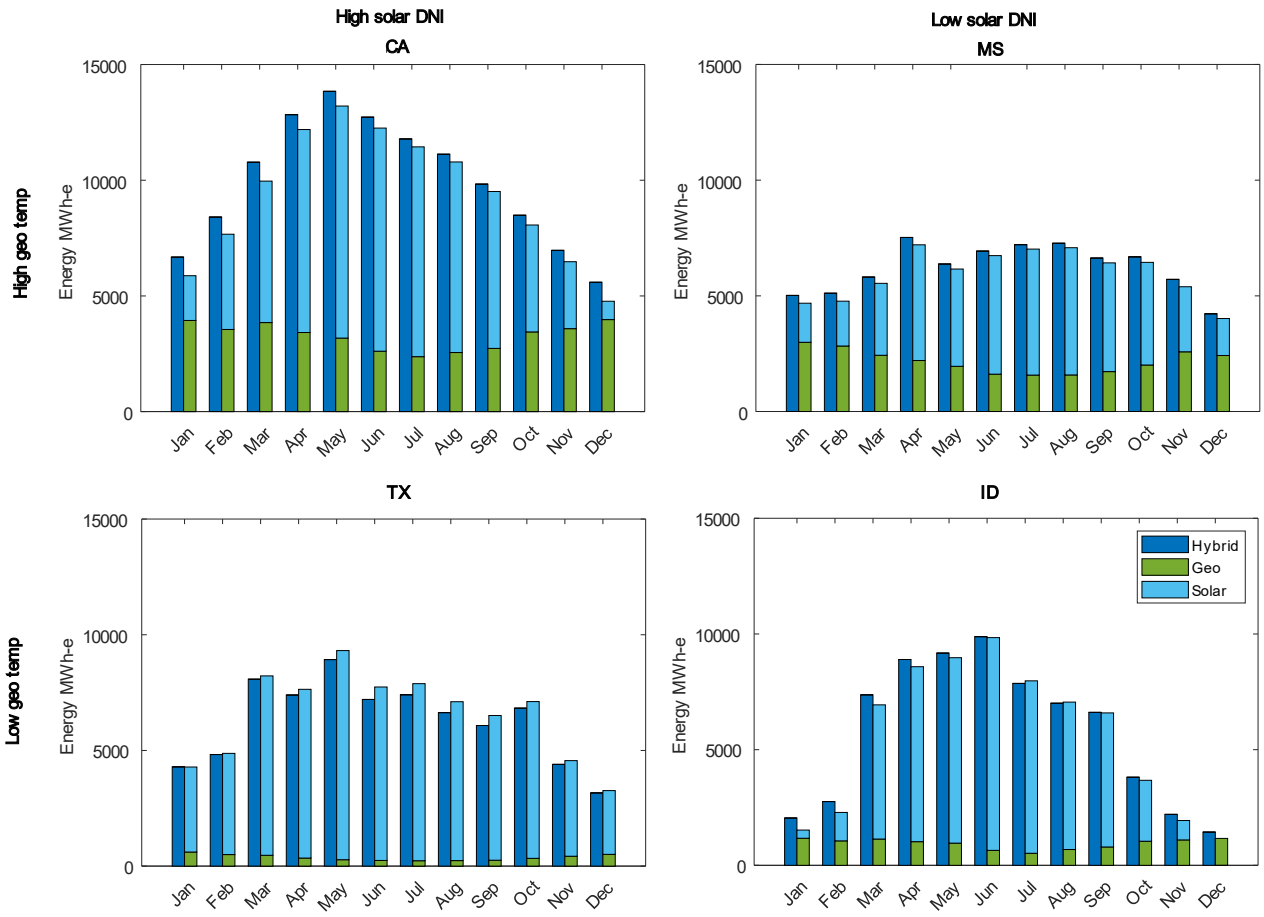

Figure 21. Monthly energy generation from standalone plants versus hybrid plants.

5.3.1.1 Baseload Design Cost Sensitivity and Comparison

The sensitivity of the total system cost and LCOE was investigated by considering changes to individual component costs. This analysis was performed for the baseload case, but similar trends would be expected from the peaking systems. A tornado chart of the results is shown in Figure 22 for Elk Hills, California. Each cost was varied by +/- 50% from the estimated value for this system. The geothermal wells and solar field are the biggest contributor to cost and thus have the highest impact when their costs are increased or decreased. Operations and maintenance are also a significant cost where improvements can be made and which requires improved estimation. Notably, the heat exchanger costs may be overestimated for this design and the 50% reduction may be likely. A 50% reduction in heat exchanger cost would reduce the LCOE in this location from \$98/MWh$_e$ to \$93/MWh$_e$.

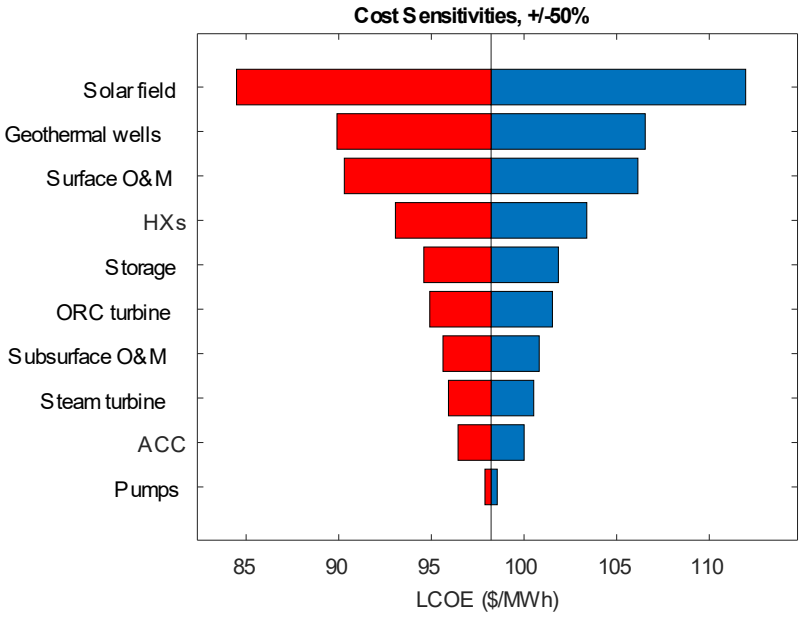

Figure 22. Tornado chart for cost sensitivities and impact on LCOE for Elk Hills, California design with SM = 3 and hours = 12.

The major capital cost components are compared between the hybrid geo-solar and geothermal-only and solar-only plants in Figure 23. Some components have the same cost because they were kept constant (e.g., the solar field and geothermal wells), while other components varied based on the cycle design (e.g., heat exchangers and pumps). The geothermal wells and solar field are notably the most expensive components. One striking difference in costs is for the heat exchangers. The hybrid design resulted in a an extremely large cost for the heat exchangers, particularly the oversized preheater. The preheater cost could be reduced using a larger minimum internal temperature approach (MITA) design specification value, although this would decrease the quantity of heat the preheater could extract from the geothermal fluid and impact the hybrid cycle performance accordingly.

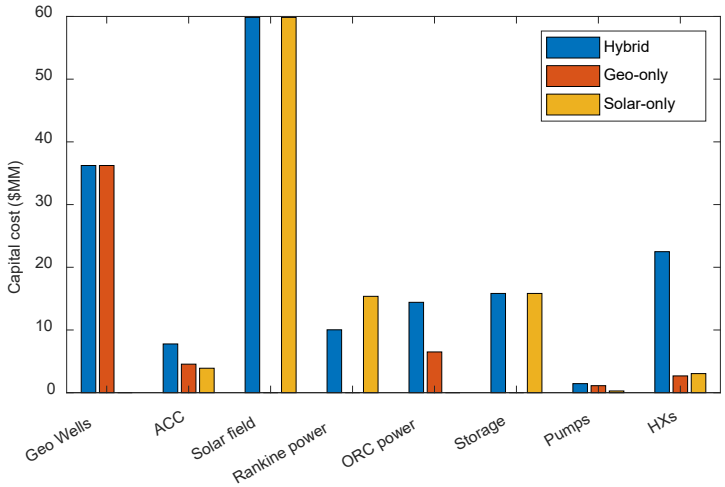

Figure 23. Capital cost components compared between standalones and hybrid system for Elk Hills, California design with SM = 3 and hours = 12.

The LCOEs for the standalone plants combined and the hybrid plants are compared in Figure 24 for all four locations. The components that contribute to the total LCOE are broken down in order by colored sections. While there is some variation in energy production between the combined standalones and the hybrid plant, the main differences come from cost.

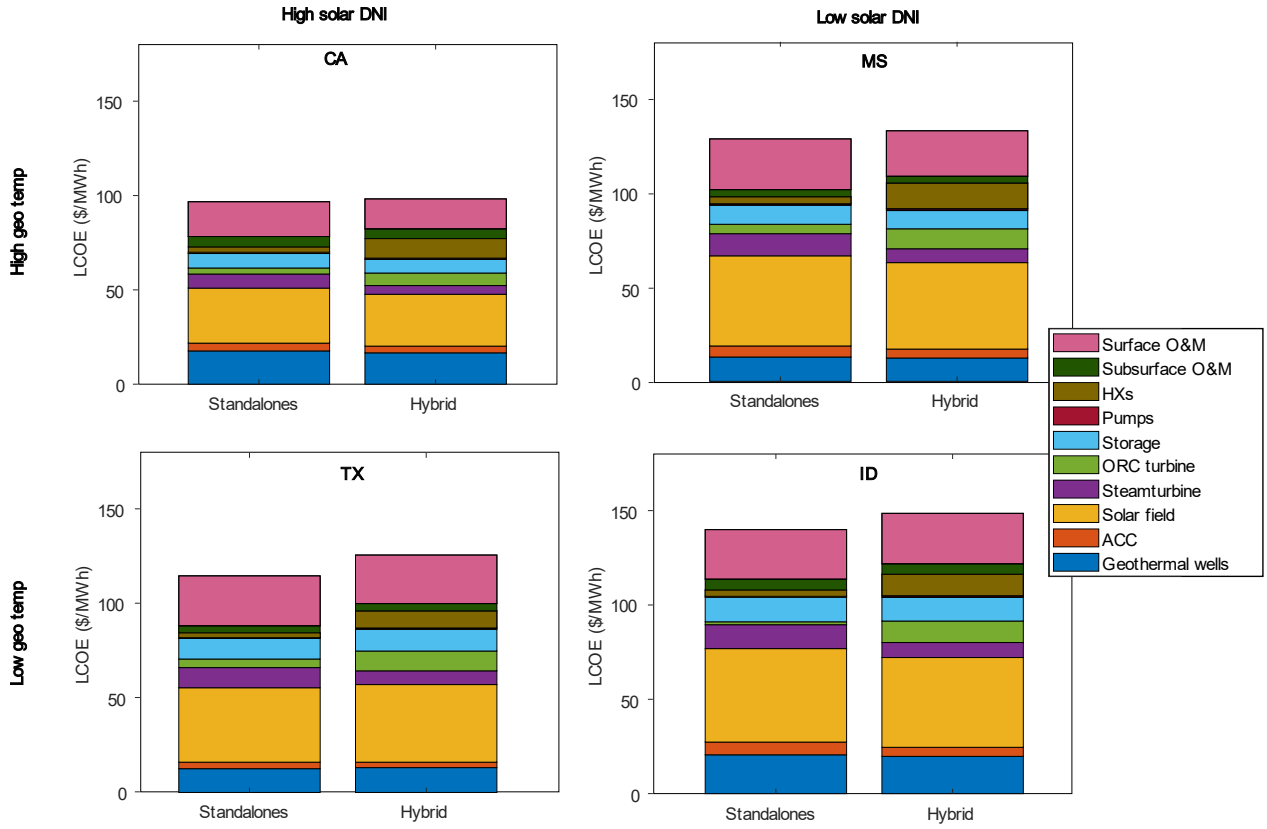

Figure 24. LCOE components for standalones versus hybrid cycle designs for each location.

The location with both high solar and geothermal resources has the lowest LCOE, while the location with the lowest resources has the highest LCOE. This is true both for the hybrid geo-solar system and the standalones combined. The costs are similar between the standalones and the hybrid system for each location, though the value in terms of both revenue and benefit to the grid may vary. There are additional challenges and complexities of the hybrid system design as well.

5.3.2 "Peaking" Hybrid Plant

The hybrid plant can also be designed to deliver power at more strategic, valuable times and a price-based dispatch strategy is used. These peaking systems have a smaller solar field compared to the baseload design, with a solar multiple of 1.5. The thermal storage has discharging durations of 8–10 hr enables the system to store large amounts of solar energy during the day when electricity prices tend to be lower. The thermal storage is then discharged when electricity prices are high, which is typically during the late afternoon, early evening, and early morning. Due to the use of a geothermal resource, these systems do deliver some energy at all times. But the strategic use of solar energy modulates the energy extracted from the geothermal resource, and the electricity delivered due to geothermal. More energy is extracted from the geothermal fluid when solar heat is added to the bottoming ORC cycle. Therefore, this hybrid peaking cycle facilitates a level of dispatchability from a fixed geothermal resource.

As an example, consider the average daily energy profiles for the Elk Hills, California location, as shown in Figure 25 (profiles for other locations are provided in Appendix C). Average electricity price profiles are also displayed that show that there is typically a spike in prices early in the morning (5:00–8:00 a.m.) and a larger spike in the late afternoon (~6:00 pm). Prices tend to be lowest during the middle hours of the day when there is an abundance of solar energy from photovoltaics being delivered to the grid. These trends are observed for all months of the year, although the magnitude of the price variations is largest during the spring and summer months. Similar trends, particularly the existence of a late-afternoon price spike, may be observed for each of the locations considered, see the figures in Appendix C. Figure 25 demonstrates the application of the price-based dispatch strategy. Solar energy is typically not dispatched during daylight hours (with the exception of avoiding curtailment), so the only electricity dispatched in low-priced hours is due to geothermal power. The solar energy is then dispatched early morning and late afternoon to coincide with the electricity price spikes. This also leads to an increase in the energy dispatched from the bottoming cycle, partly due to the increased thermal input from the back-pressure turbine exhaust, and partly from the increased thermal energy extracted from the geothermal resource.

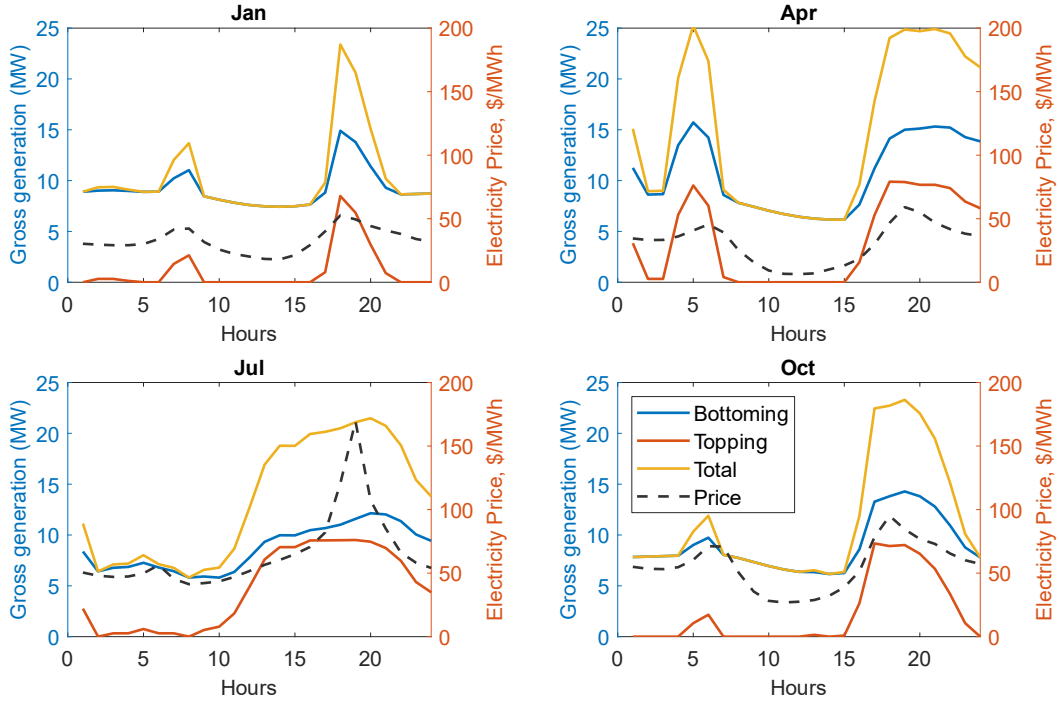

Figure 25. Average daily power and electricity price profiles for 4 months in Elk Hills, California, 2021.

These trends can be observed in more detail by considering the heatmap in Figure 26, which shows the electricity price and energy delivered for every hour of the year. Days of the year are plotted on the x-axis, while the y-axis shows the hour of that day. Darker colors correlate to higher electricity prices and power outputs. The heat map is useful for showing trends as well as the granular detail of unusual events that average profiles do not capture as well. For example, the heatmap also displays the higher prices and energy delivery that occurs early morning and late afternoon. It also shows an unusual pricing event in February in which higher-than-expected prices were observed for several days, mainly overnight.

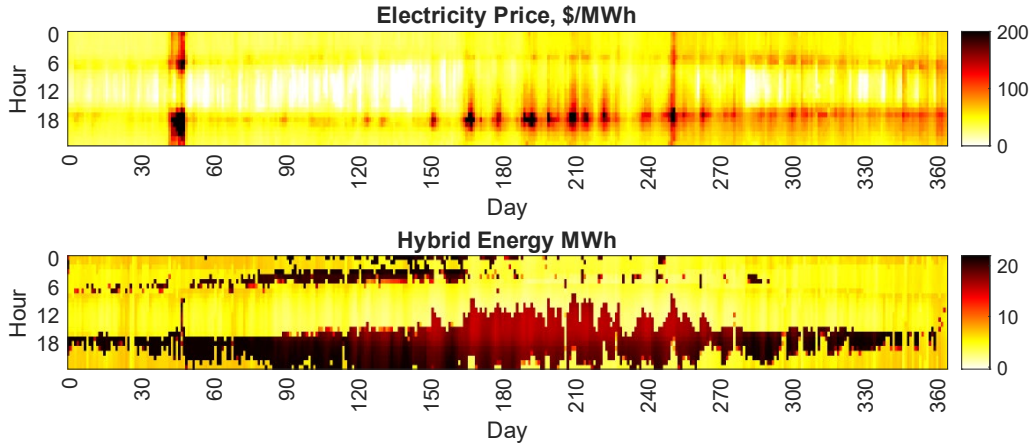

Figure 26. Heatmap showing electricity price and hybrid power plant energy output for each hour of the year in Elk Hills, California, 2021.

Figure 27 shows a heatmap of the bottoming ORC with the objective of illustrating the dispatchable nature of this hybrid plant design. The bottoming cycle energy output is normalized by the value at the design point, which enables a comparison of the dispatch profile with a standalone geothermal power plant operating with the same geothermal resource. The energy output from the bottoming cycle is a function of primarily two factors: the ambient temperature and the solar heat input, which itself is a function of the electricity price when using price-based dispatch. The standalone geothermal power output is affected only by the ambient temperature so that the largest energy output occurs overnight during the winter months when ambient temperatures are low and the plant power output can exceed the design capacity. While the standalone geothermal plant can fortuitously dispatch more energy at some high-value times, such as early in the morning and later in the evening in the autumn and winter months, the power output is reduced during the most valuable times, which occurs late afternoon in the summer. At these times, ambient temperatures are still high enough to reduce the geothermal power output. In comparison, the bottoming cycle of the hybrid plant increases its power output at these most valuable times due to its integration with the solar topping cycle and thermal energy storage. Therefore, these graphs demonstrate how hybridization with solar enables a fixed[a] geothermal resource to be operated in a dispatchable manner.

[a] By "fixed," we mean the geothermal temperature and flow rate is kept constant. But the injection temperature varies depending on the additional solar heat added to the bottoming cycle, thereby extracting more or less energy from the geothermal resource.

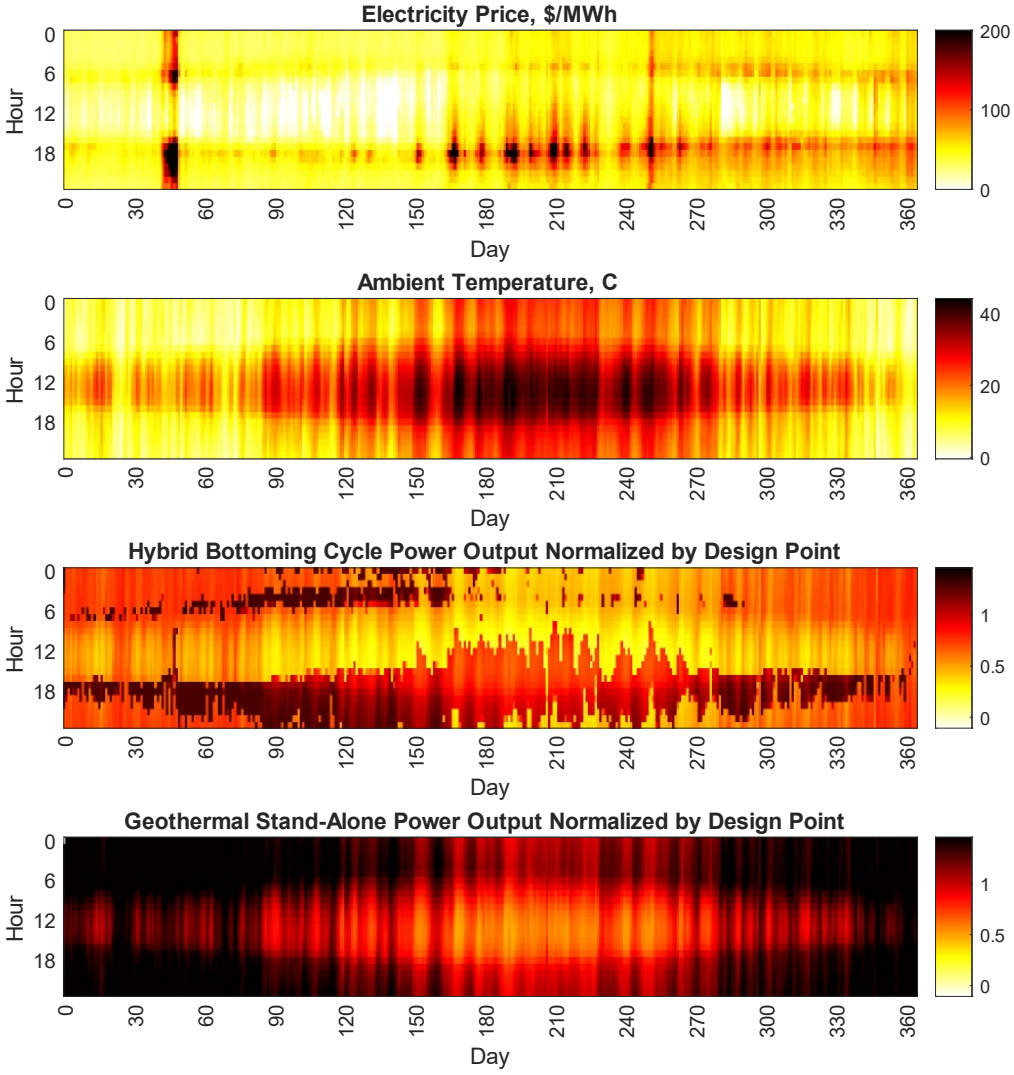

Figure 27. Heatmaps showing hourly values of electricity price, ambient temperature, energy output from the bottoming cycle (normalized by the design value), and energy output from a standalone geothermal plant (normalized by the design value). Results are for Elk Hills, California, 2021.

Financial results are provided in Table 8. As would be expected, compared to the baseload plant results in Table 7, the peaking plant produces less annual energy and has a lower capacity factor, due to the smaller field. Consequently, the annual revenue is also reduced. However, this revenue is earned at higher-value times, which can be seen by considering that the peaking plant achieves a higher VF than the baseload plant. Alternatively, the peaking plant AEP is 70% of the baseload plant, but the revenue is 80% for California, which demonstrates that the energy is delivered at high-value times. As would be expected, the LCOE is higher for the peaking plant because fixed investments, such as the power cycles and heat exchangers, are used less (due to the lower capacity factor). However, LCOE is not the best metric for dispatchable plants and instead metrics such as the levelized revenue of electricity (LROE) and VF demonstrate the value proposition of the peaking hybrid plant.

Full results that compare the hybrid plant output to two standalone plants are provided in Appendix C. In these results, the standalone solar thermal plant is also operated with the price-based dispatch scheme to ensure a fair comparison. It is challenging to make definitive statements about the benefit of the hybrid system compared to standalone systems operating with price-based dispatch due to large variations in electricity prices which has a significant impact on revenues and other financial metrics. For example, the hybrid revenue increased from $4.5M to $7.2M from 2021 to 2022 in California. Therefore, fair evaluation of these systems requires electricity prices and dispatch over the full lifetime of the plant to be estimated.

Some general conclusions can be drawn despite the limitations and uncertainty of the data. The California hybrid plant generally produces more energy, generates more revenue, and has a higher VF than two combined standalone plants. However, the capital cost and LCOE are also higher, while the NPV is worse. These trends are also true in Mississippi and Idaho. However, the margin in revenue is best in California. Results indicate that the hybrid peaking plant performs worse in Texas than combined standalone plants, as the AEP is reduced, which reduces the revenue. Despite this, the hybrid VF is larger, which demonstrates the dispatch scheme operates well even though the delivered energy has reduced.

Table 8. Annual simulation results for 2021 for four locations for hybrid geo-solar cycle. Each location uses a solar multiple of 1.5 and 8 hours of storage (except California, which uses 10 hours)

	CA	TX	MS	ID
Annual energy production (MWh_e)	80,946	37,324	50,823	41,109
Capacity factor	0.49	0.30	0.34	0.28
Capital Cost ($MM)	$111.90	$80.76	$90.33	$92.09
Revenue ($MM/yr)	$4.54	$3.57	$1.89	$1.89
LCOE ($/$MWh_e$)	$120.75	$198.40	$156.38	$199.54
LROE ($/$MWh_e$)	$56.08	$95.52	$37.26	$45.90
VF	2.47	1.39	4.73	4.94
NPV ($MM)	-$75.57	-$55.57	-$91.59	-$95.79
Benefit/cost ratio	0.32	0.31	-0.01	-0.04

6. Hybrid Geo-Gas Reciprocating Engine Results

A case study analysis of the hybrid geothermal – natural-gas reciprocating engine plant design was performed using the geothermal resource and ambient conditions associated with the Elk Hills, California case study location. Based on the geothermal resource assessment, the Elk Hills geothermal resource temperature is estimated as 135°C.

6.1 Design Point Results

Four separate power plant configurations were considered. These configurations include the standalone natural-gas reciprocating engine without WHR, standalone natural-gas reciprocating engine with WHR, standalone geothermal power plant, and hybrid geothermal-natural-gas reciprocating engine power plant. As described in Section 3.4, the hybrid plant uses geothermal heat to preheat the ORC-bottoming cycle working fluid and natural-gas engine waste heat to vaporize the ORC-bottoming cycle working fluid. The standalone plants were assumed to use a geothermal resource and gas engine configuration equivalent to that used for the hybrid plant analysis. Performance and cost analyses were performed for each plant configuration with the results used to inform comparisons between the hybrid plant versus the combined standalone plants. Since two standalone gas engine configurations were considered (i.e., with and without WHR), results are provided for two standalone gas + geothermal cases.

The hybrid plant natural-gas engine capacity was specified at the value that resulted in a geothermal resource flow rate equal to that for the geo-solar hybrid plant such that the geothermal resource flow rate, parasitic load, costs, etc., would be consistent for both the geo-solar and geo-gas hybrid plant analyses. This specification resulted in a natural-gas reciprocating engine with a large capacity (~50 MW_e), which is assumed to be provided using multiple ~10 MW_e reciprocating engine units operating in parallel. The natural-gas reciprocating engine capacity specified for the hybrid plant was also used in the standalone gas engine simulations. Similarly, the geothermal resource flow rate and temperature specifications used for the hybrid plant were also used for the standalone geothermal plant simulations.

Table 9. Summary of standalone (SA) and hybrid power plant design point operation.

	SA recip gas engine w/o WHR	SA recip gas engine w/WHR	SA geo	Hybrid geo-WHR	
Plant design capacity	49.5	55.2	4.2	61.6	MW_e
NG recip engine capacity	49.5	49.5	–	49.5	MW_e
NG fuel flow rate	2.6	2.6	–	2.6	kg/s
NG fuel LHV	48,300	48,300	–	48,300	kJ/kg
Heat rate	8750	8750	–	8750	BTU/kWh_e
NG fuel thermal input	126.8	126.8	–	126.8	MW_{th}
Geothermal heat input	#N/A	#N/A	63.4	76.3	MW_{th}

6.2 Off-Design Behavior

Power cycles that include ORC cycles (i.e., the standalone gas engine with WHR, standalone geothermal plant, and hybrid geo-gas plant) are impacted by changes in the ambient temperature. When the ambient temperature is elevated the working fluid condensing pressure increases; this increase in the ORC turbine back-pressure reduces the power generation of the ORC-bottoming cycle.

Figure 28 illustrates the net power generation versus time for the standalone gas engine w/WHR, standalone geothermal plant, and hybrid geo-gas cycle during a 1-week time period in July at the Elk Hills, California case study location with a natural-gas engine dispatch schedule specified as daily from 6:00 p.m. to 10:00 p.m., which is a time in which fossil generators are often dispatched to meet end-of-day power demand as the sun sets and PV solar generation ramps down. Note that since all these plant configurations include an air-cooled condenser, they each illustrate increasing power output with lower ambient temperature and decreasing power output with higher ambient temperature.

It can be observed from Figure 28 that the hybrid plant power generation is less than that of the standalone geothermal plant when only the geothermal resource is available. This illustrates that the hybrid plant ORC is not optimized for operation using only the geothermal resource. When the gas engine waste heat is not available the ORC-bottoming cycle operates at conditions that deviate significantly from its design point. In turn, the performance of the individual equipment components within the ORC-bottoming cycle is impacted (the heat exchangers extract less heat from the geothermal brine, the decreased ORC working fluid flow rate reduces the efficiency of the ORC turbine, etc.). Therefore, the hybrid plant ORC-bottoming cycle design is a possible area for future study, in which use of supercritical or dual-pressure level bottoming cycles could be considered to improve bottoming cycle performance when heat input from the gas engine is not available.

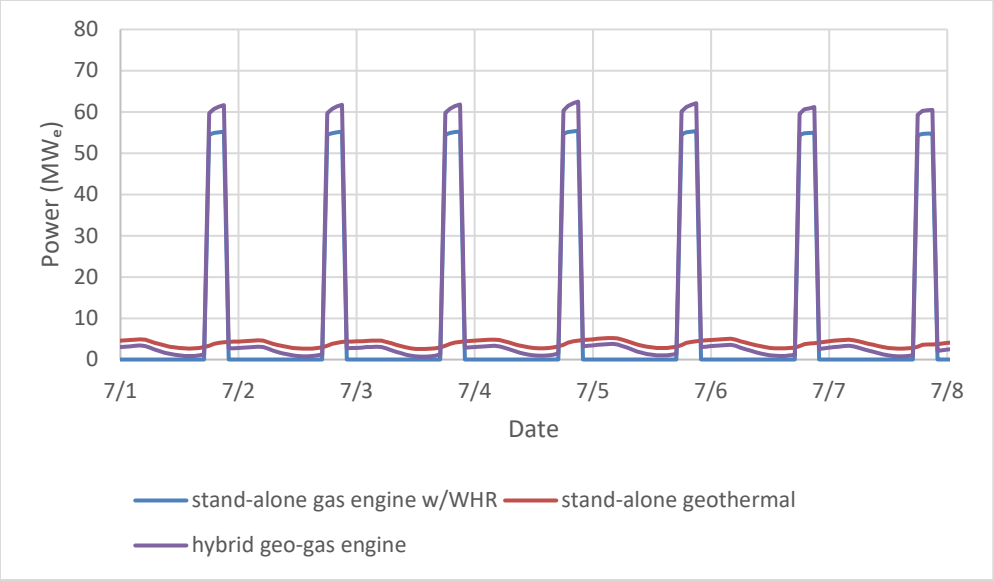

Figure 28. Standalone gas engine, standalone geothermal, and hybrid geo-gas-cycle net power generation at Elk Hills, CA case study location during a sample one-week period with gas engine operated daily between the hours of 6:00 p.m. and 10:00 p.m.

6.3 Annual Results

Standalone and hybrid power plant simulations were performed for the Elk Hills, California case study location. The annual simulations include calculation of the net power generation of each power plant type on an hourly time interval using Elk Hills, California historical ambient temperature data along with the specified geothermal resource temperature of 135°C.

Both power plant configurations that include geothermal heat input (standalone geothermal plant and hybrid geo-gas plant) were assumed to utilize the geothermal resource on a 24/7 continuous basis. The standalone geothermal power plant's hourly power output varies with the ambient temperature as described above. The hybrid geo-gas power plant's hourly power output varies with the ambient temperature as well as the availability of waste heat input from the natural-gas reciprocating engine.

The annual simulations investigated a range of natural-gas reciprocating engine operating capacity factors. Scenarios in which the natural-gas reciprocating engine was operated from 2 hours per day to 24 hours per day were evaluated. During the hours in which the reciprocating gas engine operation was not dispatched, the standalone gas engine-based plant configurations (i.e., the reciprocating gas engine power plants with and without WHR) have zero net-power output. As noted above, the hybrid geo-gas plant was assumed to continue operating using geothermal heat only during periods in which waste heat from the gas engine was not available.

A summary of the power generation performance and costs associated with each of the plant types considered is included in Table 10 for the scenario in which the gas engine is operated continuously on a 24/7 schedule. This scenario represents use of a distributed natural-gas generator providing baseload generation in poor grid quality geographies or remote locations [46]. In this scenario the hybrid geo-gas plant provides the highest net power generation and lowest normalized CO_2 emissions at an LCOE comparable to that of the standalone natural-gas reciprocating engine gen sets (both with and without WHR).

Table 10. Standalone (SA) reciprocating gas engine (without and with WHR), standalone geothermal plant, and hybrid geo-gas plant annual simulation results for Elk Hills, CA case study in which all plants operate in baseload mode (24/7 utilization of gas engine and geothermal resource).

	SA recip gas engine w/o WHR	SA recip gas engine w/WHR	SA geo	Hybrid geo-gas WHR	
Design point net power output	49.5	55.2	4.2	61.6	MW_e
CAPEX	$67,701,084	$94,591,124	$49,284,690	$151,969,674	
Fixed O&M	$1,820,324	$2,030,108	$601,524	$4,731,013	$/yr
Variable O&M	$2,581,864	$2,910,091	$49,467	$2,306,020	$/yr
Fuel cost	$20,846,709	$20,846,709	$0	$20,846,709	$/yr
Annual generation	433,199	488,270	40,882	552,319	MWh_e
LCOE	$68.63	$65.64	$95.73	$68.70	$/MWh_e$
CO_2 emissions	227,650,500	227,650,500	0	227,650,500	kg CO_2/yr
Normalized CO_2 emissions	526	466	0	412	kg CO_2/MWh_e

Table 11 provides a comparison of the annual power generation, LCOE, and normalized CO_2 emissions of the hybrid geo-gas plant versus the combined standalone gas engine w/WHR plant plus the standalone geothermal plant versus the combined standalone gas engine w/o WHR plant plus the standalone geothermal plant. This comparison assumes baseload operation of all plants (i.e., 24/7 utilization of both the gas engine and the geothermal resource). The table indicates that the hybrid plant provides greater generation than the combined standalone geothermal and standalone gas engine plants (both for gas engines with and without WHR). Additionally, the normalized CO_2 emissions of the hybrid are lower than the combined standalone gas and geothermal plants. The hybrid plant LCOE is slightly lower than the LCOE for the combined standalone geothermal plant and standalone gas engine w/o WHR. The hybrid plant LCOE is slightly higher than the LCOE for the combined standalone geothermal plant and standalone gas engine w/WHR. However, in both cases the difference between the LCOE for the hybrid plant and combined standalone plants is within the margin of error associated with these estimates.

Table 11. Comparison of LCOE and CO_2 emissions of hybrid plant relative to combined standalone (SA) geothermal and standalone gas plant for Elk Hills, California case study in which all plants operate in baseload mode (24/7 utilization of gas engine and geothermal resource).

	SA Gas w/o WHR + SA Geo	SA Gas w/WHR + SA Geo	Hybrid Geo-Gas WHR	
Annual generation	474,080	529,152	552,319	MWh_e
LCOE	$70.97	$67.96	$68.70	$/MWh_e$
CO_2 emissions	480	430	412	kg CO_2/MWh_e

In addition to the baseload operation mode, the operation of the hybrid and combined standalone geothermal and gas plants were evaluated for simplified dispatchable gas engine get set operating scenarios. The annual generation, CO_2 emissions, and LCOE of the hybrid and standalone plants was computed as a function of the number of hours per day that the gas gen set is operated. In these simplified scenarios, the gas gen set is assumed to startup at midnight and run for the specified number of hours before shutting down. This dispatch schedule is assumed to repeat during every day of the annual simulation independent of seasonal energy demand, energy pricing, or ambient temperature conditions.

Figure 29 provides a comparison of the hybrid geo-gas with the combined standalone plant annual generation as a function of the number of gas engine gen set dispatch hours per day. This figure illustrates that all configurations achieve increased annual power generation with increasing hours of daily gas engine gen set dispatch. Figure 30 presents the hybrid geo-gas plant generation versus the combined standalone geothermal and standalone gas gen set generation on a relative basis. This figure indicates that the hybrid geo-gas power plant provides more annual power generation than the combined annual power generation from the standalone geothermal plant and standalone gas engine gen set w/o WHR when the gas engine is dispatched for more than about 3 hours per day. Similarly, the hybrid geo-gas power plant provides more annual power generation than the combined annual power generation from the standalone geothermal plant and standalone gas engine gen set w/WHR when the gas engine is dispatched for more than about 8 hours per day.

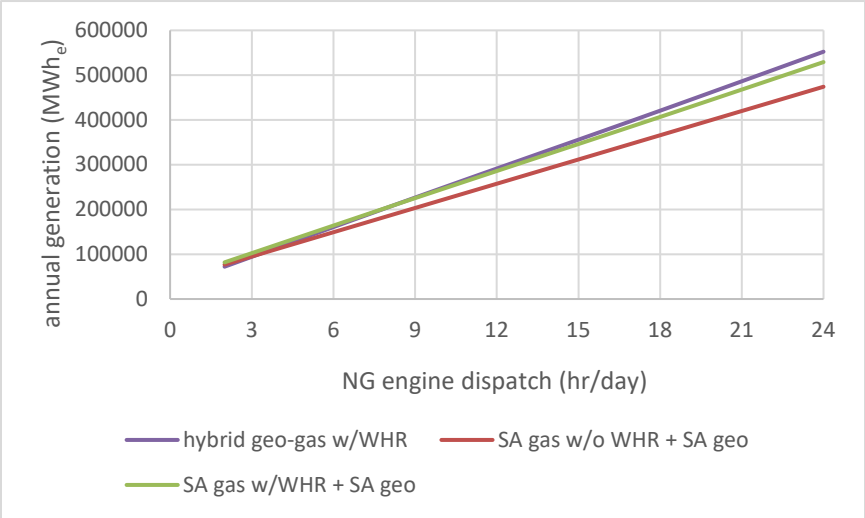

Figure 29. Comparison of annual power generation for hybrid geo-gas versus sum of standalone geothermal and gas plants based on Elk Hills, California resource and ambient conditions.

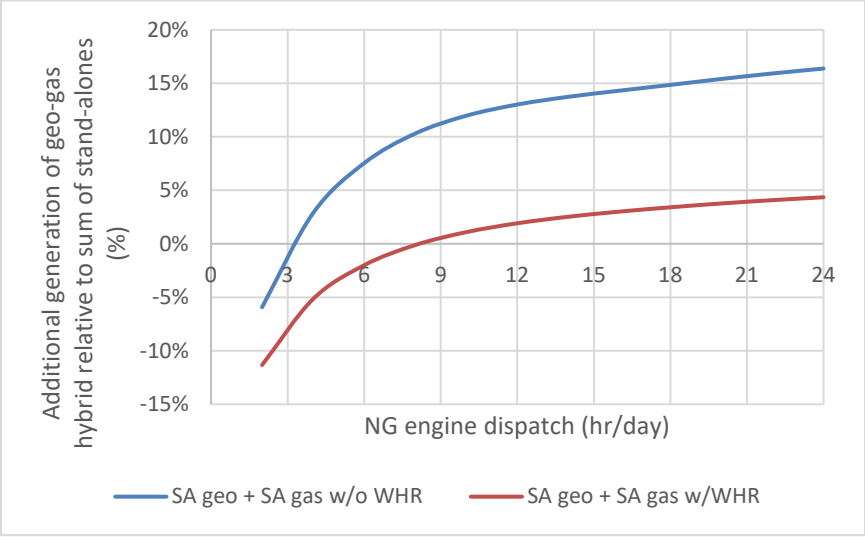

Figure 30. Additional generation of hybrid geo-gas plant relative to sum of standalone geothermal and gas plants based on Elk Hills, California resource and ambient conditions.

The hybrid plant provides more net power generation relative to the combined standalone geothermal plant and standalone gas gen set when it operates using energy from both the gas engine and geothermal resource but underperforms the standalone geothermal plant when only energy from the geothermal resource is available. The relative magnitude of the performance differences between the hybrid and standalone plants with and without energy input from the gas engine gen set determines the number of daily dispatch hours for which the hybrid generation exceeds the combined standalone plant generation (i.e., the point at which the curves in Figure 30 cross the x-axis).

The combination of the standalone geothermal plant and standalone gas engine gen set with WHR includes the more efficient gas engine gen set configuration and therefore in Figure 30 the curve for this combination of standalone plants appears below that for the combined standalone geothermal and standalone gas engine gen set without WHR. This indicates that the hybrid geo-gas plant provides increased annual power generation benefits relative to the standalone geothermal and gas gen set without WHR than relative to the standalone geothermal and gas gen set with WHR (provided that the gas gen set is dispatched for at least 3 or 8 hours, respectively).

The CO_2 emission intensity for the hybrid geo-gas plant, the combined standalone geothermal plant and standalone gas engine gen set without WHR, and the combined standalone geothermal plant and standalone gas engine gen set with WHR are shown in Figure 31. This figure illustrates that when the gas engine gen sets are operated with a high-capacity factor the hybrid plant provides lower CO_2 emissions per unit power generation than the combined standalone geothermal plant and standalone gas gen set configurations. The hybrid geo-gas plant results in lower CO_2 emission intensity than the standalone geothermal plant plus standalone gas engine gen set without WHR when the gas engine gen set is dispatched for approximately 4 hours per day. The hybrid geo-gas plant results in a lower CO_2 emission intensity than the standalone geothermal plant plus standalone gas engine gen set with WHR when the gas engine gen set is dispatched for approximately 8 hours per day. The dispatch schedule associated with these breakeven points is driven by the relative efficiency of the hybrid plant in comparison with the standalone plants during operating modes when the waste heat from the gas engine gen set is or is not available.

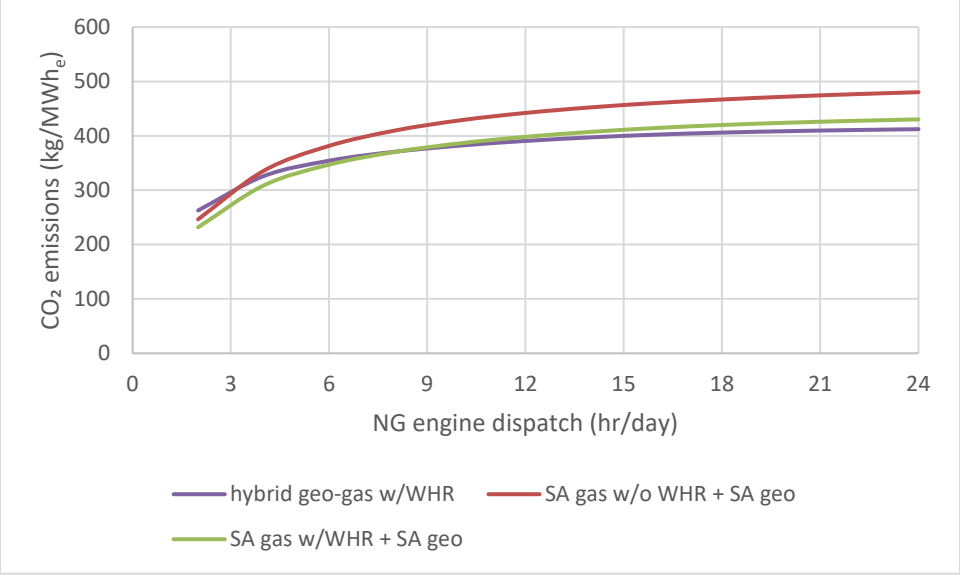

Figure 31. Comparison of CO_2 emissions for hybrid geo-gas plant versus sum of standalone geothermal plant and standalone gas engine based on Elk Hills, California resource and ambient conditions.

Figure 32 is a plot of the LCOE of the hybrid geo-gas plant, standalone geothermal plant, and standalone gas engine with and without WHR as a function of hours per day of gas engine dispatch. Note that the standalone geothermal plant has no gas engine integration; therefore, its LCOE is independent of the gas engine dispatch schedule. Figure 32 illustrates that the standalone geothermal plant has a lower LCOE than the standalone gas reciprocating engine gen sets when the gas engines are dispatched for about 9 hours per day or less. However, when the gas engines are dispatched for greater than about 12 hours per day the standalone gas engine and hybrid geo-gas engine configurations provide a lower LCOE than the standalone geothermal plant. Since the normalized CO_2 emissions of the hybrid plant are lower than those of the standalone gas engine plant when the gas engine is dispatched for 8 hours or more per day (Figure 31), the hybrid plant provides a pathway for deploying geothermal resources at an LCOE below that of a standalone geothermal plant, while increasing the generation and decreasing the normalized CO_2 emissions relative to the standalone gas engine gen set. Furthermore, it is possible that the standalone geothermal plant LCOE may be too high to be economically viable in certain markets, so the hybrid geo-gas engine configuration may provide a pathway for deploying geothermal resources that otherwise may not be developed and/or utilized.

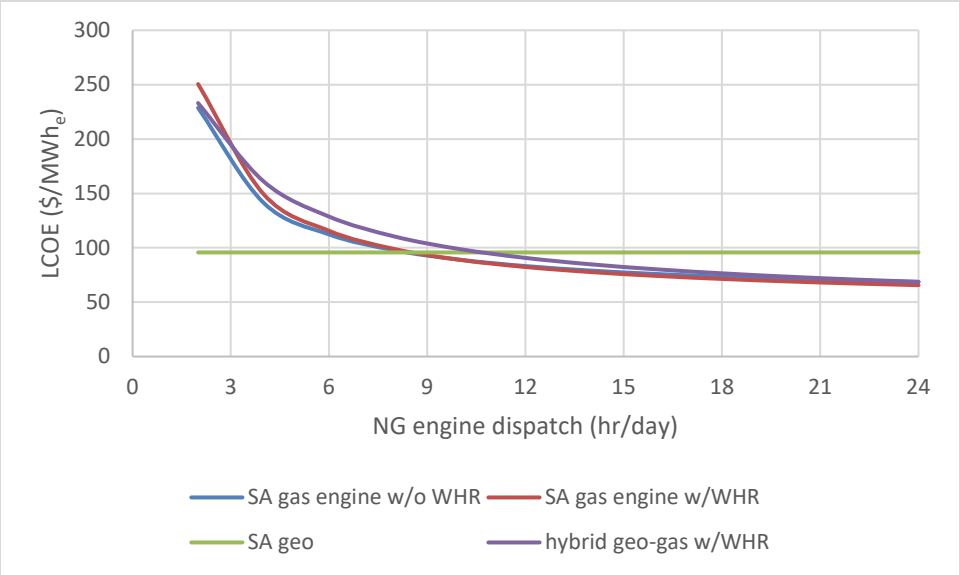

Figure 32. LCOE comparison of hybrid geo-gas plant, standalone geothermal plant, and standalone gas engine with and without WHR as a function of hours per day of gas engine dispatch.

Figure 33 provides a comparison of the LCOE for the hybrid geo-gas plant with that of the combined standalone geothermal plant and standalone gas engine gen set (with and without WHR). This figure indicates that the hybrid plant LCOE is higher than that from the combined standalone plants unless the gas engine gen sets are dispatched for most of the day throughout the year (i.e., greater than about 18 hours per day). This figure indicates that the increased efficiency of the hybrid geo-gas plant (relative to the combined standalone plants) does not offset its higher capital costs (again, relative to the combined standalone plants) unless the gas engine gen set is operated for most of the year as would be the case for a distributed natural-gas generator providing baseload generation in poor grid quality geographies or remote locations.

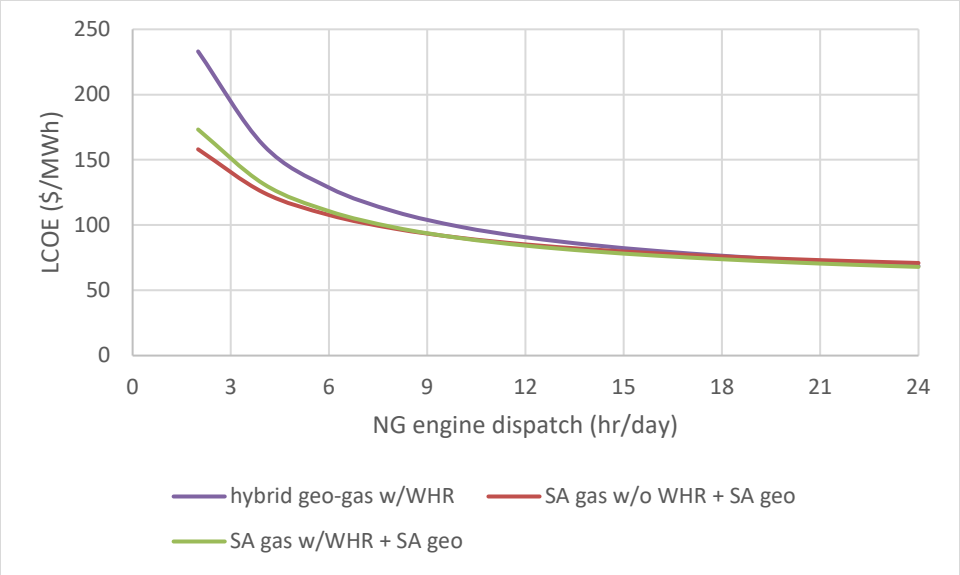

Figure 33. Comparison of LCOE for hybrid geo-gas plant versus sum of standalone geothermal plant and standalone gas engine based on Elk Hills, CA resource and ambient conditions.

7. Hybrid Geo-Gas-Solar Results

The motivation behind the triple geo-gas-solar hybrid is to note that NGCTs are likely to be deployed on the electricity grid to provide security of supply. We propose integrating the NGCT into the hybrid geothermal-solar system, which effectively converts the combustion turbine power plant into a combined cycle power plant without the full expense of the steam turbine and heat rejection system, although an HRSG is required.

7.1 Design Point Results

The system can therefore be thought to operate in two modes: solar-driven and gas-driven mode.

1. Solar-driven mode. Solar heat is used to drive the topping steam cycle and bottoming ORC.
2. Gas-driven mode. Natural gas is combusted to produce power in the gas turbine, which then rejects heat to drive the topping steam cycle and bottoming ORC.

The gas turbine is sized such that the heat rejected in the turbine exhaust is equal to the design point heat input to the geo-solar hybrid cycle. As a result, the geo-solar hybrid cycle does not require any modification from the cycle described earlier and its off-design behavior and models are the same. In this case, the gas turbine power output is 27.9 MW_e, which is a similar order of magnitude to the total power output of the hybrid cycle. Therefore, the total power output in gas-driven mode is more than double that of the solar-driven mode, as illustrated in Table 12 for the California design.

Table 12. Comparison of power outputs from each cycle in gas-driven and solar-driven mods for a plant located in California.

		Solar-driven Mode	Gas-driven Mode
Gas cycle power	MW_e	–	27.9
Steam cycle power	MW_e	9.9	9.9
Organic Rankine cycle power	MW_e	13.4	13.4
Parasitics	MW_e	3.9	3.9
Total net power	MW_e	19.3	47.2

7.2 Off-Design Behavior

Since the hybrid plant is unchanged, it has the same off-design performance as outlined in Section 5.2. The gas turbine is assumed to either run at 0% or 100% load; therefore, an off-design map is not required. (Ambient temperature variations impact the air-cooled condenser, which is handled within the off-design hybrid model.)

7.3 Annual Results

To illustrate annual performance, a contrived scenario is examined. In this scenario, it is assumed that a new NGCT added to the Californian grid would operate for a block of 5 hours per day, from 4:00 p.m. to 9:00 p.m., thereby capturing the most valuable hours of each day. While this is a simple assumption, available data in Figure 34 suggests that many natural-gas power plants in California do operate such that they mainly target high-value price hours. Figure 35 demonstrates that natural-gas energy generation is ramped up in the evening hours for every month of the year.

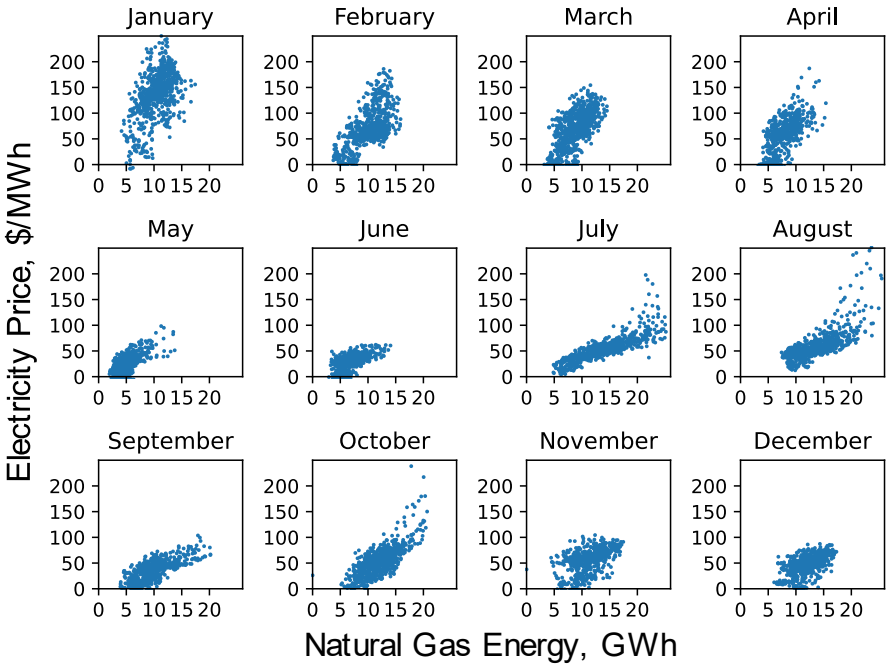

Figure 34. Scatter plot showing the electricity price and energy delivered by natural-gas power plants for each hour of the year in California 2023 [56].

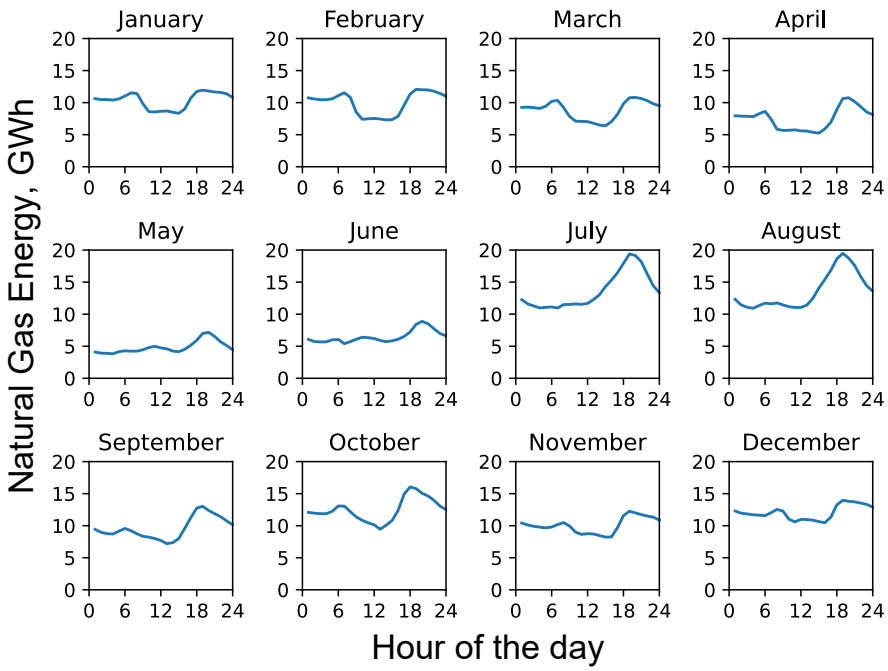

Figure 35. Average energy generated by natural-gas power plants for each month in California, 2023 [56].

Rather than building the gas plant in isolation, we examine the impact of integrating it with a hybrid geo-solar power plant. The combustion turbine cycle benefits from the hybrid plant's steam cycle and bottoming cycle, which increases the total electricity delivered in those high-value periods. However, solar energy is not able to be dispatched during those times since the gas cycle takes priority. Therefore, the solar energy is stored and dispatched at other times. Since the gas cycle dispatches during hours that are typically the most profitable, this means the value of the solar thermal system is reduced as it is forced to dispatch at lower value times. Therefore, thermal energy storage is an important component in this system as it enables the solar energy to be delivered at the most valuable times that remain, which are typically in the morning. The solar energy is dispatched using the price-based dispatch algorithm discussed in Section 5.3.2; although this algorithm is modified so that solar energy is dispatched at the most valuable hours outside of the gas-cycle operating periods.

Average daily energy profiles for seasonally representative months are illustrated in Figure 36. The large energy output of the gas cycle plus bottoming cycles is evident in the evening hours. The steam cycle typically does not operate in the middle of the day when electricity prices are low; instead, solar energy is dispatched overnight and in the early morning price peak.

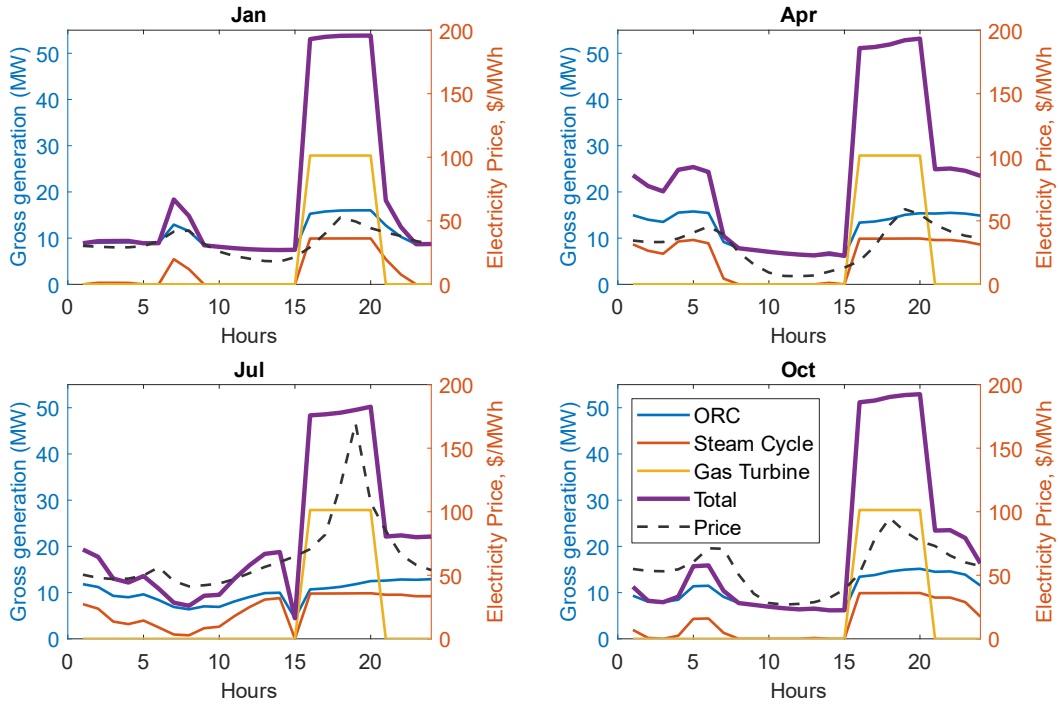

Figure 36. Average daily energy profiles for several months for a triple-hybrid gas-geo-solar plant located in California, 2021. Solar multiple = 1.5 and TES duration = 12 hr.

Data for triple-hybrid cycles with three different sizes of solar field and thermal energy storage are shown in Table 13. This table separates out the annual energy generated during solar-driven mode in the steam cycle and ORC, and the annual energy generated during gas-driven mode in those same cycles. The energy generated during gas-driven mode is about 60% of the electricity generated by the gas turbine itself. Therefore, this represents an efficient use of the gas turbine waste heat and is representative of the reduction in energy generation from fossil fuel assets that can be achieved. For instance, with a solar multiple of 1.5, the gas turbine generates 50.1 GWh_e (and emits 33,360 tonnes of CO_2) annually and using the waste heat in the hybrid cycle generates another 32.8 GWh_e. Therefore, using the hybrid cycle reduces the energy generation from gas cycles by 32.8 GWh_e a year, which corresponds to reducing carbon emissions by 21,490 metric tonnes. The "cost" of saving these carbon emissions is estimated by comparing the additional cost incurred by integrating the combustion turbine with the hybrid cycle (i.e., the capital cost of the HRSG). The cost per metric tonne of CO_2 saved is shown in Table 13 and is approximately 38 \$/tonne-CO_2. This is similar to the current cost of carbon credits in California [57].

Table 13. Techno-economic results for a triple-hybrid gas-geo-solar plant with different solar field sizes.

		Solar multiple = 1	Solar multiple = 1.5	Solar multiple = 2
TES discharge duration	h	4	12	14
Solar-driven Energy	MWh_e	49,283	66,518	79,411
Gas-turbine-driven Energy	MWh_e	32,803	32,765	32,723
Gas turbine Energy	MWh_e	50,863	50,863	50,863
Total Energy	MWh_e	132,950	150,150	163,000
Capital cost	M$	157.4	174.3	184.7
LCOE	$/$MWh_e$	129.2	122.3	117.2
Revenue (annual)	M$	8.27	9.19	9.65
Carbon Emissions (annual)	Metric tonnes	33,360	33,360	33,360
Carbon Emission Reduction (annual)	Metric tonnes	21,515	21,490	21,462
Cost of reducing carbon emissions	$/tonne	–	38.0	38.0

Economic results are also reported in Table 13. Increasing the solar field size increases the capital cost but leads to a better LCOE and larger revenue as more electricity is generated. The LCOE of the triple-hybrid with a solar multiple of 1.5 (122.3 $/$MWh_e$) is similar to that of the geothermal-solar hybrid plant in Table 8 (120.8 $/$MWh_e$). However, the revenue doubles from $4.5M to $9.2M as a result of the inclusion of the gas turbine.

The triple-hybrid results can be compared to a NGCT cycle operating in isolation and to a hybrid geothermal-solar cycle with the same size solar field and thermal energy storage. Contributions to the LCOE are shown in Figure 37 and the standalone NGCT has a slightly larger LCOE than either of the hybrid plants: predominantly due to the high cost of natural gas and its inefficient conversion to electricity (32%) in the gas cycle. The natural-gas contribution to LCOE is significantly lower for the triple-hybrid since exhaust gas exergy is exploited in the steam cycle and ORC.

More detailed results are shown in Table 14, which shows that integrating the NGCT into a hybrid plant reduces the LCOE and increases the revenue, AEP, and capital cost. For small solar multiples (1-1.5), the triple-hybrid plant has a lower LCOE than the geothermal-solar hybrid plant. However, at larger solar multiples, the triple-hybrid has a worse LCOE, although its revenue and AEP outperforms the geothermal-solar hybrid. The revenue increases at a diminishing rate, as the average price solar energy is sold at reduces as the solar field gets larger.

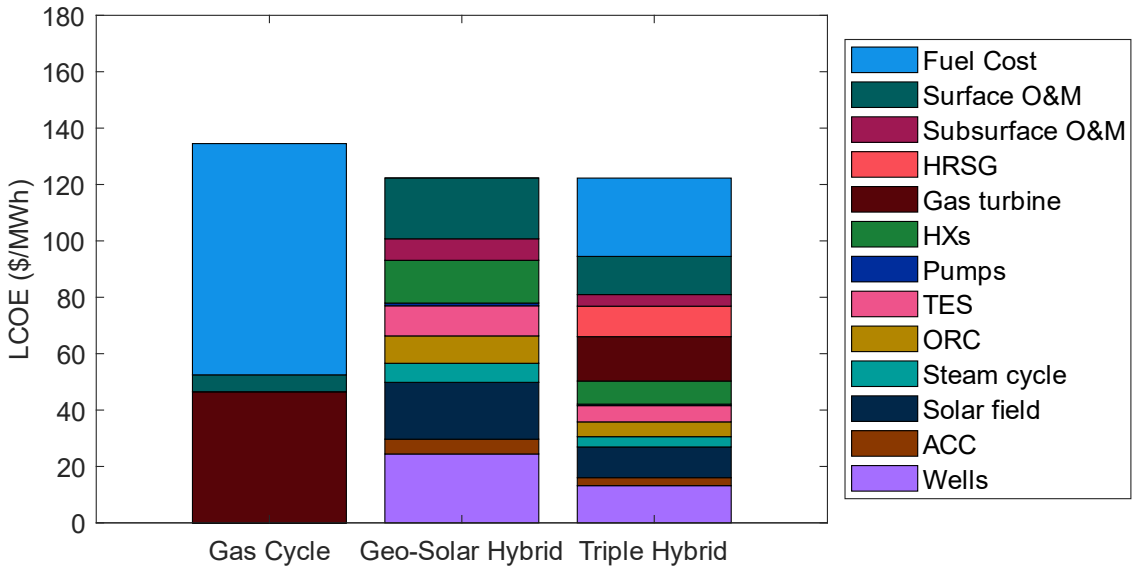

Figure 37. Breakdown of contributions to the LCOE for a standalone NGCT, a hybrid geothermal-solar system, and a triple-hybrid gas-geothermal-solar system. Solar multiple = 1.5 and thermal storage duration is 12 hr. California, 2021.

Table 14. Results comparing a standalone NGCT, with solar-geothermal hybrid, and triple gas-geothermal-solar hybrid for three solar field sizes, in California, 2021

		Solar multiple = 1.		
		Standalone NGCT	Geothermal-solar hybrid	Gas-geothermal-solar hybrid
AEP	MWh_e	50,863	67,758	132,950
Capital cost	M$	35.7	97.1	157.4
LCOE	$/$MWh_e$	134.5	129.1	129.2
Revenue	M$	3.66	3.68	8.27
		Solar multiple = 1.5		
		Standalone NGCT	Geothermal-solar hybrid	Gas-geothermal-solar hybrid
AEP	MWh_e	50,863	81,140	150,150
Capital cost	M$	35.7	116.3	174.3
LCOE	$/$MWh_e$	134.5	124.1	122.3
Revenue	M$	3.66	4.55	9.19
		Solar multiple = 2.		
		Standalone NGCT	Geothermal-solar hybrid	Gas-geothermal-solar hybrid
AEP	MWh_e	50,863	94,288	163,000
Capital cost	M$	35.7	124.5	184.7
LCOE	$/$MWh_e$	134.5	113.0	117.2
Revenue	M$	3.66	5.16	9.65

8. CONCLUSIONS

Conclusions regarding each of the hybrid plant configurations examined in this analysis are presented below. Conclusions are presented first for the geothermal-solar hybrid plant, second for the geothermal-gas reciprocating engine hybrid plant, and third for the gas-geothermal-solar triple hybrid plant.

Concluding remarks on the geothermal-solar hybrid plant:

- Designing a greenfield geothermal-solar hybrid plant enables the relative sizes of the geothermal flow, solar field size, and thermal energy storage discharge duration to be chosen. The optimal relative sizes depend on location-dependent properties (e.g., ambient temperature, geothermal resource, and solar resource).
- Two concepts were investigated: (1) a system with a large solar field suitable for providing baseload capabilities and (2) a system with a smaller solar field that provides peaking capabilities, at four locations that have different solar and geothermal resources.
- The hybrid cycle is compared to equivalently sized, co-located, independent geothermal power plant and concentrating solar power plant.
- The hybrid cycle tends to produce slightly more power than the standalone geothermal and solar plants combined. Thus, if new designs can reduce the cost of the hybrid plant or better prove the value of the hybrid plant, then the cycle would be more competitive in comparison to the two standalones.
- Generally, the hybrid plant achieves a similar capital cost, annual energy output, and LCOE to the combined output of two standalone plants and the differences in results are small enough that they may not be statistically significant. Based on these values alone, the hybrid plant may not have sufficient benefits to outweigh the added complexity of the hybrid system. Additional analysis with a focus on grid value may be needed to show the benefits of the proposed hybrid plant.
- For the baseload case, the geothermal-only plant has a high LCOE at locations with low geothermal resource temperature (Texas and Idaho), suggesting that geothermal systems are not economical here. Adding solar thermal to these systems leads to a hybrid plant with an LCOE lower than the geothermal-only system, though the standalone plants combined have an even lower LCOE. Thus, hybrid plants may enable the economic development of geothermal resources in locations with a low geothermal resource temperature. In areas with higher geothermal resource temperature (Mississippi and California), the geothermal-only plant has a lower LCOE than the hybrid cycle and could be developed without the need for solar heat addition. However, the use of high-temperature solar heat enables the power output to be significantly increased without the risk and uncertainty of drilling large numbers of wells.
- For the baseload case, the standalone CSP plant has a lower LCOE than the hybrid plant at all locations except Mississippi. This suggests that developers may prefer not to include geothermal systems and instead develop only CSP plants. The geothermal component must provide some value to be worth the increased LCOE. For example, the geothermal resource can help stabilize the seasonal energy output: geothermal power production increases in winter months due to lower ambient temperatures, whereas solar power production drops off sharply. This is particularly true for the systems located in CA and ID.
- The peaking plant design uses a price-based dispatch algorithm to deliver electricity at the most valuable times. Therefore, thermal energy storage is an important component in this system. The LCOE is a less suitable metric to assess this design because it produces less energy in total than the baseload design as a result of the smaller solar field. The objective is to increase the revenue and flexibility of the system. Results were generated across four locations and 2 years of data, but

electricity prices vary significantly so conclusions need to be carefully considered and further analysis is required.

- Across the eight scenarios, the hybrid plant generates slightly more revenue than the combined revenue of two standalone systems in seven cases. When solar heat is dispatched through the topping cycle, heat rejected from the topping cycle is added to the bottoming cycle which enables more energy to be extracted from the geothermal fluid and therefore increases the bottoming cycle power output. Therefore, the hybrid cycle enables the geothermal resource to be dispatched flexibly, while maintaining a constant brine flow rate. The geothermal resource is thus used to generate power at the most valuable times in the hybrid plant, whereas, with a standalone geothermal plant, the power output is dictated only by variations in ambient temperature. Therefore, the peaking hybrid plant provides significant value to the grid due to its flexibility and could enable geothermal resources to be developed in regions where high-renewable generation and curtailment are a problem.
- The peaking hybrid plants have lower capital costs than the baseload hybrid plants, due to the smaller solar field, and might be easier to finance. The solar field could then be expanded in later years if different dispatch characteristics were required from the hybrid plant or if the geothermal resource quality declined.

Concluding remarks on the hybrid geo-gas reciprocating engine:

- The Elk Hills case study analysis indicates that for a scenario in which the gas reciprocating engines are dispatched for greater than 12 hours per day the standalone gas engine and hybrid geo-gas engine configurations provide a lower LCOE than the standalone geothermal plant. This dispatch schedule also results in hybrid geo-gas plant normalized CO_2 emissions that are lower than those from standalone gas reciprocating engine plants with and without WHR.
- For the hybrid geo-gas plant to realize these advantages relative to the standalone natural-gas engine gen sets, the gas engine gen sets would have to be dispatched for 12+ hours per day, as may be the case for a distributed natural-gas generator providing baseload generation in poor grid quality geographies or remote locations.
- Therefore, for scenarios with high gas reciprocating engine gen set capacity factors, the hybrid geo-gas reciprocating engine plant configuration could provide a pathway for using a geothermal resource in a plant configuration that results in a lower LCOE than a standalone geothermal plant, while increasing the annual generation and decreasing the normalized CO_2 emissions relative to standalone gas reciprocating engine gen sets (either with or without WHR).
- Since it is possible that the standalone geothermal plant LCOE may be too high to be economically viable in certain markets, the hybrid geo-gas engine configuration may provide a pathway for deploying geothermal resources that otherwise may not be developed and/or utilized.

Concluding remarks on the triple-hybrid gas-geothermal-solar cycle:

- A triple-hybrid plant that combines natural gas, solar thermal, thermal energy storage, and geothermal is investigated. A NGCT is added to the geothermal-solar hybrid such that the hot exhaust gas from the gas turbine provides an alternative source of heat to the steam turbine of the hybrid cycle. The combustion turbine cycle is effectively converted into a more efficient combined cycle gas turbine with only the additional cost of the HRSG. The dispatch strategy determines whether to deliver heat from the gas turbine or the solar field based on electricity prices and time of day.
- Results suggest that the triple-hybrid plant has a significantly higher energy generation and revenue than a standalone NGCT or the original geothermal-solar hybrid. This is because the waste heat from the gas cycle is used efficiently to generate energy and revenue. The triple-hybrid design benefits most from using a smaller solar field so that the solar energy can be dispatched at the most valuable times available. The triple-hybrid plant also has a lower LCOE than the standalone NGCT.

- The triple-hybrid plant was evaluated making simple assumptions about the dispatch profile of the gas cycle, and more nuanced and realistic dispatching schedules should be analyzed in future work.

9. FUTURE WORK

A list of potential topics for future work and the corresponding benefits of further analyses in each area is provided below:

- ORC preheater size, cost, and operational considerations:
  - The preheater for the geo-solar cycle was designed for high performance, but without consideration for size. Consequently, the hybrid plant design includes a preheater with a very large heat transfer area and correspondingly high capital cost. Revising the design to use a smaller heat exchanger could significantly reduce capital costs at the expense of a reduction in the heat extracted from the geothermal brine and therefore the hybrid plant net power generation. However, since the decreased heat extraction would be the lowest grade heat input to the cycle, it is expected that the reductions in capital cost would outweigh the reductions in hybrid plant performance.
  - Future studies of the steam-topping cycle hybrid plant configuration should consider the costs and operational implications of a geothermal preheater design that functions as a preheater at the design condition but as a preheater/vaporizer at off-design operating conditions.
- ACC control: future analysis could incorporate advanced ACC control strategies to reduce the parasitic load from the ACC fans when the ambient temperature is low. Preliminary evaluation of this strategy indicates that the gross power generation decreases at a lower rate than the ACC fan power as the fan power is reduced during periods of low ambient temperature. Implementation of a more advanced ACC control strategy would be expected to improve the AEP of all standalone and hybrid plant configurations that include an ACC, with the net effect of decreasing the LCOE for these plants.
- Impacts of steam extractions for standalone CSP steam Rankine cycle: Since the standalone CSP steam Rankine cycle condenses steam at low pressure and temperature, feedwater heating must be used to minimize the temperature differential in the steam generator. The steam extractions required for this purpose may have a negative impact on net power generation. Since the hybrid plant uses a back-pressure turbine that condenses the steam at an elevated pressure and temperature, less steam extractions for feedwater heating may be needed to provide the correct steam generator feedwater inlet temperature, which may provide a marginal performance gain in comparison with the standalone solar plant. The simplified steam Rankine cycles used in this analysis do not capture the potential performance differences that may result from the back-pressure steam turbine used in the hybrid plant configuration and the condensing steam turbine used in the standalone plant configuration. Future work could investigate potential performance differences associated with these different turbine types and the corresponding feedwater heating configurations.
- The annual simulations highlighted the lower performance of the hybrid plant ORC relative to the standalone geothermal plant ORC when the ORC operates using geothermal heat only. Extensive efforts were made to optimize the performance of the standalone geothermal power plants to ensure that the comparison of hybrid and combined standalone plant performance did not overstate the potential benefits of the hybrid plants. However, some of the cycle design attributes considered in the standalone geothermal plant analysis could also be applied to the hybrid plant bottoming ORC to investigate whether improved hybrid plant bottoming ORC performance may be possible when the high-temperature solar or natural-gas heat is not available, and the hybrid plant bottoming ORC operates from geothermal heat only. Therefore, future work could consider use of a dual-pressure level or supercritical bottoming cycle in the hybrid plant bottoming ORC, which may allow increased performance at both on- and off-design operating conditions and/or reduced hybrid plant capital costs.

- Improved valuation of the hybrid design:
  - Evaluating the "value" of a system based solely on the spot market energy prices misses multiple ways that a plant can add value to a grid. Capacity payments were not considered herein and may be able to increase the revenue, based on the location. Additionally, value from either providing baseload power to the grid, or flexible dispatch, or both, may be relevant in future electrical grids. One benefit of a hybrid cycle is the ability to flexibly dispatch from storage while also feeling confident in continuous power output from the geothermal cycle, regardless of weather. That benefit was difficult to quantify in the analysis herein.
  - Uncertainty of electricity prices. Significant year-by-year variation was present in the historical electricity pricing data used in this analysis. Evaluation of the plant performance in each of the selected case study locations using multiple years of historical and/or projected electricity pricing data would increase the confidence of the economic analyses as well as to allow quantification of uncertainty and variability in the results.

10. REFERENCES

[1] White House. 2021. "The Long-Term Strategy of the United States, Pathways to Net-Zero Greenhouse Gas Emissions by 2050." United States Executive Office of the President. November 2021.

[2] Lazard. 2023. "Lazard's Levelized Cost of Energy: Version 16.0," Lazard. April 2023.

[3] Robins, J. C., et al. 2021. "2021 U.S. Geothermal Power Production and District Heating Market Report." National Renewable Energy Laboratory. 2021.

[4] GTO. 2019. "GeoVision: Harnessing the Heat Beneath Our Feet." U.S. Department of Energy Geothermal Technologies Office. 2019. http://www.osti.gov/scitechonlineordering:http://www.ntis.gov/help/ordermethods.aspx

[5] Wendt. D. S., et al. 2015. "Stillwater Hybrid Geo-Solar Power Plant Optimization Analyses." in *GRC Transactions*, 2015.

[6] McTigue, J. D., et al. 2018. "Hybridizing a geothermal power plant with concentrating solar power and thermal storage to increase power generation and dispatchability." *Appl Energy* 228: 1837–1852, October 2018. doi: 10.1016/j.apenergy.2018.07.064.

[7] McTigue, J. D., D. Wendt, K. Kitz, J. Gunderson, N. Kincaid, and G. Zhu. 2020. "Assessing geothermal/solar hybridization – Integrating a solar thermal topping cycle into a geothermal bottoming cycle with energy storage." *Appl Therm Eng* 171: 115121. May 2020. doi: 10.1016/j.applthermaleng.2020.115121.

[8] Wendt D., et al. 2019. "Flexible Geothermal Power Generation utilizing Geologic Thermal Energy Storage." INL/EXT-19-53931. Idaho National Laboratory. May 2019.

[9] Sharan, P., K. Kitz, D. Wendt, J. McTigue, and G. Zhu. 2021. "Using concentrating solar power to create a geological thermal energy reservoir for seasonal storage and flexible power plant operation." *Journal of Energy Resources Technology, Transactions of the ASME* 143, no. 1: 010906, January 2021, doi: 10.1115/1.4047970.

[10] McTigue, P. D. Joshua, G. Zhu, D. Akindipe, and D. Wendt. 2023. "Geological Thermal Energy Storage Using Solar Thermal and Carnot Batteries: Techno-Economic Analysis." Presented at the 2023 *Geothermal Rising Conference*, Reno, Nevada. October 1–4, 2023.

[11] Mctigue, J. D., J. G. Simpson, G. Zhu, G. Neupane, and D. Wendt. 2023. "Design of a Geothermal Power Plant with Solar Thermal Topping Cycle: Preprint." Presented at the 2023 *Geothermal Rising Conference*, Reno, Nevada. October 1–4, 2023.

[12] Manente, G., A. Toffolo, A. Lazzaretto, and M. Paci. 2013. "An Organic Rankine Cycle off-design model for the search of the optimal control strategy," *Energy* 58: 97–106. September 2013. doi: 10.1016/J.ENERGY.2012.12.035.

[13] Keshvarparast, A., S. S. M. Ajarostaghi, and M. A. Delavar. 2020. “Thermodynamic analysis the performance of hybrid solar-geothermal power plant equipped with air-cooled condenser.” *Appl Therm Eng* vol. 172: 115160. May 2020. doi: 10.1016/J.APPLTHERMALENG.2020.115160.
[14] Hu, S., Z. Yang, J. Li, and Y. Duan. 2021. “Thermo-economic optimization of the hybrid geothermal-solar power system: A data-driven method based on lifetime off-design operation.” *Energy Convers Manag* 229, February 2021. doi: 10.1016/J.ENCONMAN.2020.113738.
[15] Ghasemi, H., E. Sheu, A. Tizzanini, M. Paci, and A. Mitsos. 2014. “Hybrid solar–geothermal power generation: Optimal retrofitting.” *Appl Energy* 131: 158–170. October 2014. doi: 10.1016/J.APENERGY.2014.06.010.
[16] Lentz, Á., and R. Almanza. 2006. “Parabolic troughs to increase the geothermal wells flow enthalpy,” *Solar Energy* 80, no. 10: 1290–1295. October 2006. doi: 10.1016/j.solener.2006.04.010.
[17] Tranamil-Maripe, Y., J. M. Cardemil, R. Escobar, D. Morata, and C. Sarmiento-Laurel. 2022. “Assessing the Hybridization of an Existing Geothermal Plant by Coupling a CSP System for Increasing Power Generation.” *Energies (Basel)* 15, no. 6. March 2022. doi: 10.3390/en15061961.
[18] Bassetti, M. C., D. Consoli, G. Manente, and A. Lazzaretto. 2018. “Design and off-design models of a hybrid geothermal-solar power plant enhanced by a thermal storage.” *Renew Energy* 128: 460–472. December 2018. doi: 10.1016/J.RENENE.2017.05.078.
[19] Mctigue, J. D., N. Kincaid, G. Zhu, D. Wendt, J. Gunderson, and K. Kitz. 2018. “Solar-Driven Steam Topping Cycle for a Binary Geothermal Power Plant.” 2018. [Online]. Available: https://www.nrel.gov/docs/fy19osti/71793.pdf.
[20] Bonyadi, N., E. Johnson, and D. Baker. 2018. “Technoeconomic and exergy analysis of a solar geothermal hybrid electric power plant using a novel combined cycle.” *Energy Convers Manag* 156: 542–554. January 2018. doi: 10.1016/j.enconman.2017.11.052.
[21] Boukelia, T. E., O. Arslan, and A. Bouraoui. 2021. “Thermodynamic performance assessment of a new solar tower-geothermal combined power plant compared to the conventional solar tower power plant.” *Energy* 232: 121109. October 2021. doi: 10.1016/J.ENERGY.2021.121109.
[22] Song, J., Y. Wang, K. Wang, J. Wang, and C. N. Markides. 2021. “Combined supercritical CO_2 (SCO2) cycle and organic Rankine cycle (ORC) system for hybrid solar and geothermal power generation: Thermoeconomic assessment of various configurations.” *Renew Energy* 174: 1020–1035. August 2021. doi: 10.1016/J.RENENE.2021.04.124.
[23] NREL. 2024. “Solar Resource Maps and Data | Geospatial Data Science.” National Renewable Energy Laboratory. Accessed: March 17, 2024. [Online]. Available: https://www.nrel.gov/gis/solar-resource-maps.html.
[24] Roberts, B. J. 2024. “Geothermal Resource of the United States: Identified Hydrothermal Sites and Favorability of Deep Enhanced Geothermal Systems (EGS).” National Renewable Energy Laboratory. 2018.
[25] Neupane, G., D. S. Wendt, J. D. Mctigue, and J. G. Simpson. 2024. “Geologic Assessment of Four Greenfield Sites for Solar-Geothermal Hybrid Power Plants.” in *49th Workshop on Geothermal Reservoir Engineering.* 2024.
[26] NREL. 2022. “Solar Electric Generating Station I | Concentrating Solar Power Projects.” National Renewable Energy Laboratory. October 21, 2022. Accessed: March 17, 2024. [Online]. Available: https://solarpaces.nrel.gov/project/solar-electric-generating-station-i.
[27] NREL. 2023. “Mojave Solar Project | Concentrating Solar Power Projects.” October 25, 2023. National Renewable Energy Laboratory. Accessed: Mar. 17, 2024. [Online]. Available: https://solarpaces.nrel.gov/project/mojave-solar-project.
[28] NREL. 2023. “Crescent Dunes Solar Energy Project | Concentrating Solar Power Projects.” National Renewable Energy Laboratory. October 25, 2023. Accessed: March 17, 2024. [Online]. Available: https://solarpaces.nrel.gov/project/crescent-dunes-solar-energy-project.

[29] NREL. 2022. “Ivanpah Solar Electric Generating System | Concentrating Solar Power Projects.” National Renewable Energy Laboratory. October 21, 2022. Accessed: March 10, 2024. [Online]. Available: https://solarpaces.nrel.gov/project/ivanpah-solar-electric-generating-system.
[30] Montes, M. J., A. Abánades, J. M. Martínez-Val, and M. Valdés. 2009. “Solar multiple optimization for a solar-only thermal power plant, using oil as heat transfer fluid in the parabolic trough collectors.” *Solar Energy* 83, no. 12: 2165–2176. 2009. doi: 10.1016/j.solener.2009.08.010.
[31] NREL. 2022. “Genesis Solar Energy Project | Concentrating Solar Power Projects.” National Renewable Energy Laboratory. October 21, 2022. Accessed: March 10, 2024. [Online]. Available: https://solarpaces.nrel.gov/project/genesis-solar-energy-project.
[32] EPA. 2015. “Catalog of CHP Technologies, Section 2. Technology Characterization – Reciprocating Internal Combustion Engines.” Environmental Protection Agency. 2015.
[33] EIA. 2020. “About 25% of U.S. power plants can start up within an hour.” U.S. Energy Information Administration. November 19, 2020. Accessed: Mar. 10, 2024. [Online]. Available: https://www.eia.gov/todayinenergy/detail.php?id=45956.
[34] Skone T. J., et al. 2014. “Life Cycle Analysis of Natural Gas Extraction and Power Generation,” Department of Energy National Energy Technology Laboratory. DOE/NETL-2014/1646. May 29, 2014.
[35] Sim Tech. 2024. “IPSEpro.” Sim Technology. 2024.
[36] Bahrami, M., F. Pourfayaz, and A. Kasaeian. 2022. “Low global warming potential (GWP) working fluids (WFs) for Organic Rankine Cycle (ORC) applications.” *Energy Reports* 8: 2976–2988. 2022. doi: 10.1016/j.egyr.2022.01.222.
[37] GE. 2006. “GE Jenbacher Technical data.” GE Jenbacher. May 10, 2006. Accessed: March 18, 2024. [Online]. Available: https://www.uspowerco.com/generator_attachments/3125-jenbacher_tech.pdf.
[38] GE. “Jenbacher gas engines technical specification.” GE Jenbacher. Accessed: March 18, 2024. [Online]. Available: https://www.energy-motors.com/sites/default/files/ge_jenbacher_j616_2681.pdf.
[39] GE Power & Water. “Jenbacher type 6.” GE Jenbacher. Accessed: March 18, 2024. [Online]. Available: https://www.clarke-energy.com/wp-content/uploads/2015/04/CEL-type-6.pdf.
[40] Turchi C. S., et al. 2019. “CSP Systems Analysis - Final Project Report.” National Energy Technology Laboratory. Golden, Colorado. 2019. [Online]. Available: www.nrel.gov/publications.
[41] Mehos, M., et al. 2017. “Concentrating Solar Power Gen3 Demonstration Roadmap,” National Energy Technology Laboratory. 2017. [Online]. Available: www.nrel.gov/publications.
[42] Mines, G. L. 2016. “GETEM User Manual.” INL/EXT-16-38751. Idaho National Laboratory. 2016.
[43] NREL. 2023. “Annual Technology Baseline: Geothermal.” National Renewable Energy Laboratory. July 15, 2023. Accessed: October 09, 2023. [Online]. Available: https://atb.nrel.gov/electricity/2023/geothermal.
[44] Chemical Engineering. “Chemical Engineering Plant Cost Index - Chemical Engineering.” Accessed: March 17, 2024. [Online]. Available: https://www.chemengonline.com/pci
[45] EIA. 2022. “Cost and Performance Characteristics of New Generating Technologies, Annual Energy Outlook 2022,” U.S. Energy Information Administration. 2022.
[46] Lazard, 2017. “Lazard’s Levelized Cost of Energy Analysis—Version 11.0.” Lazard. 2017.
[47] Oakes, M., et al. 2023. “Cost and Performance Baseline for Fossil Energy Plants, Volume 5: Natural Gas Electricity Generating Units for Flexible Operation.” 2023.
[48] EIA. 2024. “California Natural Gas Prices.” Energy Information Administration, Accessed: March 17, 2024. https://www.eia.gov/dnav/ng/ng_pri_sum_dcu_SCA_a.htm
[49] EPA. 2016. “Combined Heat and Power Technology Fact Sheet Series.” U.S. Department of Energy. 2016.
[50] EPA. 2015. “Catalog of CHP Technologies, Section 4. Technology Characterization – Steam Turbines.” U.S. Environmental Protection Agency. 2015.

[51] Black & Veatch. 2012. “Cost and Performance Data for Power Generation Technologies,” Prepared for the National Renewable Energy Laboratory. February 2012.
[52] AspenTech. 2024. “Aspen Process Economic Analyzer.” AspenTech. Accessed: March 17, 2024. [Online]. Available: https://www.aspentech.com/en/products/engineering/aspen-process-economic-analyzer
[53] AspenTech. 2024. “Aspen Exchanger Design and Rating (EDR).” AspenTech. Accessed: Mar. 17, 2024. [Online]. Available: https://www.aspentech.com/en/products/engineering/aspen-exchanger-design-and-rating
[54] Benato A., and A. Stoppato. 2019. “Integrated Thermal Electricity Storage System: Energetic and cost performance.” *Energy Convers Manag* 197. October 2019. doi: 10.1016/J.ENCONMAN.2019.111833.
[55] Astolfi, M., L. Xodo, M. C. Romano, and E. Macchi. 2011. “Technical and economical analysis of a solar-geothermal hybrid plant based on an Organic Rankine Cycle.” *Geothermics* 40, no. 1: 58–68. March 2011. doi: 10.1016/j.geothermics.2010.09.009.
[56] EIA. 2023. “Opendata - U.S. Energy Information Administration (EIA).” U.S. Energy Information Administration. Accessed: March 27, 2024. [Online]. Available: https://www.eia.gov/opendata/.
[57] Qin, B. 2023. “California Carbon Price Hits a Peak as Supply Cuts Loom,” Bloomberg NEF. August 3, 2023. Accessed: March 17, 2024. [Online]. Available: https://about.bnef.com/blog/california-carbon-price-hits-a-peak-as-supply-cuts-loom/.
[58] Manente, G. 2011. “Analysis and Development of Innovative Binary Cycle Power Plants for Geothermal and Combined Geo-Solar Thermal Resources.” Universita di Padova. 2011.
[59] Schuster, S., C. N. Markides, and A. J. White, 2020. “Design and off-design optimisation of an organic Rankine cycle (ORC) system with an integrated radial turbine model.” *Applied Thermal Engineering* 174. June 25, 2020. doi: 10.1016/j.applthermaleng.2020.115192.
[60] Bergman, T. L., A. S. Lavine, F. P. Incropera, and D. P. Dewitt. 2011. *Fundamentals of Heat and Mass Transfer*, 7th ed. Wiley, 2011.
[61] Nagorny, A. S., N. V. Dravid, R. H. Jansen, and B. H. Kenny. 2005. “Design aspects of a high speed permanent magnet synchronous motor / generator for flywheel applications.” in *2005 IEEE International Conference on Electric Machines and Drives.* IEEE Computer Society. 2005: 635–641. doi: 10.1109/iemdc.2005.195790.

Appendix A

Design Considerations and Set Points in IPSEpro and SAM

Page intentionally left blank

Appendix A

Design Considerations and Set Points in IPSEpro

A general listing of standalone and hybrid plant design parameters is included in Table A-1, with additional discussion and off-design decisions listed below.

Table A-1. Standalone and hybrid plant design parameters.

Design Parameter	Specification
Solar HTF – steam generator outlet temperature difference	20°C
Steam condenser – ORC vaporizer mean temperature difference (MTD)	10°C
ORC preheater minimum internal temperature approach (MITA)	5°C
Heat exchanger ΔP (liquid or two-phase mixture)	0.1 bar
Heat exchanger ΔP (molten salt)	0.001 bar
Condensing steam turbine efficiency	85% (based on Stillwater plant [58])
Back-pressure steam turbine efficiency	78% (based on [50])
ACC inlet ΔT (difference between the air inlet temperature and the condensate outlet temperature)	20°C
ACC hot side ΔP	0.15 bar
ACC cold side ΔP	0.002 bar
ACC air outlet temperature	40°C
ACC fan efficiency	65%
Pump efficiency	80% (based on Ref. [58])
Generators and motors	98% electrical and 98% mechanical efficiency

- ACC
  - Off-design: heat transfer coefficient does not change, assuming there is not significant change in heat transfer coefficient because condensing heat transfer is high
- ORC turbine
  - Off-design: using off-design table from Schuster et al.'s 2020 article [59]
- Steam turbine
  - Off-design: using Spencer-Cotton-Cannon (SCC) method built into IPSEpro for steam turbine off-design
- Heat exchangers
  - Using off-design relations built into IPSEpro based on exponents for mass flow and pressure changes effect on heat transfer coefficients
    - Using 0.8 for mass-based changes based on Dittus-Boelter relation [60]
    - Using 2 for pressure-based changes based on Navier-Stokes, assuming constant density

- Pumps
  - Assuming variable speed drives (VSDs), allowing to vary power output in off-design conditions
- Generator
  - Off-design table based on Nagorny et al.'s 2005 article [61].

Appendix B

Detailed Results Tables

Page intentionally left blank

Appendix B

Detailed Results Tables

Table B-1–Table B-4 includes the detailed results comparing standalone cycles to the geo-solar hybrid cycle with a solar multiple of 3 and 12 hours of storage (except for Mississippi where it is 10 hours). Storage durations were chosen based on minimizing LCOE for a given solar multiple.

Table B-1. California annual simulation results for baseload operation.

	2021					2022			
	Solar-only	Geo-only	Combined	Hybrid		Solar-only	Geo-only	Combined	Hybrid
Annual energy production (MWh_e)	73,016	39,210	112,226	115,516		74,414	38,996	113,409	120,358
Capacity Factor	0.58	1.18	0.70	0.70		0.59	1.17	0.71	0.73
Cost ($MM)	$81.17	$42.19	$123.36	$138.81		$80.37	$42.19	$122.56	$138.01
Revenue ($MM/yr)	$3.46	$1.89	$5.35	$5.67		$5.14	$3.27	$8.41	$9.01
LCOE ($/$MWh_e$)	$97.50	$95.29	$96.73	$98.22		$95.06	$95.81	$95.32	$96.76
LROE ($/$MWh_e$)	$47.38	$48.19	$47.66	$47.61		$69.02	$83.95	$74.15	$74.85
VF	0.97	0.98	0.97	0.97		0.83	1.01	0.89	0.90
NPV ($MM)	-$52.51	-$26.36	-$78.88	-$85.91		-$23.79	-$3.20	-$26.99	-$29.28
Benefit / cost ratio	0.35	0.38	0.36	0.38		0.70	0.92	0.78	0.79

Table B-2. Texas annual simulation results for baseload operation.

	2021					2020			
	Solar-only	Geo-only	Combined	Hybrid		Solar-only	Geo-only	Combined	Hybrid
Annual energy production (MWh_e)	74,064	4,458	78,522	75,227		74,158	4,556	78,713	75,158
Capacity Factor	0.59	1.78	0.61	0.61		0.59	1.82	0.61	0.61
Cost ($MM)	$78.51	$21.95	$100.45	$109.43		$76.67	$21.95	$98.61	$107.59
Revenue ($MM/yr)	$4.33	$1.07	$5.41	$5.42		$3.60	$0.33	$3.93	$3.79

	2021					2020			
	Solar-only	Geo-only	Combined	Hybrid		Solar-only	Geo-only	Combined	Hybrid
LCOE ($/MWh$_e$)	$93.82	$463.96	$114.83	$125.88		$92.07	$454.02	$113.01	$124.39
LROE ($/MWh$_e$)	$58.52	$240.26	$68.84	$71.99		$48.49	$72.50	$49.88	$50.39
VF	0.41	1.69	0.48	0.51		0.81	1.22	0.84	0.85
NPV ($MM)	-$35.31	-$14.33	-$49.63	-$56.06		-$45.82	-$26.72	-$72.55	-$81.49
Benefit / cost ratio	0.55	0.35	0.51	0.49		0.40	-0.22	0.26	0.24

Table B-3. Mississippi annual simulation results for baseload operation.

	2021					2022			
	Solar-only	Geo-only	Combined	Hybrid		Solar-only	Geo-only	Combined	Hybrid
Annual energy production (MWh$_e$)	45,564	25,931	71,495	74,514		53,845	25,780	79,625	82,993
Capacity Factor	0.36	1.29	0.49	0.49		0.43	1.29	0.54	0.55
Cost ($MM)	$81.14	$24.61	$105.75	$118.38		$79.51	$24.61	$104.12	$116.75
Revenue ($MM/yr)	$1.67	$0.85	$2.52	$2.63		$3.74	$1.41	$5.15	$5.35
LCOE ($/MWh$_e$)	$152.94	$85.62	$128.53	$132.84		$128.25	$86.12	$114.61	$118.34
LROE ($/MWh$_e$)	$36.76	$32.71	$35.29	$35.29		$69.46	$54.60	$64.65	$64.43
VF	1.11	0.99	1.07	1.07		1.18	0.92	1.09	1.09
NPV ($MM)	-$79.86	-$20.31	-$100.17	-$108.89		-$44.42	-$10.95	-$55.37	-$62.32
Benefit / cost ratio	0.02	0.17	0.05	0.08		0.44	0.56	0.47	0.47

Table B-4. Idaho annual simulation results for baseload operation.

	2021					2017			
	Solar-only	Geo-only	Combined	Hybrid		Solar-only	Geo-only	Combined	Hybrid
Annual energy production (MWh_e)	55,004	11,308	66,312	69,051		46,663	11,533	58,195	61,410
Capacity Factor	0.43	1.14	0.48	0.49		0.36	1.16	0.42	0.44
Cost ($MM)	$83.10	$25.08	$108.18	$121.39		$82.92	$25.08	$108.00	$121.20
Revenue ($MM/yr)	$2.31	$0.43	$2.74	$2.83		$0.92	$0.23	$1.15	$1.22
LCOE ($/$MWh_e$)	$129.98	$188.51	$139.96	$148.60		$151.99	$184.83	$158.50	$166.44
LROE ($/$MWh_e$)	$41.91	$38.42	$41.32	$41.04		$19.74	$20.07	$19.80	$19.88
VF	1.04	0.95	1.02	1.02		0.94	0.96	0.95	0.95
NPV ($MM)	-$72.12	-$25.70	-$97.82	-$111.22		-$94.35	-$29.10	-$123.45	-$137.57
Benefit / cost ratio	0.13	-0.02	0.10	0.08		-0.14	-0.16	-0.14	-0.14

Appendix C

Additional Results for a “Peaking” Hybrid Plant

Page intentionally left blank

Appendix C

Additional Results for a “Peaking” Hybrid Plant

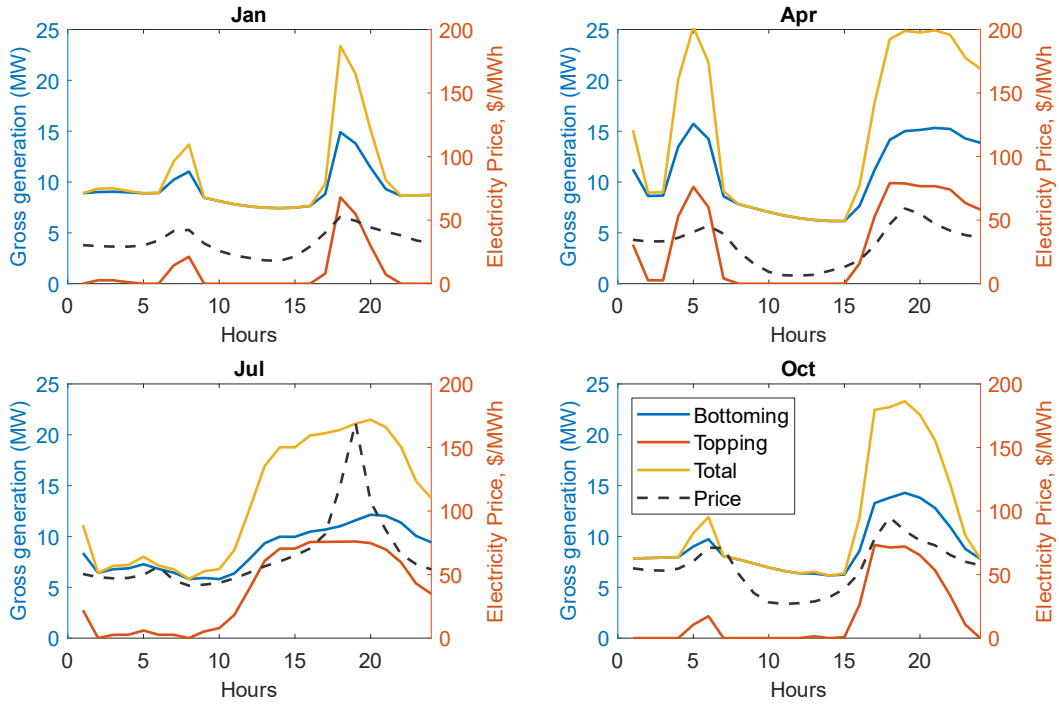

Figure C-1. Heatmap showing electricity price and hybrid power plant energy output for each hour of the year in Elk Hills, California, 2021

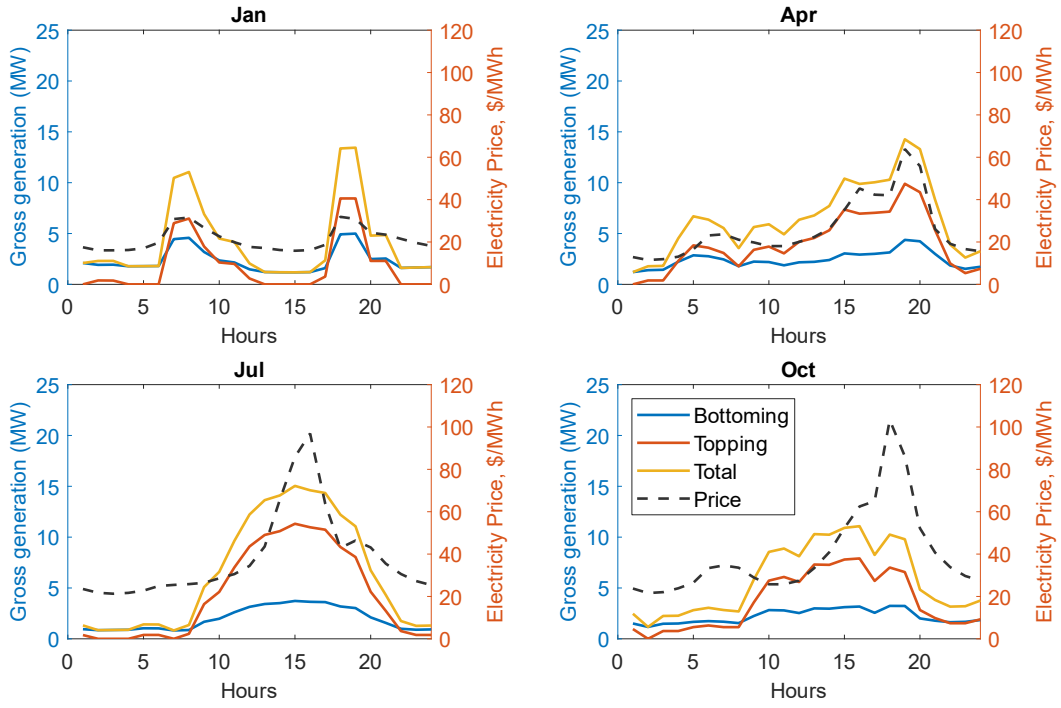

Figure C-2. Heatmap showing electricity price and hybrid power plant energy output for each hour of the year in Fort Bliss, Texas, 2021

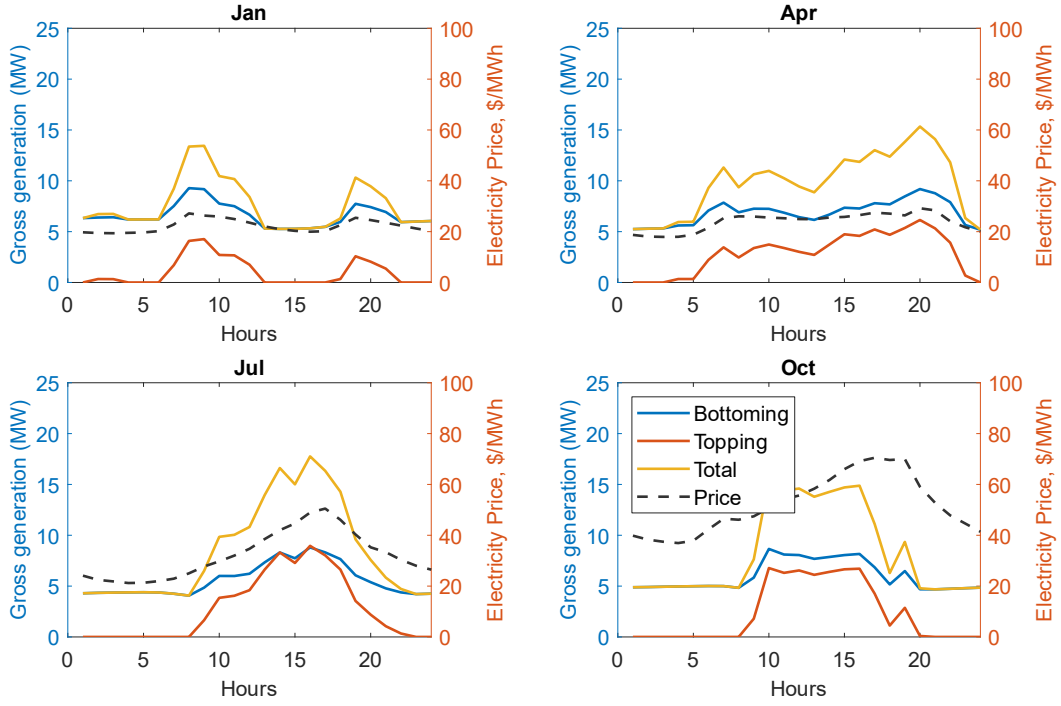

Figure C-3. Heatmap showing electricity price and hybrid power plant energy output for each hour of the year in Mississippi, 2021

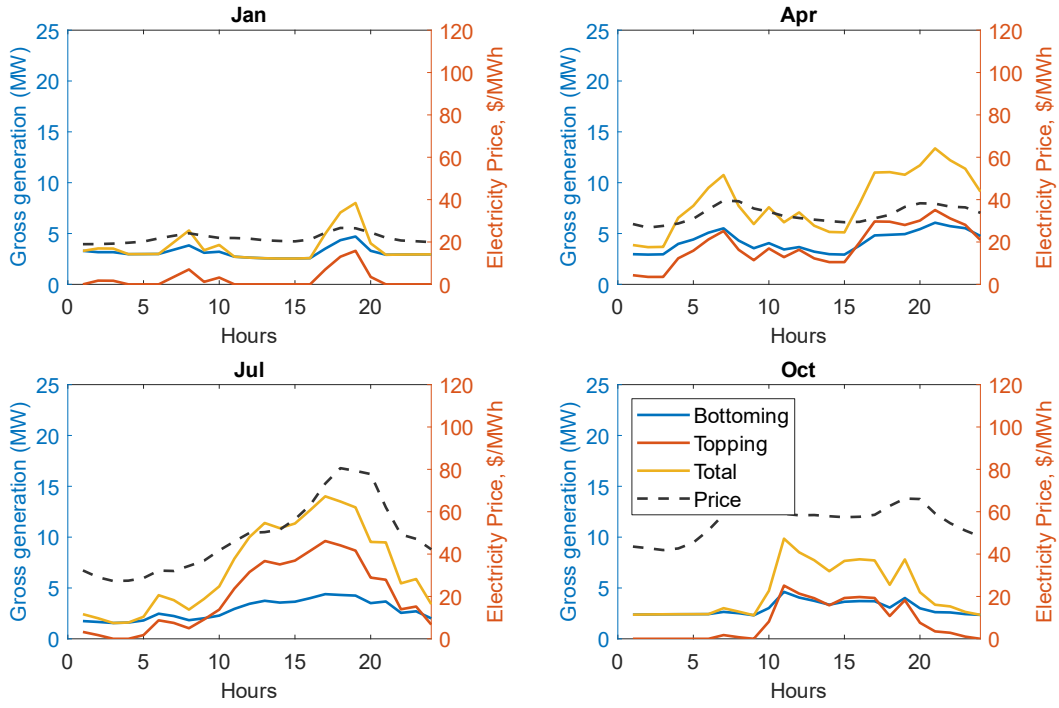

Figure C-4. Heatmap showing electricity price and hybrid power plant energy output for each hour of the year in Idaho, 2021

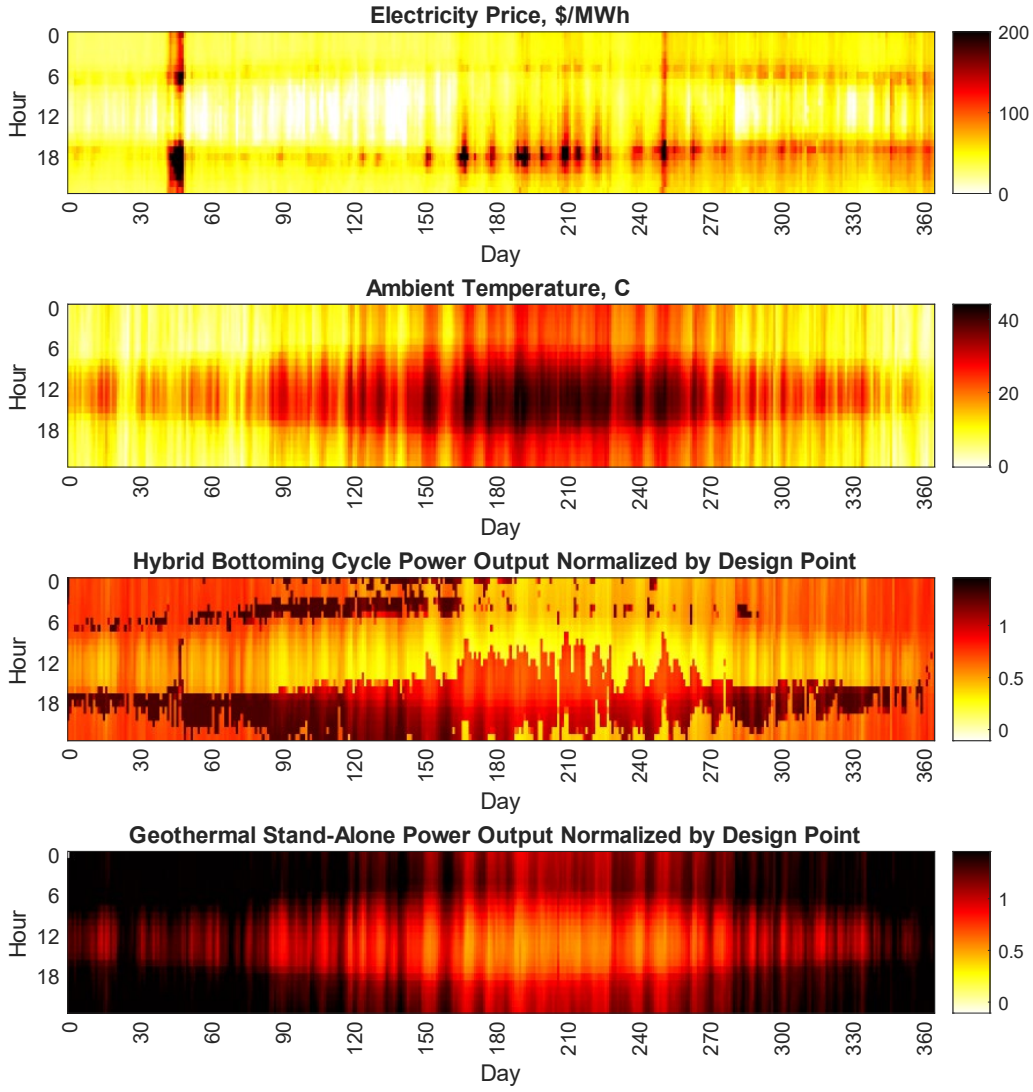

Figure C-5. Heatmaps showing hourly values of electricity price, ambient temperature, energy output from the bottoming cycle (normalized by the design value), and energy output from a standalone geothermal plant (normalized by the design value). Results are for California, 2021

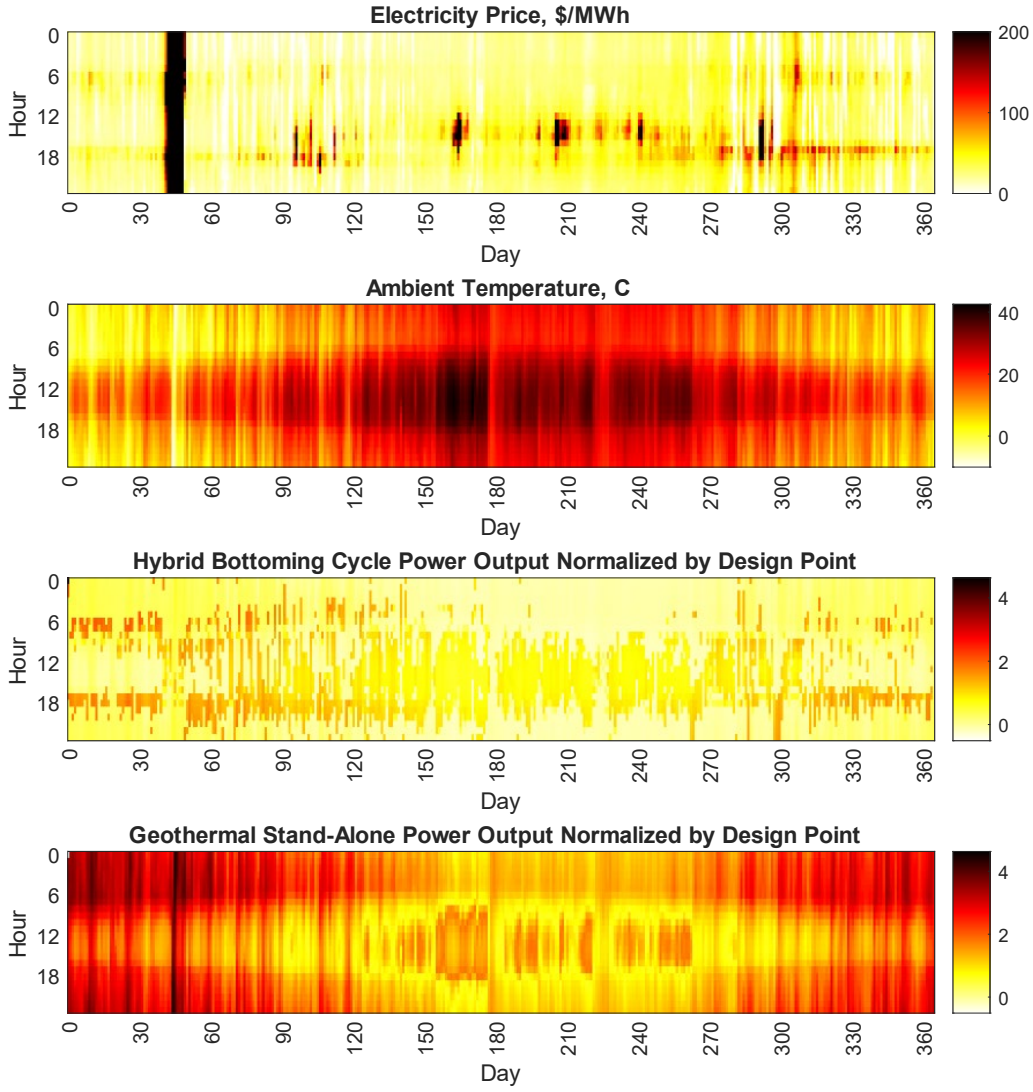

Figure C-6. Heatmaps showing hourly values of electricity price, ambient temperature, energy output from the bottoming cycle (normalized by the design value), and energy output from a standalone geothermal plant (normalized by the design value). Results are for Texas, 2021

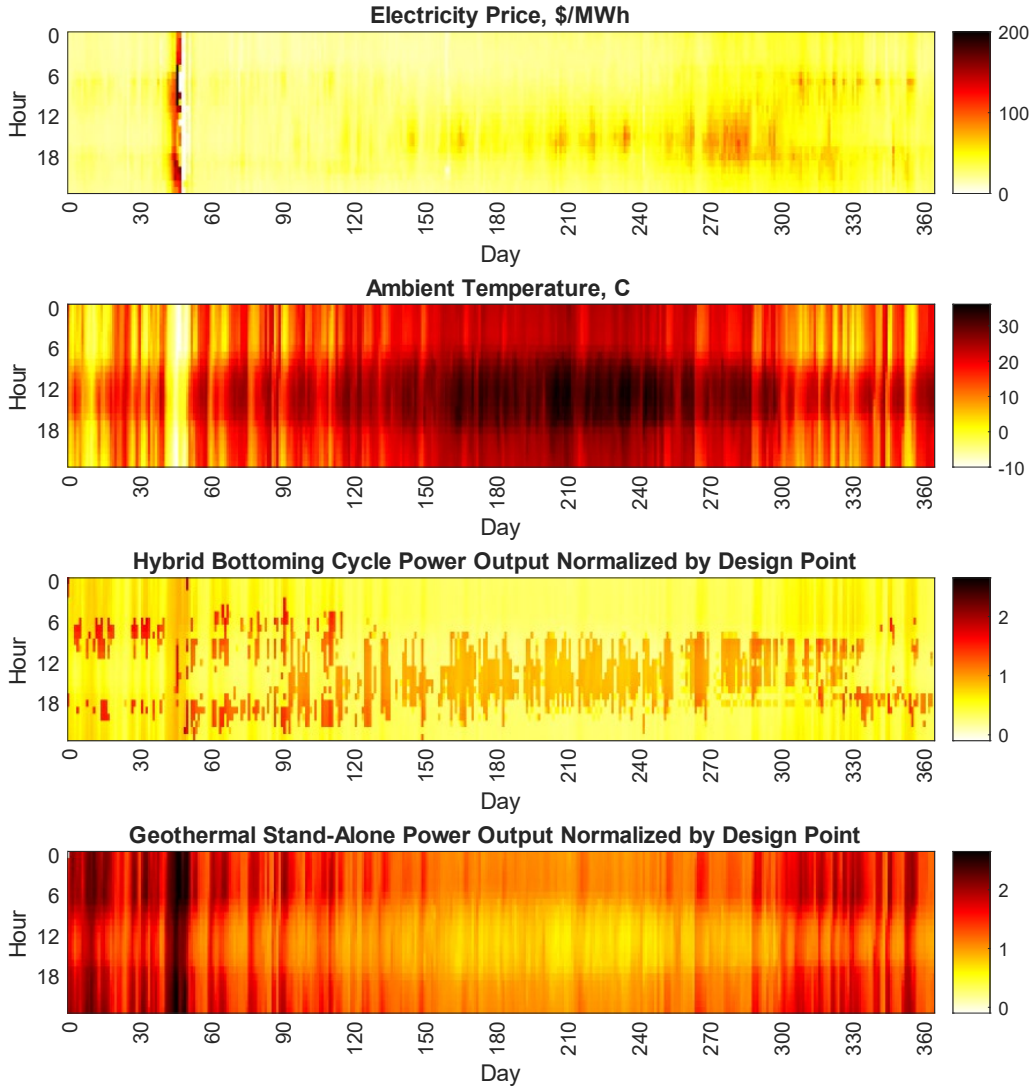

Figure C-7. Heatmaps showing hourly values of electricity price, ambient temperature, energy output from the bottoming cycle (normalized by the design value), and energy output from a standalone geothermal plant (normalized by the design value). Results are for Mississippi, 2021

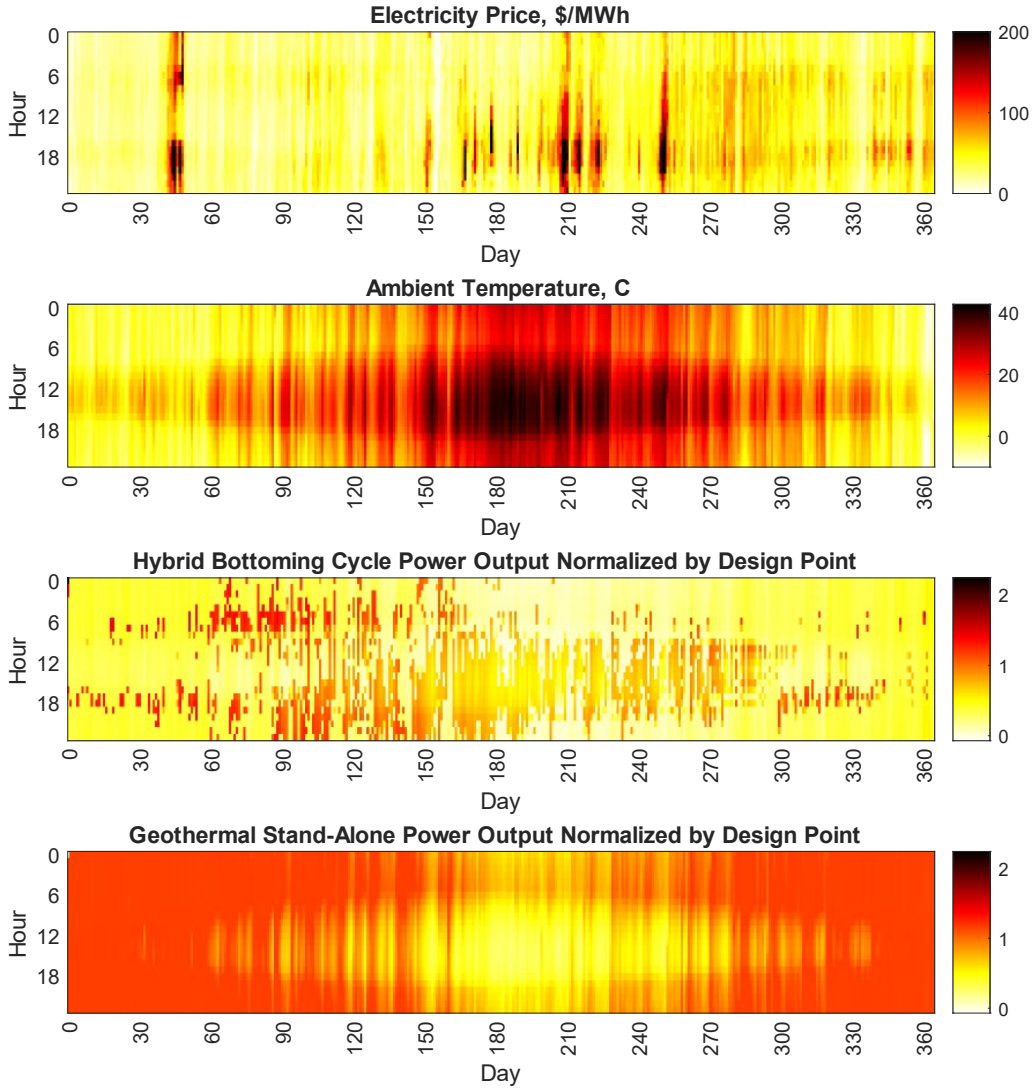

Figure C-8. Heatmaps showing hourly values of electricity price, ambient temperature, energy output from the bottoming cycle (normalized by the design value), and energy output from a standalone geothermal plant (normalized by the design value). Results are for Idaho, 2021

Table C-1. California annual simulation results for peaking operation.

	2021					2022			
	Solar-only	Geo-only	Combined	Hybrid		Solar-only	Geo-only	Combined	Hybrid
Annual energy production (MWh_e)	37,592.17	39,209.51	76,801.68	80,946.43		32,825.94	41,685.89	74,511.83	79,702.25
Capacity Factor	0.30	1.18	0.48	0.49		0.26	1.25	0.47	0.48
Cost ($MM)	$54.26	$42.19	$96.44	$111.90		$54.69	$42.19	$96.88	$112.33
Revenue ($MM/yr)	$2.41	$1.89	$4.30	$4.54		$3.21	$3.51	$6.72	$7.24
LCOE ($/$MWh_e$)	$136.90	$95.29	$115.65	$120.75		$156.86	$89.63	$119.25	$122.78
LROE ($/$MWh_e$)	$64.09	$48.19	$55.97	$56.08		$97.80	$84.09	$90.13	$90.84
VF	2.80	1.95	2.36	2.47		1.89	1.08	1.44	1.48
NPV ($MM)	-$39.97	-$26.36	-$66.33	-$75.57		-$26.56	$0.68	-$25.88	-$30.52
Benefit / cost ratio	0.26	0.38	0.31	0.32		0.51	1.02	0.73	0.73

Table C-2. Texas annual simulation results for peaking operation.

	2020					2021			
	Solar-only	Geo-only	Combined	Hybrid		Solar-only	Geo-only	Combined	Hybrid
Annual energy production (MWh_e)	38,541.31	4,555.54	43,096.85	39,203.48		36,526.64	4,457.95	40,984.59	37,323.70
Capacity Factor	0.31	1.82	0.34	0.32		0.29	1.78	0.32	0.30
Cost ($MM)	$49.81	$21.95	$71.76	$80.74		$49.84	$21.95	$71.78	$80.76
Revenue ($MM/yr)	$2.21	$0.33	$2.54	$2.39		$2.49	$1.07	$3.56	$3.57
LCOE ($/$MWh_e$)	$126.02	$454.02	$160.69	$189.08		$132.72	$463.96	$168.75	$198.40
LROE ($/$MWh_e$)	$57.24	$72.50	$58.86	$60.95		$68.14	$240.26	$86.86	$95.52
VF	2.12	7.63	2.70	3.18		0.93	3.26	1.19	1.39
NPV ($MM)	-$39.00	-$26.72	-$65.72	-$75.37		-$34.11	-$14.33	-$48.44	-$55.57
Benefit / cost ratio	0.22	-0.22	0.08	0.07		0.32	0.35	0.33	0.31

Table C-3. Mississippi annual simulation results for peaking operation.

	2021					2022			
	Solar-only	Geo-only	Combined	Hybrid		Solar-only	Geo-only	Combined	Hybrid
Annual energy production (MWh_e)	23,263.51	25,930.66	49,194.17	50,822.50		27,376.41	25,780.10	53,156.51	54,977.00
Capacity Factor	0.18	1.29	0.34	0.34		0.22	1.29	0.36	0.36
Cost ($MM)	$53.09	$24.61	$77.70	$90.33		$52.31	$24.61	$76.92	$89.55
Revenue ($MM/yr)	$0.98	$0.85	$1.83	$1.89		$2.23	$1.41	$3.64	$3.75
LCOE ($/$MWh_e$)	$214.56	$85.62	$146.59	$156.38		$181.24	$86.12	$135.11	$143.90
LROE ($/$MWh_e$)	$42.15	$32.71	$37.18	$37.26		$81.45	$54.60	$68.43	$68.26
VF	6.49	2.59	4.44	4.73		3.07	1.46	2.29	2.44
NPV ($MM)	-$61.40	-$20.31	-$81.71	-$91.59		-$40.09	-$10.95	-$51.04	-$59.96
Benefit / cost ratio	-0.16	0.17	-0.05	-0.01		0.23	0.56	0.34	0.33

Table C-4. Idaho annual simulation results for peaking operation.

	2017					2021			
	Solar-only	Geo-only	Combined	Hybrid		Solar-only	Geo-only	Combined	Hybrid
Annual energy production (MWh_e)	24,397.20	11,532.77	35,929.97	38,262.59		28,022.79	11,307.99	39,330.78	41,109.43
Capacity Factor	0.19	0.97	0.25	0.26		0.21	0.95	0.28	0.28
Cost ($MM)	$53.81	$25.08	$78.89	$92.10		$53.80	$25.08	$78.88	$92.09
Revenue ($MM/yr)	$0.65	$0.23	$0.88	$0.93		$1.39	$0.43	$1.82	$1.89
LCOE ($/$MWh_e$)	$206.79	$184.83	$199.74	$214.10		$180.71	$188.51	$182.95	$199.54
LROE ($/$MWh_e$)	$26.46	$20.07	$24.41	$24.41		$49.57	$38.42	$46.37	$45.90
VF	9.87	8.82	9.53	10.22		4.47	4.66	4.53	4.94
NPV ($MM)	-$67.83	-$29.10	-$96.93	-$111.55		-$55.71	-$25.70	-$81.41	-$95.79
Benefit / cost ratio	-0.26	-0.16	-0.23	-0.21		-0.04	-0.02	-0.03	-0.04